2012-11-13

Ultrasound-Induced Phase Change of Emulsion Droplets for Targeted Gene and Drug Delivery

James R. Lattin
Brigham Young University - Provo

Ultrasound-Induced Phase Change of Emulsion Droplets for Targeted Gene- and Drug-Delivery

James R. Lattin

A dissertation submitted to the faculty of
Brigham Young University
in partial fulfillment of the requirements for the degree of

Doctor of Philosophy

William G. Pitt, Chair
Randy S. Lewis
Thomas A. Knotts
David O. Lignell
Morris D. Argyle

Department of Chemical Engineering

Brigham Young University

November 2012

ABSTRACT

ULTRASOUND INDUCED PHASE CHANGE OF EMULSION DROPLETS FOR TARGETED GENE- AND DRUG-DELIVERY

James R. Lattin
Department of Chemical Engineering, BYU
Doctor of Philosophy

This dissertation explores the potential of using perfluorocarbon emulsion droplets to add an ultrasound-sensitive element to drug delivery systems. These emulsion droplets may be induced to vaporize with ultrasound; during the rarefactional phase of an ultrasound wave, the pressure around the droplets may fall below the vapor pressure of the liquid forming the emulsion, providing a thermodynamic potential for vaporization. This ultrasound-induced phase change of the emulsion droplet could release therapeutics attached to the droplet surface or aid in drug delivery due to mechanical effects associated with vaporization and expansion, similar to the ability of cavitating bubbles to aid in drug delivery. In contrast to bubbles, stable emulsions can be formed at nano-scale sizes, allowing them to extravasate into tissues and potentially be endocytosed into cells. Perfluorohexane and perfluoropentane were selected to form the emulsions due to their relatively high vapor pressure, low water solubility, and biocompatibility.

Acoustic droplet vaporization was explored for its potential to increase ultrasound-induced drug release from liposomes. Liposomes have proven to be versatile and effective drug carriers, but are not inherently responsive to ultrasound. eLiposomes, defined as a liposome with encapsulated emulsion droplets, were developed due to the potential of the expanding vapor phase to disrupt bilayer membranes. The resulting vesicle retains the advantages of liposomes for drug delivery, while adding an ultrasound-sensitive element. eLiposomes were loaded with calcein, a fluorescent molecule, as a model drug in order to quantify ultrasound-mediated drug release compared to release from conventional liposomes. Upon exposure to ultrasound, eLiposomes typically released 3 to 5 times as much of the encapsulated load compared to conventional liposomes, with some eLiposome samples approaching 100% release. Emulsion droplets were also added to the outside of conventional liposomes, but resulted in little to no increase compared to control samples without emulsions.

Lastly, in vitro experiments were performed with HeLa cells to explore the ability of emulsion droplets and eLiposomes to deliver calcein inside of cells. Calcein delivery to the cytosol was accomplished, and the emulsion-containing samples demonstrated the ability to aid in endosomal escape.

Keywords: James Lattin, drug delivery, ultrasound, emulsion, liposome, eLiposome

ACKNOWLEDGMENTS

I would first like to express my appreciation and gratitude to my wonderful wife, Lindsay, for her unconditional love, support, and patience throughout school and in all areas of our life. I would also like to thank my parents and family for their encouragement, love, and support throughout the years. I would next like to thank Dr. William Pitt, my graduate advisor, for his guidance and help. His patient mentoring has helped to make graduate school an enriching, challenging, and meaningful experience. His style of teaching and counseling epitomize the aims and mission of Brigham Young University. Along with Dr. Pitt, I would like to thank all of the members of his research group that have helped with this project in countless ways. Thank you as well to the other professors and staff of the Chemical Engineering Department for their dedication and hard work.

TABLE OF CONTENTS

LIST OF TABLES

LIST OF FIGURES

1 INTRODUCTION

Targeted drug delivery is currently an important and promising research area. There are a number of conventional and potentially useful therapeutic techniques that sometimes have widespread negative side effects and risks. These techniques often have a specific target, such as a cancerous tumor or a specific target organ where treatment is beneficial. Side effects and risks could be greatly reduced if the therapeutics could be directed specifically to the target area. One of the most obvious examples of this is chemotherapy used in cancer treatment. The devastating side effects of this treatment include fatigue, hair loss, widespread pain, sores, diarrhea, nausea, and vomiting. If the chemotherapy drugs could be delivered only to the cancer cells, then the benefit of this treatment could be maintained while avoiding most of the negative side effects.

Another major candidate for targeted delivery is gene therapy. This treatment allows selected genes to be inserted into a patient's cells. These inserted genes may replace abnormal genes, turn on inactive genes or suppress a disease-causing gene. Heart disease, lung disease, cancer, and genetic disorders are just a few of the diseases that could be targeted with such a treatment. However, because of potential negative effects of exposing the entire body to these foreign therapeutic genes, they should be delivered only to the target cells.

For the last decade, ultrasound has been investigated as a targeting modality for drug and gene delivery to preferentially deliver therapeutics to a specific target. Ultrasound has been shown to temporarily increase the permeability of cell membranes, allowing for more effective

delivery of therapeutics to the area exposed to ultrasound. Cavitation is believed to be the mechanism that causes this permeability. Cavitation is the formation, vibration, and collapse of bubbles caused by pressure oscillations in the ultrasonic field. It is believed that cavitation events introduce mechanical shear that temporarily creates tears and holes in the cell membrane, increasing the delivery of therapeutics to the interior of the cell.

Ultrasound can also aid in drug and gene delivery by breaking apart or otherwise activating a vesicle serving as a drug carrier, thus releasing the drug in the specific location where ultrasound is applied. These drug carriers can be micelles, polymer particles, liposomes, or bubbles. Bubbles are of particular interest as ultrasound activated drug carriers because they can serve as cavitating bubbles while simultaneously carrying drugs. One disadvantage to bubbles, however, is that they cannot easily be formed at sub-micron sizes due to the high Laplace pressure found in small bubbles. This minimum size limitation prevents bubbles from being able to pass beyond capillaries into tissues where delivery is desired because the junctions between endothelial cells lining normal capillaries are typically less than 10 nm in size. Microbubbles are even excluded from cancerous tumors, despite the potential for cancerous tissues to have large capillary fenestrations of up to 1000 nm [1].

Another useful carrier that has been investigated in drug delivery is a liposome. Liposomes can be loaded with drugs or DNA, sequestering the therapeutics inside of a bilayer lipid membrane until they are released from the liposome. Liposomes have many advantages, including a high encapsulation efficiency, relative low cost, and biocompatibility of lipids. Perhaps the most-often cited advantage for cancer treatment is that their sub-micron size allows liposomes to permeate deep into tissues, especially cancerous tumors with leaky capillaries. These advantages have led to the active research of liposomes as drug carriers for decades.

However, one disadvantage of liposomes is that drug delivery is achieved by gradual diffusion out of the liposome or the eventual rupture or break down of the membrane over time. While liposomes are very useful as drug delivery vehicles, their potential in targeted delivery could be increased if drug release could be induced by ultrasound. One way to make liposomes susceptible to ultrasound may be to encapsulate emulsion droplets with a relatively high vapor pressure inside of the liposomes. During the low pressure phase of the acoustic cycle the encapsulated liquid will vaporize, resulting in a sufficient volume of gas to break apart the lipid bilayer of the liposome, allowing targeted drug release from the liposome. This release would be localized to where the ultrasound was applied, and the time and rate of release could be controlled by ultrasound. Throughout the rest of this dissertation, liposomes containing encapsulated emulsion droplets will be referred to as eLiposomes.

This vaporizing fluid could also address another concern with drug delivery: endosomal escape. Drugs that cannot diffuse through cell membranes often enter the cell through an endosome, where they are digested and broken down by the cell before they can be therapeutically effective. If several emulsion droplets were trapped within a liposome inside of the endosome, they could provide sufficient volume increase during vaporization to not only break through the liposomal membrane, but also to break open the bilayer membrane of the endosome, thus allowing release of the drug into the cell cytosol.

My dissertation research has included the synthesis of perfluorocarbon emulsions and the synthesis of eLiposomes. Nano-scale perfluorocarbon emulsions were formed and characterized. Once formed, eLiposomes were investigated as ultrasound activated drug carriers. The ability of eLiposomes to deliver model drug in vitro and the ability of expanding emulsion droplets to aid in endosomal escape was also investigated.

2 LITERATURE REVIEW AND BACKGROUND

2.1 Drug and gene delivery

Chemotherapeutic drugs are one of the main treatments used against cancerous tumors. However, this treatment is often limited by the high toxicity of the drugs and the lack of tumor-specific targeting [2]. Current chemotherapy techniques usually involve systemic circulation of the drug. This exposes the whole body to the chemotherapy, resulting in anemia, vomiting, diarrhea, nausea, and hair loss [3]. Methods for targeting drugs to specific target sites are an active research area. The goal of this research is to selectively deliver drugs to tumors without harming other cells. By targeting the drug to the tissue where it is needed, the dose delivered to the target tissue could be maintained or even increased while lowering exposure in other areas of the body. Alternatively, a reduced administered dose could be used to achieve a therapeutic dose at the target site. This would allow for more effective treatment of the tumor while reducing or eliminating negative side effects [4].

Another type of treatment requiring targeting is gene therapy. In this treatment selected genes are transfected into a patient's cells. Transfection is the incorporation of foreign genetic material into a cell. These inserted genes may replace abnormal genes, suppress active genes or stimulate inactive genes. In principle, inserted genes may code for specific proteins that would allow a wide variety of problems to be alleviated at the cellular level. The treatment of cancer, infectious diseases, liver diseases, vascular diseases, and genetic disorders are just a few of the

potential uses for such a treatment [5, 6]. However, the effect of exposing the entire body to foreign DNA that is designed to be therapeutic for a certain type of tissue is a major concern. It is important to be able to deliver the genetic material to the targeted cells without delivery to the rest of the body. The most promising method for delivery of therapeutic genes was previously thought to be viral vectors. Because this method utilizes an efficient viral mechanism for inserting genetic material into cells, viral delivery has been shown to have very high transfection rates [6]. However, this method has a number of drawbacks, including toxicity of viral vectors and decreased efficiency of treatments over time due to the body's immune response. Also, viral delivery methods have very low tissue specificity, raising safety concerns about the effects of the inserted genes on non-targeted cells, and the potential of these genes being integrated into the patient's cells at random sites in the body [7].

Over the last decade, non-viral drug targeting carriers for both conventional drugs and nucleic acids have been an area of intense research. Drug delivery systems seek to increase site-specific delivery and to sequester the drug load except at the target site. Potential targeting techniques that have been investigated include attaching a targeting ligand to the surface of the drug carrier, using a pH-sensitive or enzyme activated carrier, targeting leaky tissues by controlling the carrier size, and making the carrier susceptible to drug release when an external trigger is applied [4, 8, 9]. "Passive targeting" typically refers to drug carrier accumulation in some tissues based on the size of the particle and the inherent properties of the target tissue's vasculature. In "active targeting," ligands are recognized by a target cell type and aid in preferential attachment and sometimes induce uptake of the therapeutics into targeted cells [10-12]. Enzyme or pH-sensitive carriers are designed to sequester drugs until release is triggered at the targeted location by environmental changes [13, 14]. "Actuated" delivery, the use of an

external trigger such as ultrasound, has the advantage of being able to control both the location of release and the amount of drug released with time [9]. Multiple targeting techniques can also be used in conjunction with each other, such as using passive targeting to concentrate drug carriers at a target site and then releasing sequestered drug by employing active or actuated targeting.

Sub-micron drug and gene carriers are especially desirable for cancer treatments in order to take advantage of passive targeting. Cancer tumors tend to have chaotic and rapidly growing vasculature. The chaotic growth of tumor vessels leads to a leaky capillary system with large fenestrations that allow sub-micron particles to pass into the cancerous tissue. The poor development of an efficient lymphatic system for clearance from the tumor allows particles that are on the order of hundreds of nanometers to accumulate in the tumor. This is referred to as the enhanced permeability and retention (EPR) effect and is cited as a method of passively targeting therapeutics to cancer tumors [15]. Typical sizes of the endothelial fenestrations in tumors range from 100 nm to about 1 um [1]. This increased permeability observed in cancer tissues allows particles that are excluded from other tissues to enter the cancer tumor. The size of these gaps and the ability of nano-sized particles to diffuse into the cancerous tissue is dependent on the type of tumor, with most types allowing particles up to about 500 nm to pass through [1]. Ideal sizes for drug carriers to both pass through these fenestrations and accumulate in tissues in order to take advantage of the EPR effect are believed to be between 100 nm and 300 nm [16]. After penetrating into the tumor, particles between these sizes tend to accumulate due to the tumor's limited ability to recycle the extracellular fluid via the lymphatic system.

2.2 Ultrasound in drug and gene delivery

Ultrasound is defined as cyclic pressure waves with a frequency above 20 kHz [17]. These pressure waves are similar to those that create sound, but at this frequency they are beyond the limit of human detection. Traditionally, ultrasound has been used in medicine for imaging and for local heating of tissues. Recently it is being investigated for several beneficial roles that it may play in therapeutic delivery systems. Beginning in the 1980's, several studies reported increased drug activity when drugs were administered along with the application of ultrasound, particularly for cytotoxic drugs and chemicals [18, 19]. For example, Saad and Hahn exposed HA1 chinese hamster cells to the cytotoxic drug Doxorubicin (Dox) with and without ultrasound [18]. The fraction of cells that survived dropped by an order of magnitude with the application of ultrasound compared to negative controls. For some time it was debated whether this effect was a result of local hyperthermia or mechanically increased cell permeability.

By the 1990's, it was believed that mechanical effects were responsible for increased cell permeability [19]. Tachibana et al. reported that low intensity ultrasound increased drug activity in HL-60 cells. These results suggested that mechanical effects were responsible for the drug effect because thermal effects of this low intensity ultrasound would be minimal. Furthermore, directly after ultrasound treatment, some of the cells were fixed for electron microscopy, providing images that showed evidence of mechanical disruption on cell surfaces. Huber, et al. showed that transfection of reporter DNA plasmids was drastically increased *in vitro* and *in vivo* with the application of ultrasound, concluding that the cell membrane had to have been disrupted to allow the plasmids into the cell [20].

Over the past decade, many studies have sought to better understand the mechanisms by which ultrasound increases membrane permeability. Although the mechanism is still not

completely clear, the current hypothesis is that ultrasound causes cavitation events which mechanically disrupt the cell membrane [7]. Cavitation is the formation and/or cyclic oscillation of a bubble entrained in liquid [17]. These oscillations are created by the cyclic pressure changes imposed by ultrasound. Beyond a threshold in negative pressure amplitude, these oscillations become erratic and eventually result in the collapse of the bubble, creating a shock wave. This is known as collapse cavitation. Furthermore, if the bubble is close to a surface, the asymmetric collapse of the bubble can result in the formation of a high-velocity jet of liquid [21]. These bubble oscillations, liquid jets, and shock waves generated with ultrasound can shear and penetrate the cell membrane, creating reversible openings through which drugs or DNA plasmids can pass [5, 7, 17, 19, 22-25]. Because of challenges in comparing the biological effects of ultrasound at different frequencies, the mechanical index (MI) was developed to create a normalized parameter for predicting the likelihood of cavitation at a given frequency. MI is defined as:

$$MI = \frac{P_{rarefactional} \ / \ 10^6 \, Pa}{\sqrt{f \ / \ 10^6 \, Hz}} \tag{1}$$

where $P_{rarefactional}$ is the peak rarefactional (negative) pressure and f is the ultrasound frequency.

To investigate this mechanism, Schlicher, et al. exposed DU 145 prostate-cancer cells to 24-kHz ultrasound in the presence of calcein, a fluorescent marker molecule that does not cross biological membranes [25]. After sonication, samples were given 5 to 10 minutes to recover. The cells were then washed to remove non-incorporated calcein. Flow cytometry was used to observe fluorescence of the cells from sonicated and non-sonicated experiments. Non-sonicated cells did not fluoresce significantly. Increased fluorescence was observed in 10% to 40% of sonicated cells, indicative of increased membrane permeability to the calcein. Furthermore,

cellular response in the sonicated samples was characteristic of membrane wounding and repair. At 500 kHz, permeabilization of the membrane occurs to some extent at a peak negative pressure of 0.6 MPa [26]. The amount of calcein that was able to pass through the membrane increased with peak negative pressure, but cell viability decreased rapidly at pressures above 1.6 MPa. The amount of calcein taken up by the cells was correlated with the total ultrasound energy to which they were exposed [26, 27]. Guzman, et al. performed similar experiments with fluorescent dextrans of larger sizes and reported that larger molecules (464 kDa dextran) were also able to diffuse into the cell cytosol [27]. However, these larger molecules were unable to enter the cell nucleus, while calcein was able to do so.

Recently, advanced microscopy techniques have allowed researchers to observe holes and tears in the cell membrane as well as subsequent membrane repair. For example, Schlicher et al. used electron microscopy to observe changes in cell membranes after ultrasound exposure including possible holes and interior vesicle fusion to patch these holes [25]. Prentice, et al. visualized cavitating bubbles using optical microscopy. Afterwards, actual holes in the cell membrane were observed using atomic force microscopy (AFM) [24]. These findings are consistent with the hypothesis of reversible membrane damage caused by cavitation events that open up holes in the membrane followed by self-healing.

Another important application of ultrasound in targeted drug and gene delivery is its ability to initiate the release of drugs or genes from particles that sequester or bind the therapeutics. The same physical effects of ultrasound that increase permeability of cell membranes can be advantageously used to release loaded drugs or genes from particles such as micelles, microbubbles, and liposomes. Polymeric micelles have been investigated as ultrasonically activated drug carriers because of their ability to sequester hydrophobic drugs. For

example, Rapoport, et al. and Husseini, et al. showed that Pluronic™ micelles could be used to sequester Doxorubicin. The drug was released from the micelles in response to ultrasound exposure at frequencies ranging from 20 kHz to 1 MHz and re-sequestered after insonation [9, 28]. This would allow a chemotherapeutic drug to be sequestered from interaction with the body except where ultrasound is used to rupture the micelles and release the drug.

2.3 Microbubbles

Microbubbles are 1-10 μm-sized gas bubbles. The pressure inside of a spherical bubble is proportional to the interfacial energy and inversely proportional to the radius. Therefore, the formation of micro-scaled gas bubbles leads to high pressure gas inside of a microbubble – as bubble size approaches 1 μm the Laplace pressure can be well over 1 atm [29]. Without being somehow stabilized, this gas will quickly dissolve into the surrounding liquid [30]. Microbubbles for medical purposes are stabilized by a surfactant. Surfactants have polar and non-polar regions and associate with the liquid-gas interface to lower the interfacial energy and thereby lower the internal pressure of the bubble. This makes it possible to form stable microbubbles. To increase their lifespan, microbubbles are often formed from gases that have low solubilities in water such as perfluorocarbons [31, 32]. These microbubbles are used as contrast agents in ultrasound imaging of blood to increase the quality and sharpness of ultrasound images [31].

There is potential benefit from applying microbubbles to targeted gene and drug delivery. They can be used to lower the threshold pressures necessary for cavitation because they introduce cavitation nucleation sites [33]. One study reported that the ultrasonic pressure threshold for collapse cavitation at 757 kHz was 1.96 MPa in pure water [34]. This threshold

was reduced to 0.53 MPa when microbubbles were introduced as cavitation nuclei. Bubbles could therefore enhance cavitation and simultaneously act as drug carriers. Several types of microbubbles have been investigated for use in drug and gene delivery. Most notably, perfluorocarbon gas bubbles are stabilized by an albumin shell (Optison) [22] or by lipid surfactants (Definity) [5]. Both Optison and Definity have been shown to undergo collapse cavitation when ultrasound was applied, resulting in increased gene transfection. Prentice et al. sonicated a monolayer of cells in the presence of Optison™ microbubbles with a 1-MHz transducer. An ultra-high-speed camera and atomic force microscopy were used to observe the bubbles and the cell surface [24]. Bubbles could be observed oscillating, forming microjets, and collapsing.

Bubbles can be used in drug delivery in a number of ways. Treat et al. used Optison microbubbles to aid in delivery of Dox to the brain by increasing the permeability of the blood-brain barrier [35]. Dox is a reasonable candidate for treatment of brain tumors, but normally cannot pass through the blood brain barrier. Dox and Optison were co-administered to rats. When ultrasound was applied, therapeutic concentrations of Dox were observed in the brain. The delivered dose of Dox was dependent on the concentration of Optison and the intensity of ultrasound.

Tinkov et al. describe the incorporation of drugs into the surfactant shell or attached to the surface of a microbubble through covalent or non-covalent interactions. Unger et al. sequestered sudan black dye in the surfactant layer of microbubbles and showed that ultrasound caused destruction of the microbubbles and release of sudan black [36]. Later, Paclitaxel, a chemotherapeutic drug, was sequestered inside of the hydrophobic surfactant shell of 3 μm

microbubbles and released with ultrasound. Without ultrasound, the Paclitaxel remained encapsulated.

Microbubbles have also been used to increase gene transfection into cells [23]. DNA plasmids can be bound to the bubble surface or encapsulated inside [31]. Upon insonation, the microbubbles undergo cavitation events that both aid in cellular transfection and release the DNA from the bubble. Lawrie *et al.* used naked DNA plasmids coding for luciferase to measure gene transfection into smooth muscle cells. Cells were exposed to a DNA-plasmid solution and 956-kHz ultrasound for 60 seconds [22]. Ultrasound alone produced a 16-fold increase in luciferase expression relative to control experiments. When Optison microbubbles were present, luciferase expression was increased by 300 times.

Using a surfactant that carries a positive charge on the surface attracts the negatively charged DNA plasmids to the surface of the bubble [37-39]. Zobel et al. showed that the DNA molecules are absorbed onto the surface of cationic particles [39]. This could result in a more efficient treatment from a smaller dose of DNA. Anwer et al. attempted to transfect tumors on mice with CAT reporter genes. It had previously been noted that these genes were transfected into tumor cells, but a significant amount of CAT was also expressed in the lungs [37]. At low DNA doses, using a positively charged stabilized bubble to deliver the gene resulted in a 270-fold increase in tumor transfection over control experiments. Transfection into the lung was unaltered compared to other treatments at this low dose. Therefore, using the cationic carrier with ultrasound allowed a smaller DNA dose to have a large effect on the tumor while transfection into other organs was limited due to the small dose that was necessary.

2.4 Nanoemulsions

One disadvantage of microbubbles is that although they are small enough to pass through capillaries, they are too large to pass through gaps in the endothelium, even in cancerous tissues. Even with surfactants to lower the interfacial energy, bubbles do not persist at sizes much smaller than 1 micron. This limits their ability to deliver therapeutics deep within tissues or to be endocytosed into most types of cells. Because stable microbubbles are very difficult to form at these sizes they are poor candidates for intra-tissue targeting via the EPR effect.

A potential nano-sized particle that can take advantage of the EPR effect while retaining the ultrasound sensitivity of microbubbles is a nanoemulsion droplet. An emulsion is a mixture of immiscible liquids. Small droplets of one liquid, referred to as the dispersed phase, are suspended within the other liquid phase, referred to as the continuous phase. In the case of a nanoemulsion, these droplets are less than a micron in diameter. In order to prevent phase separation or droplet coalescence, the droplets are stabilized by surfactants similar to those used to stabilize microbubbles. These surfactant molecules lower the interfacial energy between the two phases and help to stabilize the nano-sized droplets. The surfactant may also create a repulsive boundary, preventing the liquid droplets from colliding and coalescing. Oil in water nanoemulsions are typically formed from non-polar liquids having low water solubility to decrease their rate of dissolution.

Surfactants that have been used to stabilize emulsions for medical applications include proteins, lipids, polymers, and traditional surfactants [40, 41]. Perfluorocarbon emulsions have been used previously as artificial oxygen carriers and as ultrasound contrast agents for imaging [42, 43]. More recently, emulsions have received attention as drug carriers [44-46]. Most perfluorocarbon emulsions that have been produced previously were larger than 300 nm. Much

of the current interest in perfluorocarbon nanoemulsions centers on the ability to vaporize emulsion droplets with heat or acoustic energy. Such a technique would require emulsion droplets to be formed from a liquid with a high vapor pressure. The leading candidates are perfluorocarbons due to their high vapor pressure, low water solubility, and low toxicity [47-51]. Because stable emulsions can be formed on the nano-scale, the emulsion droplets could passively target tumors by taking advantage of the EPR effect. After reaching the target site, nanoemulsions could be transformed into cavitating microbubbles, thus overcoming some of the challenges of microbubbles and ultrasound-induced drug delivery while retaining many of the advantages of these methods [52].

Giesecke et al. measured cavitation thresholds for various perfluorocarbon emulsions to show that the droplets could be vaporized and that the resulting bubbles would cavitate [53]. Perfluoropentane, perfluorohexane and perfluoromethylcyclohexane emulsions were stabilized with albumin and threshold negative pressures for collapse cavitation were determined by observing a jump in broadband noise. The threshold negative pressure for collapse cavitation was reported to be approximately 0.7 MPa at 0.74 MHz and 1.75 MPa at 3.3 MHz. At high frequency, this threshold was comparable to the cavitation threshold for Optison, a commercial microbubble formulation. This work showed that emulsion droplets can be readily vaporized in an ultrasound field and that the threshold for observing cavitation from these vaporizing emulsions was much lower than the cavitation threshold in pure water.

There are a number of parameters that effect droplet vaporization. Shiraishi formed similar emulsion droplets for vaporization with mixtures of perfluorohexane and perfluoropentane [54]. It was reported that these mixtures allowed the emulsion to persist above the boiling temperature of perfluoropentane. These emulsions were prepared by sonication

rather than high-speed shaking or high pressure emulsification used previously. Sonication resulted in emulsion diameters that were as small as or smaller than these other methods while maintaining a higher final concentration of perfluoropentane. These emulsions were stabilized with block copolymers. In contrast to other polymer-stabilized drug carriers, the characteristics of the polymer did not have a large effect on the pharmacokinetics of the emulsion. Kawabata, et al. demonstrated that the threshold value for vaporization of emulsion droplets is dependent on liquid used to form the emulsion droplets [55]. Perfluorocarbons with higher boiling points had higher amplitude thresholds for ultrasonic vaporization. Furthermore, the acoustic threshold for vaporization of an emulsion was tuned and controlled by mixing perfluorocarbons with different boiling points. Fabiilli, et al. demonstrated that emulsion droplet size had an effect on vaporization [44]. Emulsions were prepared from perfluoropentane and stabilized with albumin. In droplets with diameters less than 2.5 um, the acoustic threshold for vaporization increased as droplet diameter decreased. Sheeran et al. have recently provided further insight to the effect of diameter on droplet formation and vaporization. Nanoemulsions were formed by condensing perfluorobutane with phospholipids as a stabilizing surfactant [56]. The resulting emulsions showed the potential to remain stable and persist in solution at 37°C for hours despite perfluorobutane having a boiling point of -1.7°C. These metastable emulsion droplets also showed the potential to vaporize back into gas droplets with the application of ultrasound [57]. Similar emulsions were formed with perfluoropropane, although they did not demonstrate the same stability or ability to persist in solution even at 22°C.

Rapoport et al. used a polymer-stabilized perfluoropentane emulsion to deliver Dox to tumors in mice [58, 59]. It was reported that Dox was sequestered inside polymer micelles as well as carried with the emulsion droplets. First, heating was used to show that the droplets

could be vaporized into micrometer-sized bubbles. This was visualized under a microscope. Ultrasound was then used to deliver Dox to tumor cells. Cells exposed to this treatment in vitro showed a higher uptake of Dox compared to negative controls. In vivo, tumors treated with ultrasound did not continue to grow while negative control tumors did grow. Later, this group used perfluoro-15-crown-5-ether (PFCE) to form emulsion droplets stabilized with block copolymers [45]. There was evidence of vaporization of droplets despite the much higher boiling point of PFCE (146°C). While the droplets did vaporize, they did not undergo collapse cavitation. Furthermore, there was evidence that the droplets re-condensed after ultrasound exposure. In contrast, perfluoropentane (PFC5) droplets went through an irreversible phase change and collapse cavitation was detected from the resulting gas bubbles [59]. Droplets were loaded with Paclitaxel and both PFCE and PFC5 emulsions were effective in reducing tumor size when ultrasound was applied [45, 59, 60].

Liquid emulsion droplets have also recently received attention as ultrasound contrast agents due to their echogenicity, and have been used to enhance ultrasonic imaging of vasculature and tissues [61]. Combining their drug carrying potential with their potential in ultrasound or MRI imaging has led to nanoemulsions sometimes being called “theranostics.” In vivo studies have already demonstrated that the drug delivery potential and echogenicity of nanoemulsions can be taken advantage of simultaneously, using emulsions to deliver drugs to a target location while simultaneously imaging the target area and/or the location of the drugs [45].

While emulsion droplets have begun to receive attention as drug-carrying particles, the amount of drug that can be encapsulated is a potential problem. Even hydrophobic drugs tend to accumulate in the surfactant shell rather than in the hydrocarbon phase [60]. The low volume of this shell would limit the amount of drug encapsulated. Dual phase emulsions seem to be

required in order to encapsulate and carry significant amount of drug; emulsions are formed with a perfluorocarbon layer and an oil layer in order to increase encapsulated drug and maintain droplet stability [44, 62]. These emulsions retain the ability to vaporize due to the inclusion of a perfluorocarbon phase, but can also carry increased amounts of drug in the oil phase. However, the threshold for vaporization is increased by the presence of an oil phase [44].

Despite these drawbacks and even though emulsion droplets are less responsive to ultrasound than microbubbles, the combination of ultrasound responsiveness with the potential to persist at nano-scale sizes make them exciting potential drug carriers for ultrasound targeting. The droplets can permeate deep into tissues, followed by activation by ultrasound that could both deliver their drug load and increase cell permeability. It is possible that they could even be endocytosed, and then be excited by ultrasound to create bubbles [46]. This could potentially target drug release not just to within a target tissue, but within targeted cells

2.5 Liposomes

Liposomes are another drug carrier of interest. A liposome is a small spherical vesicle made up of a phospholipid bilayer enclosing a volume of aqueous liquid [63]. These lipid vesicles have been studied for several decades for a variety of uses in medicine, chemistry and biology. They are formed by dissolving phospholipids in an aqueous environment. The strong interactions of the non-polar lipid tails drive the spontaneous formation of spherical bilayer membranes and vesicles [63]. The shape and size of these vesicles can then be altered by freeze thawing, exposure to ultrasound, or by extrusion through membranes. Over the past decade liposomes have been investigated as drug carriers in a wide variety of applications, including transdermal delivery and intravenous delivery of a wide range of therapeutics [63]. After

liposomes reach their target site, release of the drug can be triggered by pH changes, degradation of the liposome by lipases, or simply by slow diffusion through the membrane. In order to increase circulation time in the body, liposomes are often formulated with a small amount of lipid that has polyethylene glycol (PEG) attached to the head groups [64]. The "PEGylation" of the liposomes prevents plasma proteins from binding and subsequent phagocytic recognition and removal of the liposomes [65].

A significant advantage of liposomes is that they can be formed and remain stable at very small (nanometer) sizes. For this reason, they have recently been investigated for use in cancer therapies due to their ability to extravasate via the EPR effect [66, 67]. The EPR effect leads to a high concentration of liposomes in cancerous tissues. When the EPR effect is combined with the high circulation times of PEGylated liposomes, drug delivery to cancerous tumors is significantly enhanced compared to other treatments. For example, Gabizon et al. used PEGylated liposomes to increase the circulation time of Doxorubicin-carrying liposomes [68]. The longer circulation time, together with the EPR effect, led to a 4 to16-fold increase of drug concentration in the tumor compared to free drug delivery techniques. When compared to non-PEGylated liposomes, these long-circulating liposomes were less toxic and demonstrated less accumulation in the liver, a typical accumulation site for standard liposomes.

Liposomes have also been investigated for gene delivery. In such an application, the liposome is usually formed from cationic lipids that will interact with DNA, attracting the negatively-charged DNA to their surface [67]. Koch, et al. formed liposomes using lipids with cationic head groups [69]. These cationic liposomes were incubated with plasmid DNA coding for green fluorescent protein (GFP) to allow the DNA to condense to the outside of the liposomes. Cells were exposed to ultrasound in the presence of these DNA-liposome complexes,

resulting in a significant increase in GFP expression compared to non-sonicated samples. Similarly, polycationic molecules have been complexed with DNA and then encapsulated in liposomes [70]. These liposomes demonstrated an increased ability deliver genetic material to cells compared to the polycation-DNA complexes alone. However, these cationic materials - both polycations and cationic lipids - are typically toxic and the increased toxicity may outweigh their benefits as gene-delivery vectors.

Liposomes have many advantages as drug carriers, including their versatility, biocompatibility, and biodegradability. The lipids that are used to form the liposomes can be custom tailored for a specific application to control the surface charge, chemical properties, rigidity, and stability of the liposome. Furthermore, the hydrophilic interior of the liposome can enclose hydrophilic drugs, while either the non-polar membrane or enclosed micelles or nanoemulsions can sequester hydrophobic drugs. Liposomes have shown the ability to effectively sequester drugs and the ability to release these drugs [71]. Usually, drugs are released from liposomes by allowing diffusion through the membrane or allowing the liposome to be degraded with time [72]. Drug release from liposomes largely depends on the lipid composition of the membrane and its stability. Inclusion of polyethylene (PEG) on the surface of the liposome has been shown to greatly increase the time that the liposomes remain in the body compared to non-PEGylated liposomes or free drug [66, 71]. Another key characteristic of liposomes is the ability to control their size [73], which allows them to be used for "passive" targeting to cancerous tumors via the EPR [74]. This ability to take advantage of the EPR is the most often quoted advantage of liposomes for targeted drug delivery; liposomes are formed at small sizes that allow them to accumulate in tumors, followed by drug release over time as the liposome degrades or as drug diffuses out.

A variety of release strategies have been investigated to further target drug delivery from liposomes and increase their efficiency. Liposomes have been designed with pH-sensitive lipids so that they will open up and release their drug load in an acidic environment [75] as well as with temperature sensitive chemistries so that hyperthermic temperatures can induce release [76, 77]. Liposomes have also been designed to be sensitive to specific enzymes in order to target and control drug delivery [78]. Light has also been explored as a method of releasing contents from liposomes [79]. These techniques have yielded mixed results and have a variety of advantages and disadvantages. Because of its non-invasive nature and ability to control both the location and time of release, ultrasound may prove to be a particularly advantageous method for targeting drug delivery from liposomes. Using this method would allow liposomes to accumulate in tissues, followed by release of the sequestered contents with ultrasound. Because of these advantages, ultrasound-sensitive liposomes have recently received a significant amount of research attention.

One potential problem with using ultrasound to release contents from liposomes is that, unlike microbubbles, they do not inherently respond to ultrasound. Many of the studies investigating ultrasound triggered release have employed high intensities of ultrasound and/or long exposure times. Chen and Wu sonicated nano-scale liposomes with continuous wave 900 W/cm^2 ultrasound at 1.1 MHz [80]. Only 21% of the encapsulated material was released after 10 seconds of ultrasound exposure and only 70% was release after 60 seconds despite the high intensity being applied. As a point of reference, these ultrasound parameters would result in a mechanical index of almost 5. Mechanical indices above 1.9 are not permitted by the FDA for medical applications and diagnostic ultrasound is typically operated at mechanical index values closer to 1. Similarly, Klibanov et al. used short exposures of very intense ultrasound (7 MPa

peak acoustic pressure) to release contents from a liposomal carrier [81]. Despite the intensity of ultrasound only 11-30% of the entrapped material was released.

In addition to high intensities, long exposure times of lower intensity ultrasound have been investigated. For example, Evjen, et al. reported 10% release from conventional PC-based liposomes after 6 minutes of exposure to 40-kHz ultrasound at approximately 2 W/cm^2 (MI = 1.2) [82]. Schroeder, et al. demonstrated 50% and higher release from liposomes exposed to 3.3 W/cm^2 (MI = 2.2) ultrasound at 20 kHz for 1 to 3 minutes [83]. This group also was able to make a connection between liposomal release and cavitation. Below cavitation thresholds, increases in liposomal release were modest, whereas above cavitation thresholds, increases in liposomal release became much more pronounced. It is believed that in order for conventional liposomes to be induced to release their contents with ultrasound, bubbles must nucleate, cavitate and create mechanical shear that disrupts the bilayer membrane of the liposomes [84-87]. This dependence on cavitation has several drawbacks. The high intensities of ultrasound that can be required may damage cells. Furthermore, there is a lack of cavitation nuclei within tissues and even in the blood. Therefore, the dependence on cavitation nuclei may limit the ability of ultrasound to disrupt liposomes deep within tissues, where delivery would be most useful.

There are also other parameters that have an effect on ultrasound-induced release from liposomes. Pong, et al. demonstrated that the size of the liposomes has a significant effect [88]. Liposomes were formed at several sizes and exposed to ultrasound. One-μm vesicles demonstrated 30% release of encapsulated contents after 100 minutes of 1-MHz ultrasound exposure at approximately 7.5 W/cm^2 with a duty cycle of 0.4. 300-nm vesicles demonstrated 20% release after the same amount of exposure and 100-nm vesicles demonstrated almost no release. It has also been shown that the inclusion of PEG-lipids in the membrane increases its

susceptibility to ultrasound [88-90]. More recently, it has been demonstrated that lipid composition has a significant effect on ultrasound mediated-release from liposomes [82, 91-93]. Evjen, et al. compared the release from conventional PC- based liposomes to liposomes containing DOPE or DSPE as their principle constituents [82]. At long exposure times DSPE liposomes demonstrated as much as 5 times more release than phosphocholine based liposomes, and DOPE released 9 times as much. In 20% serum the ultrasound sensitivity of all three formulations was greatly reduced, with only DOPE still releasing a significant amount of drug. Small, et al. similarly investigated the effect of membrane composition on ultrasound-mediated release from liposomes containing various mixtures of DOPE, DPPC and cholesterol [93]. As the concentration of DOPE was increased, the amount of release caused by ultrasound also increased. Increasing the amount of cholesterol decreased the amount of release. Another parameter that has an effect on liposomal release is the frequency of ultrasound applied. It has been shown that lower frequencies of ultrasound release more of the encapsulated materials from liposomes than do high frequencies [88, 92].

While studies have shown that liposomes can be induced to release their contents with ultrasound, the ultrasound parameters required to do so typically require long times and/or high intensities. These parameters can lead to unwanted heating and cell death in healthy tissues. In order to avoid these negative effects, liposomes have been modified to attempt to increase their ultrasound susceptibility while retaining their versatility and ability to deliver drugs. Klibanov, et al. attached small liposomes to microbubbles to increase ultrasound sensitivity [81]. This increased sonosensitivity, but resulted in large complexes and limited the versatility of the liposome. Other groups have also developed liposomes that either encapsulate small bubbles [94] or contain more air than conventional liposomes [95, 96]. These “bubble liposomes” or

"acoustically active liposomes" demonstrate increased release of encapsulated contents compared to conventional liposomes. They have also been used to simultaneously deliver therapeutics and enhance diagnostic imaging, a field that has become known as theranostics. These acoustically active liposomes, however, are typically quite large. While they have significant advantages in combining therapeutics and diagnostics, they cannot take advantage of the EPR effect and would not be internalized into cells. Lastly, increased sensitivity to ultrasound has been achieved by varying the lipid compositions. Liposomes without cholesterol tend to be more susceptible to ultrasound and PEGylated lipids increase sonosensitivity [89, 90]. Replacing conventional phosphocholines with other lipids can also increase sonosensitivity [82, 91-93]. These liposomes, however, are typically more susceptible to ultrasound due to increased membrane permeability and loss of stability that may limit the liposomes' ability to carry and sequester drugs efficiently.

2.6 Liposomal encapsulation

There are a number of techniques that are commonly used to encapsulate materials inside of liposomes. These techniques include passive diffusive, reverse phase evaporation, dehydration–rehydration of preformed empty liposomes, freeze–thaw cycling and pH induced loading [97]. While these common loading techniques typically encapsulate small molecules, it is an additional challenge to encapsulate relatively large emulsion droplets inside of lipid vesicles. One technique that has been used to encapsulate relatively large particles inside of liposomes is sheet formation and refolding [98]. This technique takes advantage of an ethanol-induced phase transition to an interdigitated lipid phase. The addition of short chain alcohols to the liposome suspension causes swelling and separation of head groups as the alcohol interacts

with the polar region of the membrane [99]. As the head groups swell and the distance between lipids increases, the tail groups from opposite sides of the membrane interdigitate, thinning and stiffening the membrane. As the membrane becomes more rigid, its ability to curve into a spherical shape is reduced and liposomes with a higher curvature unfold and fuse into sheets [100]. This transition is observed even at temperatures below the lipid melting transition temperature (T_m) [98]. These sheets remain stable even after the removal of the alcohol if temperature is maintained below the T_m due to the inability of the lipids to move and flow at these temperatures. However, if the temperature is increased above the T_m in the absence of alcohol, the sheets refold into closed vesicles [101]. When the sheets refold into spherical vesicles, even relatively large particles in the solution adjacent to the sheet will be encapsulated inside the newly reformed liposomes. Boyer et al. used this technique to encapsulate small liposomes inside of larger lipid vesicles [102]. Drug was encapsulated in the smaller, inner vesicles. Release of the drug, therefore, required either the gradual breakdown of two membranes or the diffusion of encapsulated drugs through these two membranes for drug release. It was shown that this double encapsulation resulted in a more gradual and sustained release of drug than from conventional single layer liposomes.

2.7 Endocytosis and endosomes

Endocytosis is a process by which many large external molecules, such as proteins and nutrients are engulfed into most living cells. This pathway is commonly used to internalize large molecules or polar molecules that could not otherwise pass through the non-polar interior of the cell membrane bilayer. Depending on the specific situation, including cell type and specific pathway, there can be a wide range of sizes and amount of material endocytosed. Chithrani et al.

used transferrin-coated gold particles with HeLa cells to study clathrin-mediated endocytotic mechanisms in this cell line [103]. It was reported that particles up to 50 nm were endocytosed, but as particle size increased the rate and amount of endocytosis decreased. Rejman et al. studied caveolin-mediated endocytosis in murine B16 cells [104]. Cells were exposed to 50, 100, 200, 500, and 1000 nm latex beads. The rate of endocytosis decreased as the particle size increased, with the smaller sizes of beads being endocytosed by 30 minutes. Endocytosis of the 500 nm beads was detected only after 2-3 hours, and microscopy revealed that although inside the cell, these beads could not penetrate deep-into the cytoplasm. In this study, 1000-nm beads were not endocytosed. Other cell lines, especially fibroblasts and macrophages, have been shown to endocytose or phagocytose particles larger than 1 μm [105, 106]. 3T3 cells may also be candidates for endocytosis of particles up to 3 μm [106].

In all types of endocytosis, the cell membrane extends and surrounds a portion of external media. The membrane then comes together and pinches off to entrap previously external molecules. The new interior vesicle is called an endosome [107]. After an endosome is formed, the pH in this vesicle is lowered initially by actively pumping hydrogen ions inside to help break down and digest newly endocytosed materials [108]. Later, these endosomes will typically fuse with acidic lysosomes to complete digestion of their contents. To be effective, therapeutics that require intracellular delivery, including genetic treatments and many drug therapies, usually must escape from the endosome before they are degraded. Escaping from the endosome is one of the major barriers to effective intracellular delivery.

Because endosomal escape remains a significant challenge for efficient drug delivery, several techniques have been investigated in order to try to increase controllable and efficient endosomal escape. These techniques include pH buffering, pore formation in the endosomal

membrane, fusion with the endosomal membrane, and photochemical disruption of the endosomal membrane.

In the pH buffering technique, or proton sponge effect, molecules with many amine groups are employed. As the amine groups are protonated in the acidic environment of the endosome, there is an influx of protons and other ions (e.g. chloride counter ions) into the endosome, causing an osmotic imbalance. This osmotic imbalance causes the endosome to swell and burst. For example polyethylenimine (PEI) has been investigated as a potential gene carrier and has been shown to increase gene transfection [109]. As a result of this "proton sponge" effect of PEI, it was found that acidification of the endosome is slowed, and more proton pumping is required than usual to lower the pH. In this study, chloride ion concentration inside the endosome also increased beyond normal levels. The osmotic pressure gradient increased as the number of ions inside of the vesicle increased, causing the endosome to swell until it burst, and its contents were released into the cytoplasm [110]. Because of the ability of the "proton sponge" effect to produce escape from the endosome, this technique has received much attention. However, although this technique has proven effective, molecules that are most efficient for the proton sponge effect, such as PEI, are also typically toxic to cells.

Pores can be formed in the endosomal membrane with peptides that have high affinity for the inside of the endosomal membrane [111]. Many of these peptides respond to low pH, which induces a conformation change and insertion into the endosomal membrane. When the peptide is inserted in the membrane it causes a pore to form, and the contents of the endosome are allowed to leak out into the cytosol.

Another method described by Akita et al. employs fusogenic delivery vesicles [70]. After being encapsulated inside of the endosome, these vesicles fuse with the endosomal

membrane, releasing their contents into the cytoplasm. The fusogenic properties of these proteins can be enhanced at low pH so that this release predominates from the endosome [112].

In another method, Fretz and coworkers used saporin-containing liposomes with LumiTrans, a photosensitive agent that localizes to the endosome membrane [113]. Upon illumination, these photosensitive agents generate reactive oxygen species that damage the endosomal membrane, releasing the liposomes into the cytosol.

All of these techniques for endosomal escape have shown some promise. However, there are a number of disadvantages. Many of these techniques involve polymeric materials that are toxic, and most of these methods lack the ability to specifically control the location and rate of release.

2.8 Summary

In summary, there are several techniques that have been investigated in order to enhance targeted drug delivery. These techniques can be classified as either active, passive, or actuated. Active targeting typically refers to the use of chemical receptors, targets, or triggers to enhance site specific delivery. Passive targeting takes advantage of inherent physical properties of a particular tissue, such as a leaky vasculature, to preferentially deliver drugs. Actuated targeting employs the use of an external trigger to release sequestered drugs from drug carriers at the target site. While all of these techniques have shown potential, they have a number of shortcomings. A drug delivery system may be made more efficient by combining several techniques.

The acoustic vaporization of emulsion droplets makes them interesting candidates for employing several targeting strategies simultaneously. The emulsion droplets may act as drug

carriers or may provide an ultrasound sensitive component to other drug delivery systems. Specifically, the goal of this project was to develop a liposomal drug delivery system that would be more useful for actuated targeting. Liposomes are often cited as being very versatile and useful drug carriers; the ability to control the size of the liposomes and functionalize their surface allows them to employ both active and passive drug targeting strategies. When liposomes combine these techniques, their drug-delivery efficiency is increased. However, once liposomes have accumulated at a target site, drug delivery can be dependent on the slow processes of liposomal degradation and/or diffusion of drug out of the liposomes. Liposomes are not inherently responsive to ultrasound. The goal of this research was to explore the potential of using emulsion droplets and liposomes in combination to add an ultrasound sensitive element to the liposomes. The potential of these expanding emulsion droplets to aid in endosomal escape was also explored.

3 OBJECTIVES

The overall objective of this research was to develop a system for gene and drug delivery from nano-scale sized drug carriers that can be triggered by ultrasound, leading to liposomal and possibly endosomal rupture. This will allow treatment to be targeted to a specific area by ultrasound and could provide a new non-toxic method for endosomal escape. The proposed method to add ultrasound sensitivity to the drug carriers is acoustically-induced vaporization of high-vapor-pressure emulsion droplets. The drug carriers that were considered include emulsion droplets as well as combinations of emulsion droplets and liposomes. In order to be effective, the drug carriers should have small enough diameters to be able to take advantage of the EPR effect for anti-cancer applications. The specific goals of this research were:

I. Form emulsion droplets with diameters between 50 – 150 nm. Characterize the droplets and show the potential to vaporize these droplets using ultrasound.
    1. Form perfluorocarbon emulsions using various surfactants and techniques, and compare advantages and disadvantages of these various surfactants and techniques.
    2. Determine size vs surfactant-to-PFC ratio for the various surfactants to minimize droplet size. Control the size of the emulsion droplets down to 50 -150 nm.
    3. Demonstrate that the emulsion droplets can be vaporized with the application of ultrasound and determine vaporization threshold parameters.

4. Explore the ability of vaporizing emulsions to aid in ultrasound-induced drug release from conventional liposomes at low ultrasound intensities.

II. Form and characterize eLiposomes.

1. Form and characterize liposomes with emulsion droplets encapsulated inside.
2. Explore the ability of these eLiposomes to sequester a model drug.
3. Explore ultrasound-mediated release of a sequestered model drug from these eLiposomes upon vaporization of the emulsion droplets. Investigate the effect of particle size, temperature and ultrasound parameters on drug release.

III. Perform preliminary in vitro experiments on cells showing model drug release from eLiposomes using ultrasound.

1. Investigate the ability of cells to endocytose eLiposomes and emulsions.
2. Explore the ability of emulsion droplets to aid in endosomal escape when exposed to ultrasound.
3. Explore the ability of eLiposomes to deliver therapeutics to the cytosol of cells when exposed to ultrasound.

4 MATERIALS AND METHODS

4.1 Materials and equipment

4.1.1 Materials

Perfluoropentane (PFC5) was purchased from SynQuest Labs., Inc. (Alachua, FL). Perfluorohexane (PFC6), and perfluoroheptane (PFC7) were purchased from Sigma-Aldrich (St. Louis, MO, USA). All perfluorocarbons were stored in a freezer until used. Phosphate buffered saline (PBS) solution was purchased from Fisher Scientific (Fair Lawn, NJ). Sodium chloride and dimethyl sulfoxide (DMSO) were purchased from Mallinckrodt (Paris, Kentucky). Sucrose was purchased from Avantor Performance Materials (Phillipsburg, NJ) and glucose form United Biochemical Corp. (Cleveland, OH). Dipalmitoylphosphatidylcholine (DPPC) in chloroform and 1,2-distearoyl-sn-glycero-3-phosphoethanolamine-N-[amino(polyethylene glycol)-2000] (DSPE-PEG2000-amine) were purchased from Avanti Polar Lipids, Inc. (Alabaster, AL). Zonyl® FSN-100 fluorosurfactant was a gift from DuPont. Perfluorooctanoic acid (PFOA), folic Acid and N,N'-dicyclohexylcarbodiimide (DCC) were purchased from Sigma-Aldrich (St. Louis, MO).

Gibco DMEM media, F-12 Nutrient Mixture, RPMI-1640 folate free media, and Fetal Bovine Serum were purchased from Life Technologies (Grand Island, NY). Trypsin for cell passaging was purchased from Invitrogen (San Diego, CA). LysoTracker Red was purchased

from Molecular Probes (Eugene, OR). Calcein was purchased from MP Biomedicals (Solon Ohio, USA).

All water used was double distilled. Calcein was dissolved in water by slowly adding NaOH to raise the pH until the color of the solution changed from light orange and cloudy to a deep red, indicating dissolution. Additional water was added to the solution to dilute the calcein concentration to 30 mM. Chloroform was evaporated away from the DPPC using a Rotovap, and DPPC-in-water solutions were prepared at 30 mg/mL by film hydration. Water used in acoustic measurements was de-gassed prior to experiments by boiling the water and exposing it to low pressure in a vacuum oven.

4.1.2 Ultrasound equipment

A 3-mm-diameter 20-kHz ultrasound probe driven by a Vibra-Cell VCX400 (Sonics and Materials, Newton, CT) was used to form and shear emulsion and liposomes samples. This same probe setup was used to perform 20-kHz release experiments. Ultrasound intensity was previously calibrated in degassed and deionized water using a low frequency hydrophone (Model 8103, Bruel & Kjaer, Naerum, Denmark). For this calibration, the hydrophone was positioned 3 mm from the transducer and connected to an oscilloscope. The hydrophone voltage signal was converted into intensity (W/cm^2) values using the factory calibration parameters.

525 kHz experiments were performed with a focused transducer (Sonic Concepts, Woodinville, WA). The signal was generated with an HP 33120A waveform generator and amplified with an Electronics and Innovation power amplifier (model 2100L). The amplified signal was passed through an external switch, an oscilloscope (Tektronix TDS 2014), and a matching network prior to the transducer. A needle hydrophone (HNR-1000, ONDA Corp.,

Sunnyvale, CA) had been used previously to determine the location of the focus of the transducer and to create an intensity calibration at the focal point. The same hydrophone and oscilloscope were used to collect acoustic emissions from emulsion samples.

4.1.3 Dynamic light scattering

Particle sizes of emulsions, liposomes and eLiposomes were determined by dynamic light scattering (DLS) using a *Brookhaven 90Plus* Particle Sizer (Brookhaven Instruments Co., Holtsville, New York). Samples were prepared at concentrations to give 800 kcounts/second to 1.2 Mcounts/second. Ten experimental runs of 1 minute each were performed on each sample and averaged.

4.1.4 TEM microscopy

Samples were viewed and imaged using several TEM techniques. Samples were viewed by negative staining on an FEI Tecnai 12 transmission electron microscope (Hillsboro, Oregon, USA) on continuous carbon grids using a Gatan single-tilt sample holder. Samples were prepared for cryoTEM on 200-mesh copper (holey-carbon) grids. Grids were plunge frozen in liquid ethane using a FEI Vitrobot. The samples were then viewed on an FEI Tecnai F30 transmission electron microscope (Hillsboro, Oregon, USA) using a Gatan 626 cryoholder. Negative staining and cryoTEM images were recorded on Gatan 1024 × 1024 CCD cameras.

4.1.5 Fluorometry

A QuantaMaster fluorometer (Photon Technology International, Birmingham, New Jersey) was used for calcein release experiments. The excitation and emission wavelengths were

set to 488 nm and 525 nm, respectively. The apertures were adjusted to limit the fluorescent counts per second (cps) to less than 1,000,000 in order to avoid damaging the detector. Experiments were typically run closer to 100,000 cps. Because the aperture openings were not precise, they were adjusted only when necessary in order to remain consistent from one experiment to the next. Data was collected at 4 points/second and exported to Microsoft Excel for analysis.

4.1.6 Fluorescent and confocal microscopy

An Olympus IX70 microscope using a 40X objective microscope was used to view emulsion samples before and after exposure to ultrasound. This microscope was also used for initial experiments with cellular calcein delivery and fluorescence. Intracellular uptake of calcein into HeLa cells was verified using an Olympus FluoView FV300 confocal laser scanning microscope. An argon laser with an excitation wavelength of 488 was used to visualize calcein within the cells. A red helium-neon laser was used to view LysoTracker Red dye within the cells.

4.2 Methods and procedures

4.2.1 Emulsion formation

Two different methods were used to form and stabilize perfluorocarbon emulsions with PFC5 and PFC6: shaking and sonication. To form emulsions by shaking, the desired amount of PFC, surfactant and water was added to a crimp-top vial. In order to exclude all air from the vial, it was prepared in a water bath. The cap was carefully placed on top crimped while the vial was submerged. In order to form the emulsion, the vial was then shaken on a COE Mix 5000

High Speed Mixer (GC America Inc., Alsip, IL) at 4200 cycles per second for two 30-second intervals.

Sonicated emulsion samples were prepared by adding the desired amount of PFC, surfactant, and water to a plastic cuvette. Typically, 0.1 to 0.2 g of PFC was added along with 1.5 mL of water, while the amount of surfactant was varied. The sample was cooled on ice and the 20-kHz ultrasound probe was inserted directly into the cuvette. The sample was sonicated while still on ice for the desired amount of time. Ultrasound parameters and the time of sonication were varied. During the beginning of sonication, care was taken to move the probe tip into the corners of the cuvette to ensure mixing and suspension of the PFC phase.

For experiments that required large emulsion droplets, low intensities (0.5 W/cm^2) were used and no further processing was required. Slightly higher intensities (1 W/cm^2) were used to form smaller emulsions. After nanoemulsion formation, droplet size of some samples was further reduced by extrusion through a 100-nm or a 50-nm polycarbonate filter using an Avanti Mini Extruder (Alabaster, AL, USA). The extrusion was carried out at 50°C by placing the extrusion apparatus on a temperature controlled heating block for 10 minutes prior to extrusion. After heating, the emulsion was passed through the filter 15 times. The syringes were removed from the heating block and allowed to cool prior to removing the emulsion sample.

4.2.2 Verification of vaporization

Ultrasonic vaporization of emulsion droplets was verified by applying ultrasound to the emulsion sandwiched between a microscope slide and cover slip at room temperature (24°C). 100 µL of emulsion was diluted in 1 mL of water. The diluted emulsion was viewed with an Olympus IX70 microscope using a 40X objective. The slide was then inverted and exposed to 1

W/cm^2 ultrasound for 5 seconds by applying a small amount of ultrasound gel to the slide and positioning the 20 kHz transducer directly into the gel. The slide was again imaged after ultrasound exposure. Control experiments were performed using plain water and a DPPC lipid solution to verify that bubbles were not formed in the absence of PFC emulsion.

This experiment was repeated at 37°C. Heating was performed in a 37°C incubator. In order to test the amount of time required for heating, a thermocouple was used to measure the temperature of the liquid film on the slide and a similar volume of water prior to experiments. Slides were prepared with diluted emulsions and were viewed after preparation, followed by 5 minutes of heating in the incubator at 37°C. The samples were then removed from the incubator and imaged quickly to observe any effects from heating. After heating again, ultrasound was applied to the slide as described above and the slide was imaged again.

Vaporization of emulsion droplets was further verified by collecting the acoustic spectra created by emulsion samples and controls when exposed to an ultrasonic field. Various acoustic signatures have been correlated with cavitation of entrained bubbles. The acoustic signal can be Fourier-transformed, with key peaks of the resulting spectra providing clues about what is happening when emulsion droplets are exposed to an acoustic field. The applied frequency, f, is expected to be the strongest peak on the spectrum. As the intensity is increased, peaks at higher harmonic frequencies (2f, 3f, 4f...) and at the subharmonic (f/2) frequency have been linked to stable cavitation [114-117]. Subharmonic frequencies and a non-frequency dependent increase of broadband sound have been linked to collapse cavitation [21, 118, 119]. For this reason, the emergence of harmonic peaks, subharmonic peaks, and a broadband baseline shift were identified as phenomena of interest.

Control and emulsion samples were placed in the bulb tip of a transfer pipette. This bulb was positioned in the focal point within the water bath on the 500 kHz insonation chamber. A hydrophone was positioned at a 90 degree angle to the sample chamber about ½ an inch away. The intensity of ultrasound was increased gradually while observing for the emergence of the key spectral phenomena on an oscilloscope. Some samples were heated by circulating 37°C water into the water bath with a Neslab RTE 110 temperature bath/circulator. Water was filtered between the temperature controller and the water bath containing the transducer to minimalize the introduction of bubbles into the bath.

4.2.3 Lipid sheet formation

DPPC liposomes were prepared using a standard film hydration technique. Briefly, DPPC in chloroform was added to a round bottom flask. The solvent was removed under vacuum with a rotary vacuum evaporator, leaving a thin dry lipid film on the flask. This film was hydrated in water to a lipid concentration of 30 mg/mL. The mixture was heated to 60°C while being stirred in the rotary evaporator for 10 minutes or until the majority of the lipid was suspended. If necessary, the solution was re-pipetted and stirred again to suspend remaining lipid. Small unilamellar vesicles (SUVs) were formed from the resulting lipid solution using two methods: extrusion and sonication. For extrusion, the hydrated lipid solution was extruded 10 times through a 50-nm filter at 50°C using the Avanti Mini Extruder. Alternatively, SUVs were also prepared by sonicating the 30 mg/mL DPPC solution at 1 W/cm^2 for 15 minutes, or until the color had changed to a translucent bluish. The sizes of the resulting SUVs were verified by DLS before proceeding. If necessary, the solution was allowed to cool and was sonicated again.

The resulting vesicles from both methods ranged in size from 30 to 80 nm in diameter as measured by DLS. SUVs prepared by extrusion were typically larger (60-80 nm), but had a narrower size distribution and less variability. Sonicated samples could be formed at smaller diameters, with median sizes as small as 30 nm. However, sonicated samples typically had a wider size distribution and median diameters were less consistent from one sample to the next. Despite increased variability and typically broader size distributions, sonication was able to form SUV's of smaller sizes with more ease than extrusion and median sizes were never larger than 50 nm after two periods of sonication. Both sonication and extrusion proved effective in forming small enough vesicles for sheet formation.

Interdigitated DPPC sheets were formed by adding ethanol dropwise to DPPC SUVs while stirring. Ethanol was added to a total concentration of 3 M. As the ethanol was added, the solution changed from translucent pale blue to opaque white and showed an increase in viscosity as the SUVs opened into lipid sheets [98, 120].

The sheets were suspended and diluted in 50 mL of water at room temperature and centrifuged at 1800 x g for 3 minutes, resulting in a large pellet of DPPC sheets. The alcohol-rich supernatant was removed and the pellet was re-suspended in water and centrifuged again to reduce the ethanol concentration to less than 10 mM. The pellet was again suspended in a small volume of water in order to transfer the sheets to microcentrifuge tubes with 10 mg of DPPC allotted to each tube. The extra water was removed through one more cycle of centrifugation. If necessary, the interdigitated sheet phase was stored at 4°C. Lipid sheets remained stable for several weeks if the temperature was maintained below the melting transition temperature (T_m) for DPPC (41°C).

4.2.4 eLiposome vesicle formation

eLiposomes were formed by adding 0.2 mL of PFC emulsion to the interdigitated sheets along with 0.2 mL of water (for TEM imaging) or of a 30 mM calcein solution (for release experiments). This solution was re-pipetted and briefly vortexed to ensure complete mixing of the sheets and the emulsion droplets. The solution was then heated to 50°C and stirred with a magnetic stir bar for 30 minutes, allowing the sheets to fold back into vesicles, trapping some nanoemulsion droplets inside (see Figure 1). The resulting eLiposomes were reduced in size by extrusion through an 800 nm polycarbonate filter at 50°C using the Avanti Mini Extruder.

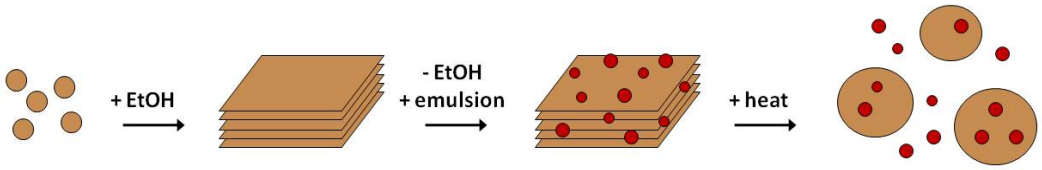

Figure 1. Schematic of the formation and refolding of DPPC sheets to form eLiposomes. The brown circles on the left represent small DPPC vesicles. These vesicles were unfolded into sheets with the addition of ethanol. Excess ethanol was removed by centrifugation and emulsion droplets (represented by small red circles) were added to the sheets. Sheets were refolded into closed vesicles with the addition of heat, and neighboring emulsion droplets were encapsulated inside.

Empty eLiposomes, or liposomes refolded from interdigitated sheets without emulsion present, were prepared as a negative control. The same method used to form the eLiposomes was employed, but emulsion was replaced with an NaCl solution, creating empty lipid vesicles as an analogous negative control.

4.2.5 Calcein encapsulation and separation

Calcein-containing samples were prepared for quantification of leakiness and ultrasound-induced release. During vesicle formation, calcein was encapsulated inside of the eLiposomes at a concentration of approximately 15 mM by adding a 30 mM calcein solution to the solution of sheets and emulsion droplets. At this concentration, the calcein was self-quenched. The external calcein concentration was reduced by allowing the sample to settle at the bottom of the microcentrifuge tube for a few hours. Due to their relatively high density, the vesicles settled to the bottom of the tube in a thick gel-like phase. The top vesicle-free layer was removed and the samples were resuspended in a NaCl solution with the osmolarity matched to the calcein solution inside of the eLiposomes. This created samples with concentrated calcein inside of the eLiposomes and dilute calcein on the outside. Osmolarity of calcein solutions was measured using a vapor pressure osmometer (Wescor Vapro 5520) in order to match this osmolarity with NaCl.

For some experiments, conventional liposomes were prepared by thin film hydration followed by extrusion through a filter with the desired pore size. Due to the lack of a large density difference between conventional liposomes and water, settling was not always adequate to remove external calcein. In these cases, external calcein was removed by centrifugation through PD-10 spin columns (GE Healthcare Biosciences, Pittsburgh, PA). Briefly, the column was prepped by adding 1-2 mL of buffer solution and spun for 2 minutes at 800 x g. The liposome solution was then added to the column and it was again centrifuged at 800 x g for 1.5 minutes.

4.2.6 Purification by sucrose cushion

Some samples were further purified by centrifugation on a "sucrose cushion" to remove unencapsulated emulsions and additional external calcein from the eLiposomes. Sucrose and NaCl solutions were prepared to match the internal osmolarity of the eLiposomes. The mixture of eLiposomes containing unencapsulated emulsion droplets was added to the bottom of a 1.5 mL microfuge tube. Approximately 0.4 mL of the NaCl solution was added to the microcentrifuge tube. Then, using a glass Pasteur pipette, approximately 0.4 mL the sucrose solution was gently pipetted to the bottom of the microcentrifuge tube, underneath the NaCl layer. As the sucrose layer was added, the salt layer was forced up, creating two distinct phases of different densities. The sucrose had a density of 1.12 g/cm^3 and the NaCl solution had a density of 1.02 g/cm^3. The sample was centrifuged for 10 min at 3000 rpm (504 g) using a fixed rotor centrifuge (Eppendorf 5415 C, Hauppauge, NY). Upon centrifugation, free emulsion droplets collected at the bottom of the sucrose layer due to their relatively high density (1.67 g/ cm^3 for PFC6 and 1.63 g/ cm^3 for PFC5). The eLiposomes, with an average density of approximately 1.05 g/ cm^3, would gather at the interphase between the sucrose and salt layers. This interphase layer was then carefully removed from the top to bottom with a pipette.

This sucrose cushion technique was also used to verify the presence of emulsion droplets in various samples. The emulsion samples were added to the NaCl phase. The tube was then centrifuged and examined to determine if a pellet had collected at the bottom of the sucrose phase, indicating the presence of emulsion droplets.

4.2.7 TEM microscopy

Some samples were imaged by cryogenic transmission electron microscopy (cryoTEM). A few μL of solution were placed on a holey-carbon-coated copper grid. The grid was then blotted with filter paper and plunge frozen in liquid ethane with an FEI Vitrobot (Hillsboro, Oregon, USA). Frozen grids were stored in liquid nitrogen until transferred to a Gatan 626 cryoholder (Pleasanton, California, USA), which maintained the samples at approximately −180°C during imaging. CryoTEM images were recorded at 300kV on an FEI Tecnai F30 transmission electron microscope. To improve contrast, the objective lens was under-focused by several micrometers and images were recorded on a Gatan 1024 × 1024 CCD camera.

Some samples were also imaged by TEM using negative staining. The sample was placed on a continuous carbon-coated copper grid and allowed to settle for 20 seconds before being blotted away by filter paper. After rinsing the grid by placing it on a large drop of water for 2-3 seconds, a uranyl acetate solution was added to the grid for 20 seconds before the solution was blotted away and the grid was allowed to dry. Negative staining images were recorded at 120 kV on an FEI Tecnai 12 transmission electron microscope with a Gatan 1024 x 1024 CCD camera.

4.2.8 Calcein release

A correlation of calcein fluorescence versus concentration was prepared for the QuantaMaster fluorometer by varying the concentration of calcein (see Figure 2). At concentrations below 8 μM calcein, the plot of fluorescence intensity versus calcein concentration is linear. At concentrations above 500 μM the fluorescence of calcein is essentially completely self-quenched.

Samples of eLiposomes were prepared in order to take advantage of the two extremes of this fluorescence curve. eLiposome samples containing self-quenched (15 mM) calcein were diluted by adding 20 µL of sample to a disposable UV/VIS-range cuvette with a 10 mm path length (Fisher Scientific cat# 14-995-130). Two (2) mL of NaCl solution were added to the cuvette to achieve a target external calcein concentration of 1 to 5 µM in order to operate in the linear region of the concentration curve for calcein. The resulting eLiposomes had very concentrated encapsulated calcein that would not contribute to the overall solution fluorescence until released and an external solution with fluorescence in the linear range for calcein. Standards were prepared at 1 µM and 5 µM to test the fluorescence emission (counts/second) expected for the target concentration range in order to verify that experiments were being run within these concentrations.

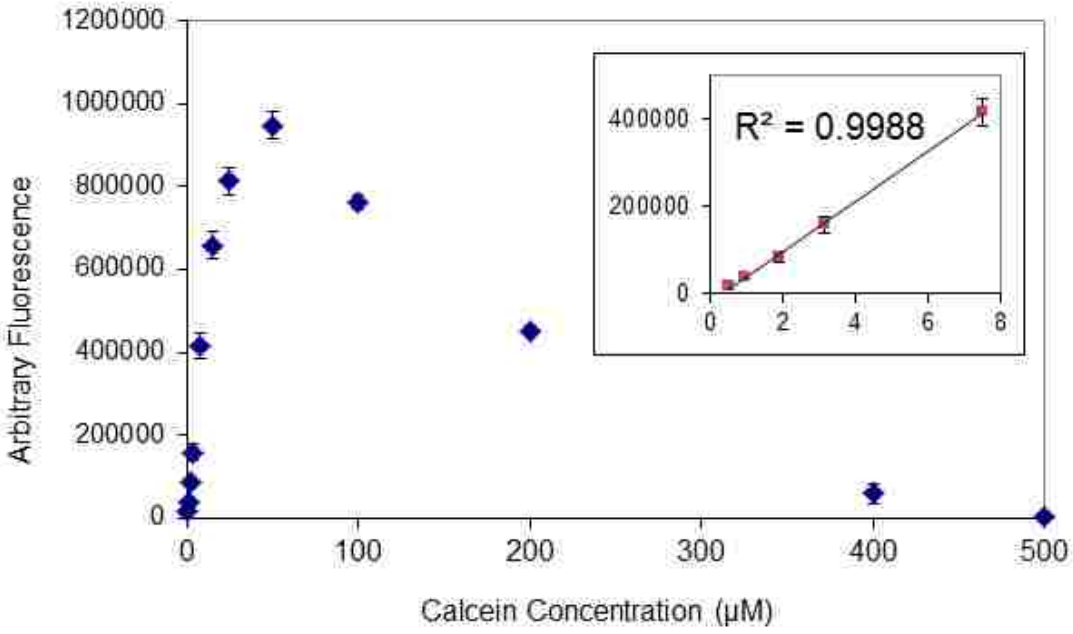

Figure 2. Plot of fluorescence versus calcein concentration in the fluorometer. The insert shows the low end of the plot; below approximately 8 µM fluorescence and calcein concentrations demonstrate a linear relationship. At concentrations above approximately 500 µM, fluorescence is essentially completely self-quenched.

For release experiments, baseline fluorescence data was collected for 10 seconds at 4 data points per second. The cuvette was then removed from the fluorometer and ultrasound was applied to the sample. As concentrated (self-quenched) calcein was released from the interior of the eLiposomes into the surrounding solution, it was diluted below its self-quenching concentration. Fluorescence was again measured after sonication. Finally 25 μL of 5% Triton X-100 was added to lyse any remaining liposomes and a final fluorescence was measured. Because experiments were performed at concentrations within the linear range of the fluorescence versus concentration plot, percent release of calcein could be determined using the following equation:

$$\%\ Release = \frac{f_{US} - f_i}{f_{full} - f_i} \cdot 100\% \quad (2)$$

where f_i is initial fluorescence, f_{US} is the fluorescent signal after sonication, and f_{full} is the fluorescence after complete calcein release using Triton X-100. Each value was determined by averaging 30 fluorescence data points. Release experiments were performed on eLiposome samples and empty control liposome samples. Experiments were also performed on empty control samples mixed with emulsion droplets after the formation of the control vesicles, such that the emulsion droplets were external to the liposomes instead of internal.

For exposure to 20-kHz ultrasound, a 3-mm transducer was inserted directly into the cuvette. For exposure to 525-kHz ultrasound the sample was transferred to the bulb of a 3-mL transfer pipet. The pipet bulb was then positioned in a water bath at the transducer's focal point. After ultrasound exposure, the sample was transferred back to the cuvette to record fluorescence after ultrasound and after the addition of Triton X-100.

4.2.9 Incorporation of folate into eLiposomes and emulsions

Folate was attached to DSPE-PEG2000-amine using techniques that had previously been established [121]. Briefly, folic acid was dissolved in dimethyl sulfoxide (DMSO). DSPE-PEG2000-amine and N,N'-dicyclohexylcarbodiimide (DCC) in pyridine were added to the solution. The reaction flask was shielded from light and the reaction was allowed to proceed under nitrogen. After 4 hours, the pyridine was removed by evaporation and water was added. Unreacted folic acid, byproducts, DCC, and DMSO were removed using a 3500 molecular weight cut-off dialysis bag. A drop of hydrochloric acid was added to the aqueous phase to protonate the product to make it more soluble in chloroform. The DSPE-PEG2000-folate was then extracted by adding an equal volume of chloroform. During this extraction, the folate shifted from the aqueous phase to the chloroform phase, as observed by the chloroform becoming yellow in color. Chloroform was evaporated to isolate the folate-conjugated lipid. Attachment of the folic acid to DSPE-PEG2000-amine was confirmed by NMR [122].

Micelles were prepared by dissolving 2 to 6 mg of DSPE-PEG2000-folate in 0.6 mL of DMSO, followed by the addition of 5.4 mL of water. The resulting solution was dialyzed against water using a 3500 molecular weight cut off dialysis bag to remove the DMSO. The original dialysate was replaced after 4 hours; then dialysis was continued overnight.

Folate was added to eLiposomes to a concentration of approximately 1.2 mol% by adding DSPE-PEG2000-folate micelles to a previously prepared sample of eLiposomes in a 1.5 mL Eppendorf tube. The micelles were allowed to incubate with the eLiposomes for at least 1 hour to allow lipid interaction and transfer [10, 122, 123]. For in vitro experiments with only emulsion, folate was added to the surface of emulsion droplets by mixing DSPE-PEG2000-folate with the DPPC prior to emulsion formation by sonication.

4.2.10 Cell culturing and ultrasound exposure

HeLa (CCL-2™) cells were grown in DMEM (Sigma Aldrich) media supplemented with 10% fetal bovine serum (FBS). Trypsin was used to passage and split the cells; the cells used in experiments were passaged less than 20 times. Cells were grown in 12-well plates and media was changed to folate-free media 48 hours prior to the addition of eLiposomes or emulsions. 200 μL of eLiposome sample or emulsion was added to each well and allowed to incubate for 2 hours before application of ultrasound. Prior to ultrasound exposure the cells were washed two times with PBS. Ultrasound was applied to the cells by adding 3 mL of media to the wells and inserting the 3-mm diameter 20-kHz ultrasonic probe directly into the culture wells with the tip approximately 2 cm above the cell monolayer. Ultrasound was applied at 1 W/cm^2 for 2 seconds. After sonication, the media was removed from all of the wells. 200 mL of fresh media or PBS was added to the wells and cells were removed from the surface with a cell scraper. Cells were stored on ice until viewed with the confocal microscope. Fluorescence intensity in the cells was measured using ImageJ software.

5 PERFLUOROCARBON EMULSIONS

5.1 Theory

Emulsions are formed when two immiscible liquids are combined in a single container and agitated such that a dispersed phase of small droplets is suspended within the continuous phase. Because the two phases are inherently immiscible, the resulting emulsion can be unstable and susceptible to the phases re-separating. Emulsions can also be susceptible to droplet coalescence. In order to overcome the challenges of emulsion instability, emulsion droplets are typically stabilized with surfactants. In general, more surfactant added to the solution can lead to the stabilization of smaller droplets, up to a certain limit. This limit is controlled by the ability of the surfactant to pack into a highly curved surface.

This study investigates emulsions of perfluorocarbon in water. Perfluorocarbons offer the intriguing possibility of ultrasound-induced phase change from liquid to vapor due to the relatively high vapor pressures of these liquids (see Table 1). As mentioned in Chapter 2.1, ultrasound is defined as cyclic pressure waves. During the low-pressure phase of an ultrasound wave the local pressure can drop below the vapor pressure of the liquid emulsions, creating a thermodynamic potential to vaporize and form bubbles.

Table 1. Normal Boiling points and Vapor Pressures of various perfluorocarbons. Values were obtained from the DIPPR database.

	Normal Boiling point	Vapor Pressure at 24°C	Vapor Pressure at 37°C
Perfluoropropane (PFC3)	-37°C	862 kPa	1,213 kPa
Perfluorobutane (PFC4)	-1°C	261 kPa	387 kPa
Perfluoropentane (PFC5)	29°C	84 kPa	135 kPa
Perfluorohexane (PFC6)	57°C	28 kPa	48 kPa
Perfluoroheptane (PFC7)	82°C	10 kPa	18 kPa

For several PFCs, the difference in vapor pressure and atmospheric pressure that must be overcome to induce vaporization is small enough to be achieved at reasonable ultrasound intensities, making them potential candidates for this strategy. The ideal choice should be liquid at temperatures of interest, but have vapor pressures that are relatively close to atmospheric pressure. For example, perfluoropentane has a relatively high vapor pressure at room temperature, and perfluorohexane has a high vapor pressure at biological temperatures, making these two liquids interesting for drug delivery applications. Nano-sized vaporizing emulsion droplets could penetrate deep into tissues due to their small size and then be induced to form bubbles for cavitation. This would retain the advantages of microbubbles (ultrasonic cavitation) while overcoming some of their shortfalls (large size). The cavitating bubbles could increase cell permeability and/or activate drug release from the emulsion droplets or from other carriers such as liposomes or micelles.

Besides vapor pressures and boiling points, another interesting factor that affects ultrasound-induce vaporization of emulsions is the Laplace pressure imposed at a curved phase boundary. Laplace pressure is the pressure difference between the inside and the outside of a bubble or droplet caused by surface tension at the interphase and the curvature of the interface. For a spherical interface, the Laplace pressure is defined as

$$P_{Laplace} = \frac{2 \cdot \gamma}{r} \quad (3)$$

where γ is the interfacial energy of the droplet/water interface and r is the radius of the droplet. The pressure on the interior of an emulsion nanodroplet is therefore the sum of the environmental pressure and the Laplace pressure, or:

$$P_{inside} = P_{\infty} + \frac{2 \cdot \gamma}{r} \quad (4)$$

where P_{inside} is the pressure inside of the droplet, P_{∞} is the local pressure of the continuous water phase. The difference between this pressure inside of the droplet and the liquid vapor pressure of the emulsion droplets is the reduction in local pressure that must be imposed by ultrasound in order to provide a driving force for vaporization.

Therefore, there are two competing effects when considering emulsion droplets for ultrasound-induced drug delivery. Small droplets are desired in order to allow extravasation into tissues. However, as the size of the emulsion droplet decreases, the Laplace pressure increases and the amplitude of ultrasound required to vaporize the droplet increases substantially.

Equation 2 helps elucidate the importance of the surfactant used to stabilize an emulsion. The surfactant stabilizes the droplets and reduces the interfacial energy, γ; therefore, surfactants that are efficient at reducing interfacial energy will result in less additional pressure on the droplet. This, in turn, translates to the ability to vaporize the droplet at relatively mild ultrasound intensity. The Laplace pressure across the interface of the nanoemulsions can be estimated by using the interfacial tension reported for other perfluorocarbon emulsions stabilized with

phosphocholines [124]. Interfacial tension for a PFC droplet in water stabilized with DPPC can be estimated to be about 4 mN/m.

The Laplace pressure imposed on emulsion droplet is intriguing for another reason. The additional pressure imposed on emulsion droplets effectively raises the boiling point of small droplets above their normal boiling point, allowing them to remain in the liquid phase well above biological temperatures [53, 56]. The Antoine equation can be used to predict and plot temperatures at which droplets will boil as the diameter decreases [56, 60]. Figure 3 demonstrates the estimated boiling point of emulsion droplets for several perfluorocarbons as a function of droplet diameter. Antoine equation constants for perfluorocarbons were obtained from the National Institute of Standards and Technology database [125].

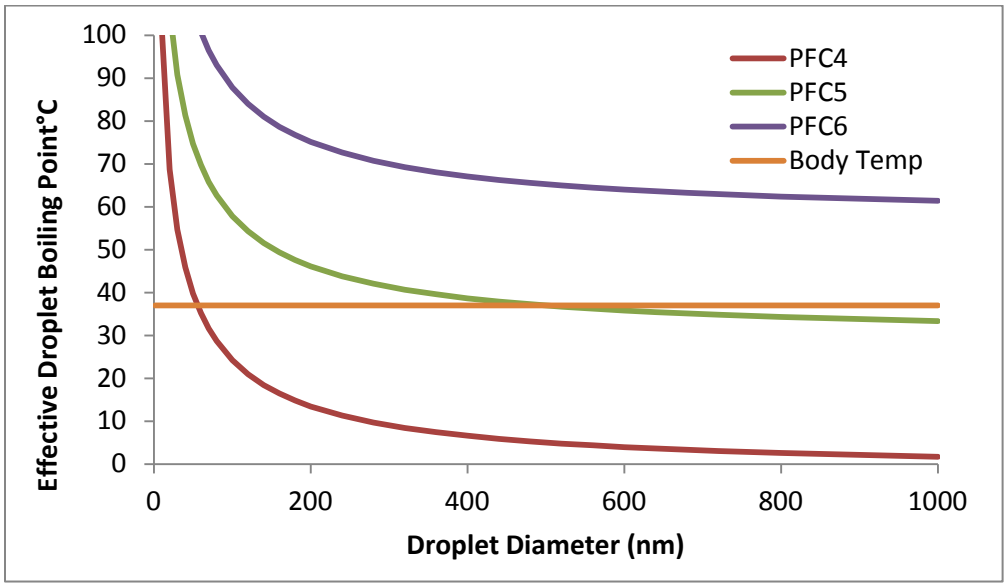

Figure 3. Predicted boiling points for emulsions formed from perfluorobutane (PFC4), perfluoropentane (PFC5), and perfluorohexane (PFC6) as a function of diameter using the Antoine Equation. Body Temperature (37°C) is also included as a point of reference.

Although the normal boiling point for PFC5 is less than body temperature, the effective boiling point of droplets exceeds the 37°C for droplets smaller than about 500 nm in diameter due to the Laplace pressure across the interphase. Therefore, if emulsion droplets can be formed from PFC5 at small sizes (for example, at low temperatures), the resulting emulsion droplets will be below their effective boiling point, even if heated to 37°C. This technique could create metastable PFC5 emulsion droplets until disrupted by ultrasound. With surfactants that result in a higher interfacial energy, it may possible to employ perfluorocarbons with an even lower boiling point such as PFC4 [56].

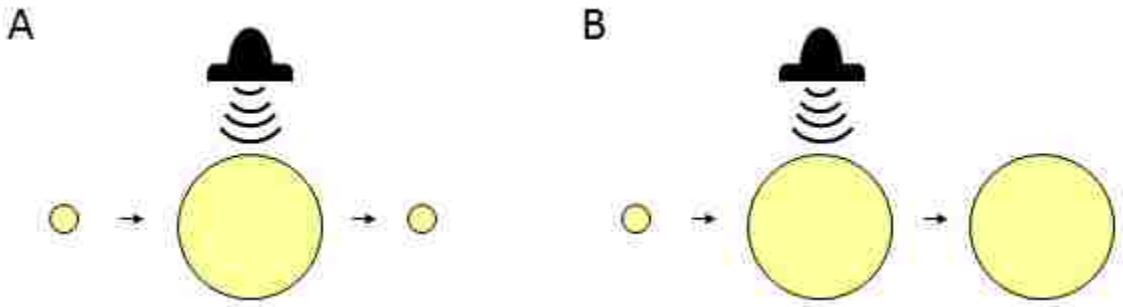

Figure 4. Two possible scenarios of ultrasound induced phase change. Droplets may vaporize during the negative phase of ultrasound, but re-condense after the ultrasound has been removed (A). This situation is likely with perfluorocarbons with high boiling points. It is also possible that perfluorocarbon emulsions could vaporize and then remain as microbubbles, even after the ultrasound field has been removed (B). This scenario is likely in the case of metastable droplet formed from liquids with low boiling points.

The ability to form metastable emulsion droplets allows the conceptualization of two scenarios for droplet vaporization (see Figure 4). For perfluorocarbon liquids that have boiling points that are higher than the temperature of the continuous phase (for example, PFC6 at 37°C or PFC5 at 24°C), droplet vaporization will be reversible, and the perfluorocarbon bubble may be able to condense back into a liquid droplet when the ultrasound is removed (Figure 4A). However, perfluorocarbon liquids that have a boiling point that is lower than the temperature of

the continuous phase (such as PFC5 droplets at 37°C) may form metastable droplets, and vaporization will be irreversible as the Laplace pressure holding the droplet in the liquid phase has been reduced (Figure 4B). This irreversible phase change would create a persistent oscillating bubble. These two scenarios each have advantages and disadvantages. In the case of reversible vaporization, the droplets could re-condense after ultrasound exposure, which may allow them to be more readily cleared from the physiological system and avoid potential embolism. Irreversible vaporization, however, will have lower ultrasound thresholds for vaporization, and the resulting bubbles may provide more efficient cavitation nuclei.

Lastly, it is likely that the ability of a vapor phase to nucleate may play a significant role in the ultrasound-induced phase change of emulsion droplets. Even when the rarefactional phase of ultrasound may overcomes the Laplace and vapor pressure of the droplet and provides a thermodynamic potential to vaporize, this process may not be instantaneous. The rate at which the vapor phase can form may limit the potential of a short ultrasound phase to vaporize the droplets.

5.2 Emulsion droplet formation

5.2.1 Shaking versus ultrasound

DPPC, Zonyl (a commercially available fluorosurfactant), and perfluorooctanoic acid (PFOA) were explored as surfactant options for stabilizing emulsion droplets. PFC6 was used in preliminary experiments to compare the ability and efficiency of these surfactants when forming emulsions. Emulsions were formed by sonication with a 20-kHz ultrasound probe and with mechanical shaking using a high speed mixer. Concentrations of approximately 10 mM of each surfactant were used in these comparisons. All three candidates demonstrated the ability to

stabilize droplets. PFOA and DPPC demonstrated the ability to stabilize emulsions formed by mechanical shaking. The median diameter of these emulsions was typically between 250 and 400 nm. Zonyl, however, was not able to sufficiently stabilize droplets formed by shaking; the mixture in the vial initially went cloudy and white, indicating mixing of phases and droplet formation during shaking, but the water and perfluorocarbon phases separated within minutes after shaking had stopped.

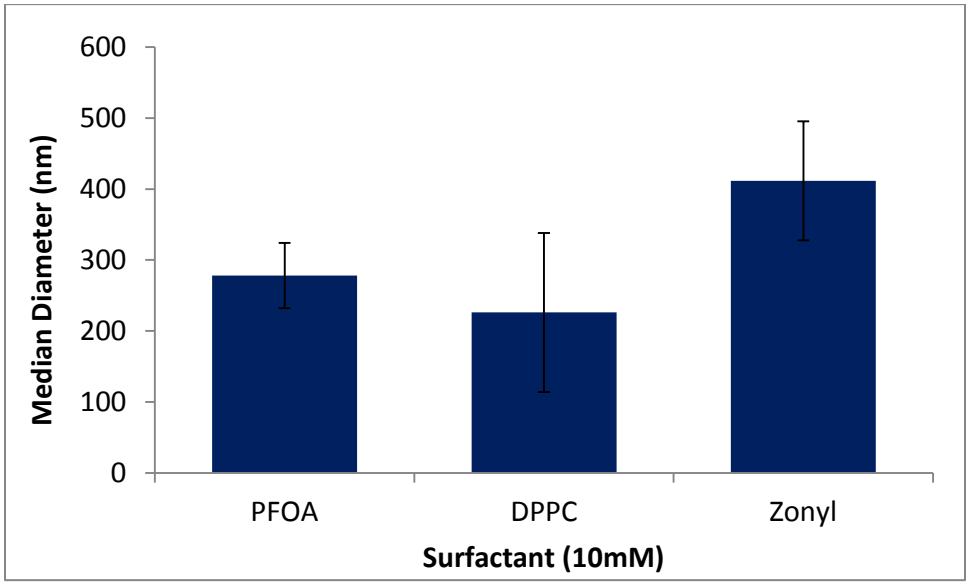

Figure 5. Median diameters of emulsion samples when prepared with ultrasound. Samples were chilled on an ice bath and exposed to 20 kHz ultrasound for 4 minutes at 1 W/cm^2. Error bars represent ± 1 standard deviation (n=10).

Ultrasound was also explored as a method for forming emulsions. As with shaking, emulsions were prepared with a concentration of approximately 10 mM of surfactant. Water, PFC, and surfactant were added to a cuvette and the solution was cooled on an ice bath for several minutes to avoid vaporization of the PFC phase during sonication. The chilled solution was sonicated on an ice bath for 4 minutes at 1 W/cm^2 via a 20-kHz probe inserted directly into

the cuvette. Each surfactant was tested 10 times at these conditions. Zonyl, PFOA, and DPPC all demonstrated the ability to stabilize PFC6 emulsions. However, there was a large amount of variation in median emulsion size from one sample to the next despite being prepared in the same way. Typical median diameters of the resulting solutions were between 250-450 nm with Zonyl and PFOA and were between 150-400 nm with DPPC (see Figure 5). While it was promising that various surfactants were able to form stable emulsions, these median sizes were larger than desired. Furthermore, the wide distribution of sizes would make it difficult to produce emulsion samples that would be consistent and repeatable enough for use as drug delivery vehicles.

The ability to stabilize more concentrated emulsions was tested for both the shaking and ultrasound methods. As the amount of perfluorocarbon was increased from 0.1 g per 1.5 mL of water to 0.2 g per 1.5 mL of water, shaking became less efficient in forming the emulsions. With the higher amounts of PFC6, emulsions were not adequately formed and stabilized by shaking and the water and PFC phases separated shortly after shaking. Ultrasound was still able to form stable emulsions even with the increased concentration of PFC6. For the remainder of the project, ultrasound was chosen as the technique for forming emulsions due to its increased versatility compared to shaking as well as being quicker and more user-friendly.

5.2.2 Comparison of surfactants

To further test the potential of each surfactant, preliminary compatibility experiments were performed. Each surfactant was added to conventional liposomes with encapsulated calcein and liposomal stability was monitored with fluorescence. When combined with liposomes it was found that PFOA had a negative effect on the bilayer lipid membrane; when

dilute PFOA was added to liposomes containing calcein, the stability of the membrane decreased and calcein was released into the surrounding solution. This increased leakiness to calcein was not observed in control liposomes or when Zonyl or DPPC was added to the liposomes. PFOA also reacted with calcein in these preliminary compatibility experiments to form a yellow precipitate. The resulting precipitate had an altered fluorescent spectra compared to calcein. Because of these effects and potential toxicity associated with PFOA it was eliminated as a candidate for stabilizing the emulsions.

The effect of Zonyl or DPPC concentration was investigated by forming emulsions with varying concentrations of surfactant. All other parameters, such as amount of PFC and preparation conditions, were maintained the same. Both Zonyl and DPPC demonstrated the ability to stabilize smaller droplets as the amount of surfactant increased. Initially, as the concentration of DPPC was increased, the median diameter decreased quickly (see Figure 6A). At approximately 5 mM DPPC, the average diameter approached 200 nm. At this PFC concentration, additional DPPC did not have a significant contribution in stabilizing smaller droplets. Zonyl-stabilized emulsions also approached 200-nm diameters, but only at much higher concentrations (see Figure 6B). At comparably low (5-10mM) concentrations, Zonyl was able to stabilize droplets, but average sizes were between 400 and 600 nm. Approximately 150 mM Zonyl was required in order to form 200-nm emulsions. In contrast, Zonyl did tend to form emulsions with narrower size distributions. DPPC was chosen to stabilize emulsion droplets throughout the rest of this study due to the much smaller amount of surfactant required to stabilize 200-nm emulsion droplets and its well-known biocompatibility. This choice had the added advantage of stabilizing emulsions with the same material that would be used to form

eLiposomes later on, thus reducing the threat to destabilize the bilayer membrane with foreign surfactants.

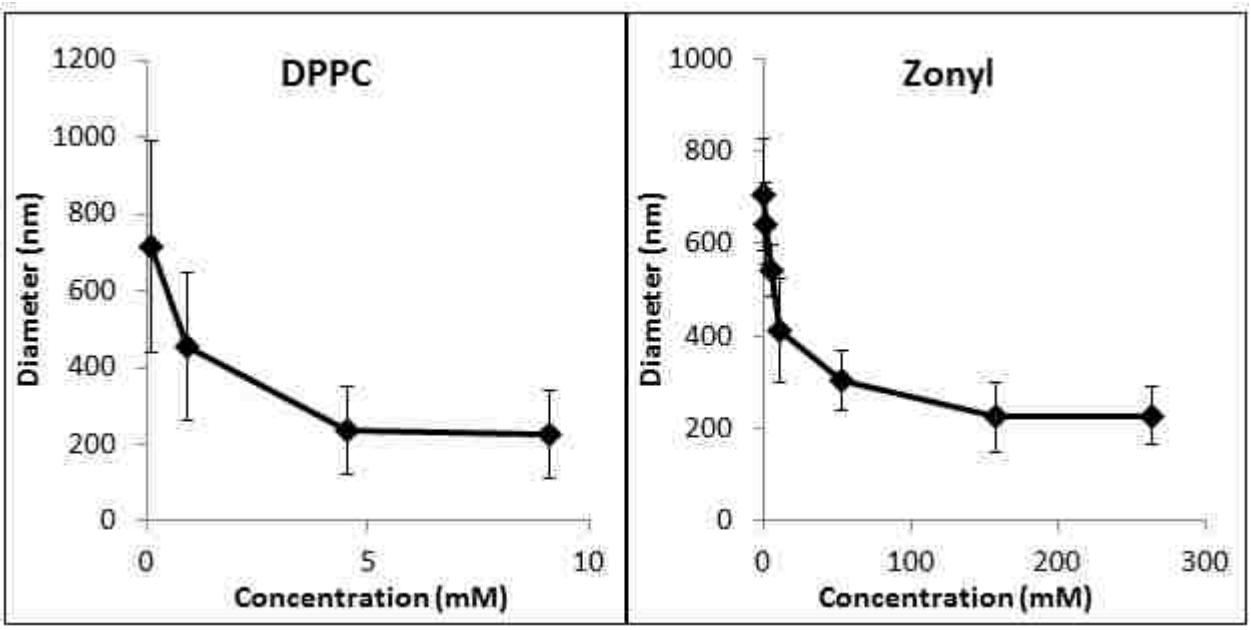

Figure 6. Emulsion diameters as measured by DLS as amount of surfactant (DPPC or Zonyl) was varied. DPPC-stabilized emulsions approached 200 nm at low concentrations. While Zonyl-stabilized emulsions approached similar median diameters, much higher concentrations were required to do so. Error bars represent ± 1 standard deviation (n=10).

5.2.3 Effect of liquid, surfactant concentration and ultrasound exposure

After choosing DPPC as the surfactant of choice for remaining studies, the ability to stabilize PFC5 emulsions was also examined. Similar to PFC6, ultrasound proved an effective method for forming PFC5 emulsions stabilized with DPPC. All emulsions were formed on an ice bath to reduce loss of PFC through vaporization and ultrasound induced heating. While this step had been largely a precaution when working with PFC6 emulsions, the cooling was mandatory when working with PFC5. It was initially discovered that PFC6 solutions emulsions could be formed without cooling. Nevertheless, cooling was introduced to avoid the possibility

of PFC6 loss. Furthermore, without cooling the diameters of the resulting emulsions tended to be less consistent, especially at longer sonication times. In contrast, when PFC5 solutions were sonicated without an ice bath a large amount of foam would form as the PFC5 was vaporized. This foam would sometimes overtake the entire sample, rendering the emulsion unusable. When the solution was cooled on an ice bath the layer of foam was either very small or completely absent. The persistence of emulsion droplets was verified by adding the emulsion to the top phase a "sucrose cushion" and centrifuging (see Chapter 4.2.6). The 1M sucrose layer had a density much greater than perfluorocarbon bubbles, slightly greater than an aqueous suspension of liposomes, but less dense than liquid perfluorocarbons. The collection of a pellet at the bottom of the sucrose layer verified the preservation of emulsion droplets.

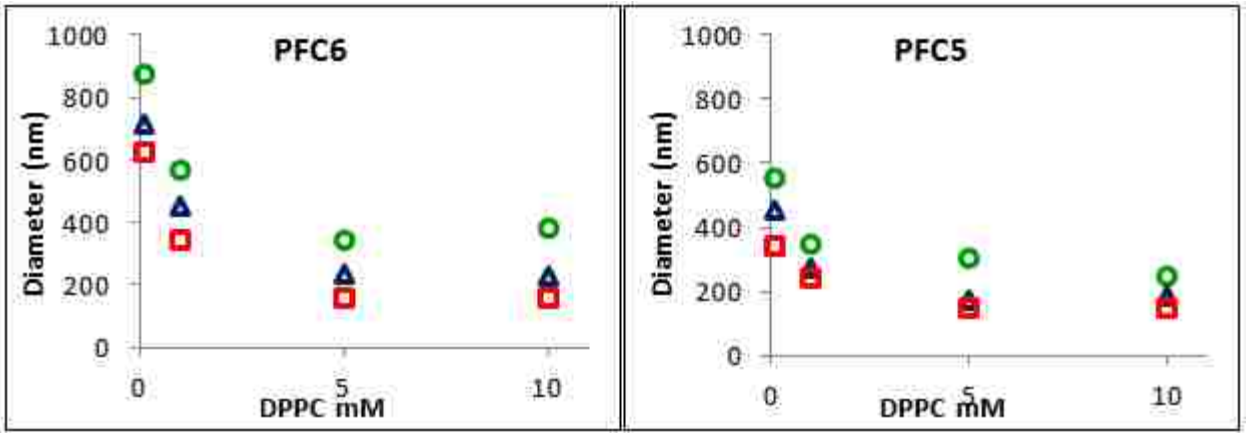

Figure 7. Median diameters of PFC6 and PFC5 emulsions at DPPC concentrations ranging from 0.1 to 10 mM. The diameter seems to level of at approximately 200 nm for both PFC5 and PFC6 emulsions. Time of ultrasound exposure was also varied. Samples were exposed to ultrasound for 1 (○), 4 (△) and 10 (□) minutes of ultrasound. The median diameter decreases as ultrasound exposure time increases. However, sizes still level off at approximately 200 nm even as time is increased. Each data point represents the average of 3 measurements (error bars are removed for clarity).

The effect of varying DPPC concentration was examined for both PFC5 and PFC6 by preparing samples with a constant amount (0.1 g) of PFC and varying amounts of DPPC. The

average diameters for both PFC6 and PFC5 emulsions decreased as DPPC concentration was increased up to about 5 mM DPPC (see Figure 7). This lipid concentration corresponds to enough lipid molecules to coat approximately 80% of the surface area of 100-nm emulsion droplets. Additional DPPC would most likely form separate liposomes or additional lipid layers on the emulsion droplet.

At low DPPC concentrations, PFC5 formed emulsions with smaller diameters than PFC6 (See Figure 7B). Once again, however, the size of emulsions formed from both PFC6 and PFC5 both leveled off at approximately 200 nm as DPPC concentration increased. The time of ultrasound exposure also had a significant effect on emulsion diameter, with samples exposed to ultrasound for longer times typically having small diameters. Some samples were exposed to up to 20 minutes of ultrasound. The diameters of these emulsions, however, still seemed to level off at slightly below 200 nm. In most cases, the presence of sufficient lipid to stabilize small emulsions seemed to have more of an impact on final diameter.

For some experiments emulsion samples with large droplets were required in order to test the effect of size on droplet vaporization. The target diameter for these samples was typically 450 nm. A variety of parameters were explored to form these larger emulsions. Intensities of 1 W/cm^2 or higher tended to form emulsions smaller than 400 nm even at short times (10, 20 and 30 seconds). The sizes produced in these samples were sporadic, ranging from 150 to almost 500 nm. More repeatable success in forming large droplets was obtained by sonicating emulsion samples at 0.5 W/cm^2. When sonicating for short times (30 seconds and less), the PFC phase was not always fully suspended. Furthermore, there was again a fairly wide range of average sizes obtained. Long times (4 minutes or more) also often resulted in diameters of less than 400 nm even at low ultrasound intensities. The most consistent results were obtained by sonicating

for 1 minute at 0.5 W/cm^2. While these parameters yielded the most consistent results, there was still a large amount of variability. Because of this variability, samples were measured after formation and were eliminated or reprocessed if the median size was not in between 400-500 nm.

5.3 Emulsion extrusion

5.3.1 Emulsion sizing via extrusion

While sonication had proven able to suspend the perfluorocarbon phase and form a DPPC-stabilized emulsion, the average droplet diameter of sonicated emulsion samples varied from 150 to 400 nm and results were not easily reproduced. Also, the size distribution generated by sonication was often multimodal and sometimes very broad. A typical size distribution of a PFC6 emulsion generated by sonication is demonstrated in Figure 8A.

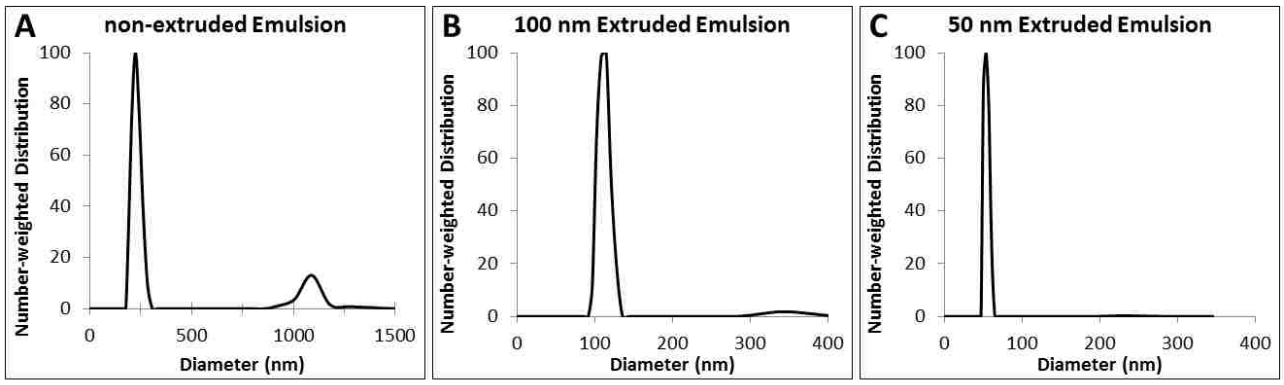

Figure 8. Typical size distributions for PFC6 emulsion samples after formation by ultrasound (A) and after extrusion through a 100-nm filter (B) or a 50-nm filter (C).

To better control the size of emulsion droplets, they were extruded through polycarbonate filters having specific pore sizes. After nanodroplets had been formed by ultrasound as described above, they were extruded 15 times through a 100-nm or 50-nm filter at 50°C to

control and reduce their size. These filter sizes were chosen in order to create emulsion droplets that could be readily encapsulated inside of sub-micron liposomes. Figure 8B and C show typical size distributions of PFC6 emulsions extruded with 100-nm and 50-nm filters, respectively. Extrusion demonstrated the ability to control the diameter of the PFC6 emulsion droplets to approximately the size of the filter pores. Additionally, size distributions after extrusion were much more monomodal than before extrusion.

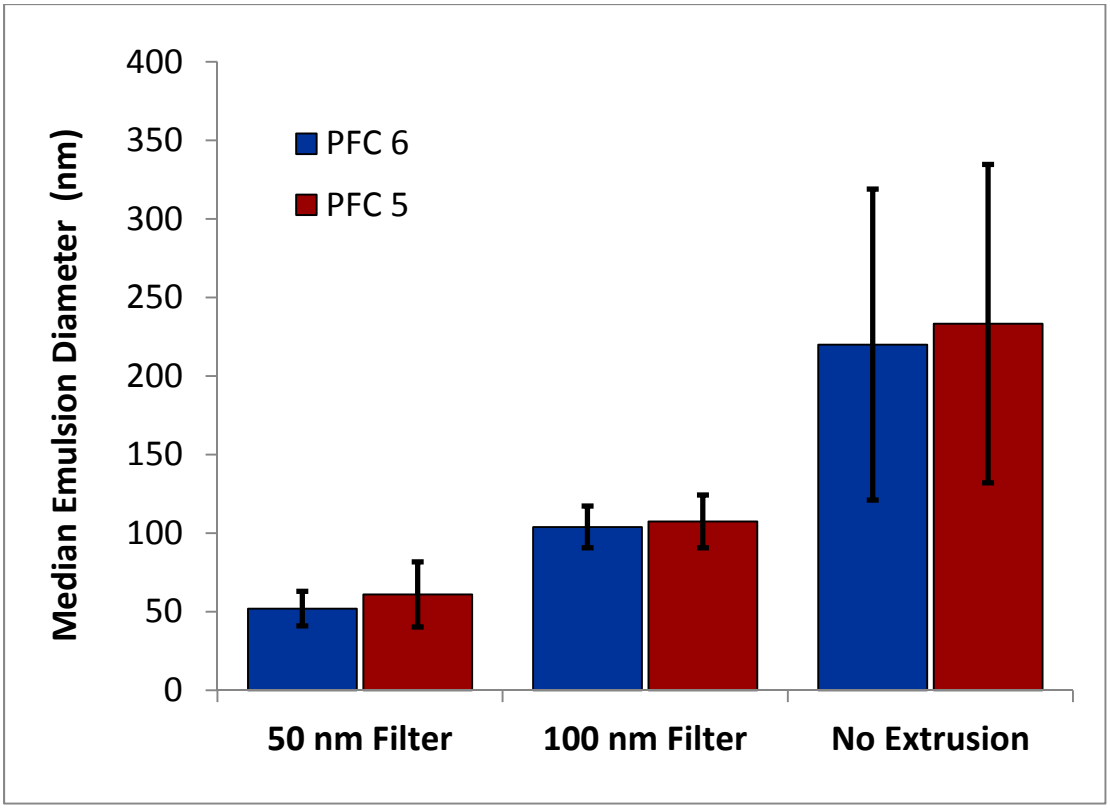

Figure 9. Average diameter of emulsions after formation by sonication at 1 W/cm^2 for 4 minutes or after extrusion through a 50 or 100 nm filter. The size of both PFC5 and PFC6 emulsions were controlled by extrusion. Not only did extrusion control the diameter to close to the filter size, but the variability from sample to sample was greatly reduced. Data is reported as the average of sample medians ± 1 standard deviation (n=10).

In order to test repeatability and efficiency of extruding, emulsions were formed and sized with DLS at least 10 times for each of the filter sizes and each PFC liquid (Figure 9). The median diameter of PFC6 samples extruded through a 100-nm filter was 104 nm with a standard deviation of 13 nm. PFC5 emulsions extruded at 100 nm had an average size of 107 with a standard deviation of 17. Similarly, when extruded through a 50-nm filter, the average diameter of the PFC6 droplets was 52±11 nm and the average diameter of PFC5 droplets was 61±21 nm. In contrast, non-extruded PFC6 emulsions had an average diameter of 220±99 nm and non-extruded PFC5 emulsions had an average diameter of 233±101 nm. Not only was the size of the emulsion controlled, but the variability from sample to sample was also greatly reduced in both PFC5 and PFC6

5.3.2 Effect of temperature

In order to effectively control droplet size, the extrusion step had to be performed above the transition temperature of DPPC (T_m = 41°C). Attempts to extrude at room temperature gave mixed results. Usually the filter would become clogged and eventually rupture, especially with PFC6 emulsions. When the filter did not break, PFC6 emulsion droplets would often stay the same size or sometimes even increase in diameter. PFC5 emulsions would sometimes decrease in size and would sometimes stay approximately the same size as before being extruded. Similar to PFC6 emulsions, PFC5 emulsions were very difficult to extrude at room temperature and the extrusion process would often break the filter. These problems were eliminated when the extrusion step was performed at 50°C; excessive amounts of force were no longer required to pass the solution though the filter and the measured sizes were typically closer to the membrane pore size. This can be attributed to stiff lipid membranes existing below the lipid transition

temperature, which is 41°C for DPPC. Droplets with a stiff DPPC layer would likely get caught in the holes of the filter. It is possible that with sufficient pressure the shape of the droplet elongated in order to pass through the pore, only to re-assume a spherical shape on the other side. This would explain the ability of droplets to stay the same size throughout extrusion as well as the higher force requirement for extrusion and the tendency to rip filters. Heating above the transition temperature of the lipid would have caused the droplet's membrane to become more shapable and fluid, allowing it to more readily elongate and form new, smaller droplets while being forced through the filter.

Despite being processed above the boiling point for PFC5, emulsion droplets persisted and their size was controlled. The ability to process PFC5 emulsions above the normal boiling point of PFC5 is most likely due to the high Laplace pressure imposed on the droplets at sub-micron sizes, additional pressure imposed in the syringes of the extruder, or some combination thereof. PFC5 emulsions would occasionally vaporize and foam when being processed or when being removed from the syringes. This problem was remedied by removing the Avanti Mini Extruder apparatus from the heating block and allowing the syringes to cool before removing the syringe from the extruder and emptying the emulsion. The presence of emulsion droplets after heating and extrusion was once again verified using a sucrose cushion. After centrifugation, a pellet had collected at the bottom of the dense sucrose phase indicating the liquid perfluorocarbon droplets were still present. Persistence of nano-sized emulsion droplets was further confirmed by TEM.

5.4 CryoTEM imaging of emulsion droplets

Emulsion droplets were imaged using cryoTEM. This technique allows structures to be frozen and viewed in their natural state. Images confirmed the average sizes observed by DLS, and better demonstrated the width of the distribution, with droplets varying from 30 to 200 nm. An unexpected wide variety of appearances was observed in the emulsion droplets. Figure 10 shows two cryoTEM images of an emulsion that was extruded through a 100 nm filter. The droplets in this particular sample have a median size of 88 nm. The two views presented in Figure 10 represent typical variability within a single sample observed during one microscope session. The dark structure with a distinct edge in the top left of the first panel is the holey carbon copper grid used to support the frozen sample.

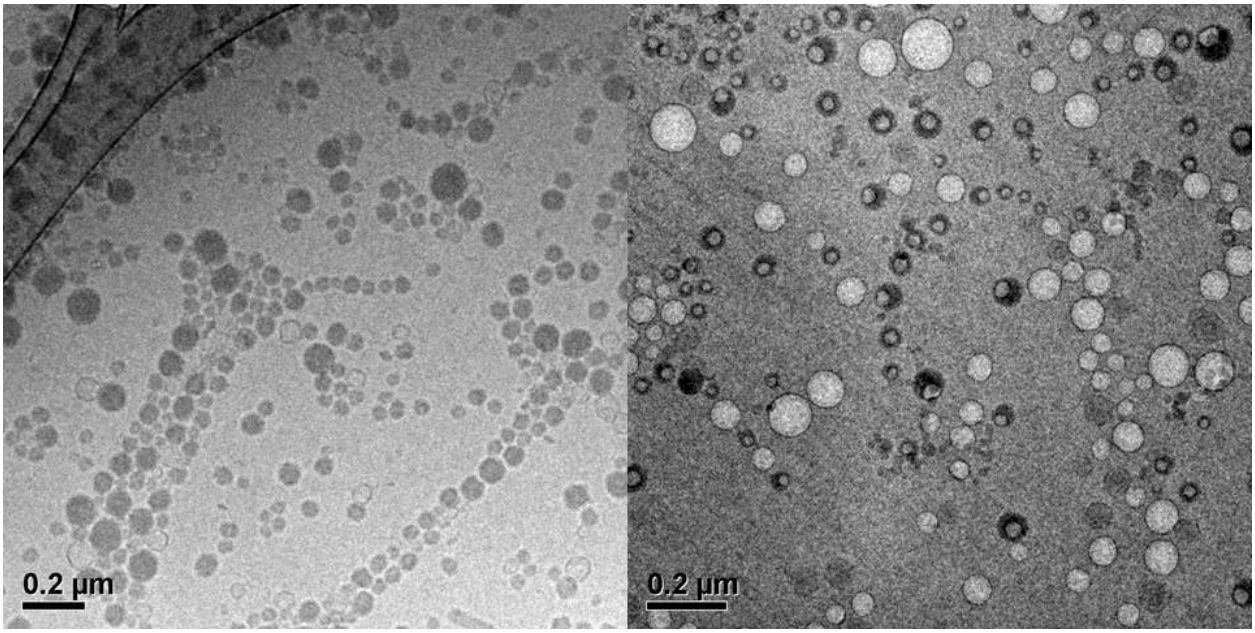

Figure 10. Two cryoTEM images of PFC6 emulsions extruded through a 100-nm filter. This emulsion sample had individual diameters ranging from 45- 140 nm and a median droplet diameter of 88 nm. The droplets demonstrated several distinct appearances. The dark structure with a distinct edge in the top left of the left panel is the holey carbon copper grid used to support the frozen sample.

The imaged droplets had three distinct appearances: 1) dark electron dense spots, 2) very light spots (brighter than the vitreous ice background), or 3) a combination of 1 and 2, with a dark circle surrounding a lighter one. Droplets were counted from six TEM images; 40% of the droplets appeared dark, 33% appeared light, and 27% appeared as a dark circle surrounding a smaller light one. A light circle surrounding a smaller dark one was never observed. When both shades were present in combination, the light spot stayed within the boundary of the dark area when the stage was rotated throughout 90°, suggesting that the lighter region was contained within the darker droplet boundary.

We speculate that these 3 distinct appearances may be due to one or more of the following possibilities. 1) Due to the low melting temperature of PFC6, the emulsion droplets may freeze slower or later than the water surrounding it. Hence, the frozen PFC6 may take on two possible formations: A crystalline phase and an amorphous phase. Differences in electron density/transparency in these phases would account for the two different droplet appearances. In some instances, one phase could be embedded within the other, causing both shades to be present simultaneously. However, upon closer examination, the emulsion droplets did not show any appearance of crystallinity in either in the real-space images or after Fourier analysis (data not shown). 2) During cryoTEM, radiation damage is commonly observed. Sometimes, this radiation damage may be observed spreading throughout a sample with time, especially as the electron beam is focused on a specific area of the sample at higher magnifications. The perfluorocarbon liquid could act as a nucleation site for this type of damage, causing some droplets to take on a white appearance. 3) The lighter regions could be areas of low fluorocarbon density, such as small bubbles of vapor or air. Frozen droplets could melt or sublime with exposure to the electron beam. This commonly happens to the ice during cryoTEM. With a

melting temperature of -90°C, the PFC6 would melt or sublime at a lower temperature than the ice, leaving a liquid phase or an empty hole where the frozen droplet had been. A void could also have been created during freezing, or some of the perfluorocarbon could have been in its vapor phase when the sample was frozen. The resulting area of low perfluorocarbon density would most likely appear as a bright area in the images. To further examine this possibility, emulsions were formed from perfluoropentane (PFC5) and perfluoroheptane (PFC7) following the same procedure outlined in Materials and Methods (Chapter 4). PFC5 has a boiling point of 29°C and PFC7 has a boiling point of 82°C. As the boiling point increases, the amount of liquid or vapor present in the sample and rate at which droplets would vaporize or sublime should decrease. Droplets were counted from 5 or more cryoTEM views. The percent of droplets that have the different appearances in the TEM images is reported in Table 2.

Table 2. The percentage of emulsion droplets that appear light, dark, or dark surrounding a light circle (combination).

	Boiling point	Light	Dark	Combination
PFC5[a]	29°C	51%	40%	8%
PFC6[b]	57°C	33%	40%	27%
PFC7[c]	82°C	25%	43%	32%

(a) n = 84
(b) n = 315
(c) n = 68

The percentage of droplets that appear lighter than the background decreases as the boiling point increases. The percentage of dark droplets with light spots inside of them increases as the boiling point increases. This trend is consistent with the hypothesis that the light regions are areas of lower perfluorocarbon density, such as small gas or vapor bubbles or liquid. The percentage of dark droplets stays relatively constant.

5.5 Verification of acoustic droplet vaporization

5.5.1 Microscope evidence of vaporization

In order to verify that ultrasound induced vaporization of emulsion droplets, PFC5 emulsions were placed on a microscope slide, and were covered with a thin glass coverslip. The coverslip was viewed initially and after 5 seconds of exposure to 1 W/cm^2 ultrasound. Figure 11 shows before and after images for large PFC5 droplets. Prior to ultrasound exposure only the largest sized droplets (approximately 3-4 um) are visible (see Figure 11A). After ultrasound exposure, many larger structures can be observed which have the appearance of gas bubbles (Figure 11B). These newly formed bubbles vary in size up to 20 µm.

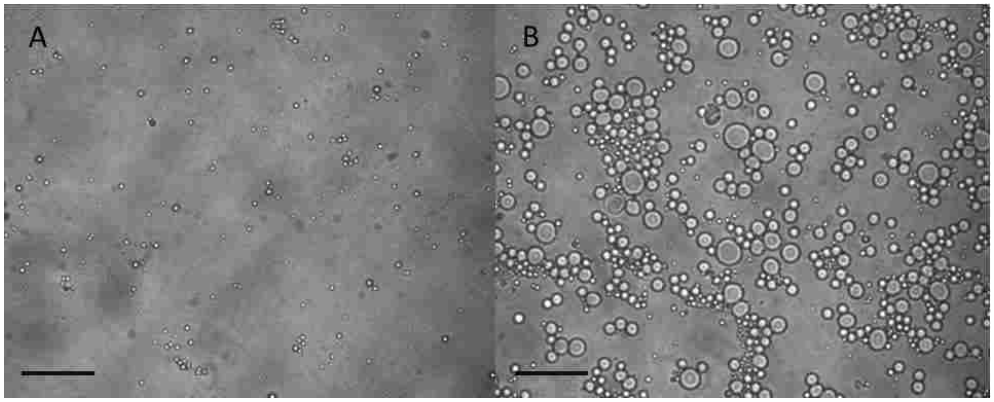

Figure 11. Large PFC5 emulsion before (A) and after (B) ultrasound exposure. Large emulsion droplets were placed on a microscope slide and imaged prior to ultrasound exposure. 20-kHz ultrasound was then applied for 5 seconds at 1 W/cm^2 and the slide was imaged again. Before ultrasound exposure only the largest droplets in the emulsion can be observed (A). After ultrasound exposure, droplets had vaporized and perhaps coalesced into much larger bubbles (B). Scale bars represent 50 µm.

Overall, the resulting bubbles were larger than expected and persisted at room temperature. For example, using the ideal gas law and liquid density, a PFC5 droplet should expand to a 137-fold larger volume at its boiling temperature and 1 atm. The expected increase in diameter would be $\sqrt[3]{137}$, or a 5.15-fold increase in diameter. The diameter of the largest

droplets observed in Figure 11B is approximately a 3.5 to 5 times the diameter of the largest droplets in Figure 11A. While this is close to the expected expansion for these droplets, there are more large bubbles in Figure 11B than expected from an emulsion with an average droplet diameter of 450 nm. The larger size could be due to bubbles colliding and combining or due to dissolved nitrogen and oxygen accumulating in the PFC bubble during and perhaps after insonation. It is worth noting that laboratory manipulations and slide preparation did not result in droplet vaporization; large droplets were not observed until after ultrasound application.

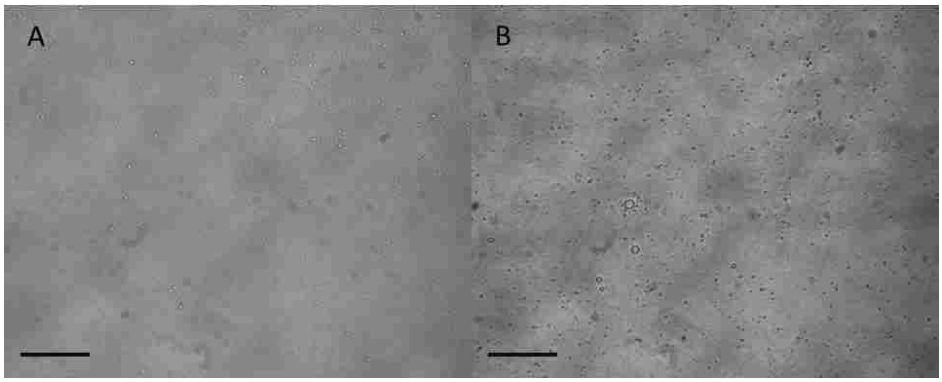

Figure 12. Small PFC5 emulsion before (A) and after (B) ultrasound exposure. 20-kHz ultrasound was applied for 5 seconds at 1 W/cm. After ultrasound exposure, droplets had vaporized and perhaps coalesced into much larger bubbles (B). While the appearance of the solution had changed, this change was not as significant as observed with large PFC5 droplets. Scale bars represent 50 µm.

Figure 12 shows before and after images for small PFC5 droplets. There was again an increase in large bubbles and structures. However, the bubbles observed after sonication were much smaller compared to the sample with large PFC5 droplets. This indicates that either the small droplets were less readily vaporized or that the resulting bubbles were less prone to combine with one another into larger droplets. Two control experiments were performed: a DPPC solution and plain water. No bubbles were observed before or after ultrasound exposure in either of the control samples (data not shown).

The experiment was repeated at 37°C by heating the microscope slides in an oven. Slides were prepared and imaged prior to heating. The slides were then allowed to sit in the oven for 5 minutes to heat to 37°C and were imaged again. Finally, the slides were exposed to ultrasound and imaged quickly to avoid cooling. Figure 13 shows results from a large PFC5 sample. It is worth noting that there is not a significant change after heating the emulsion (Figure 13B). After ultrasound was applied large bubbles had formed similarly to the results at room temperature (Figure 13C).

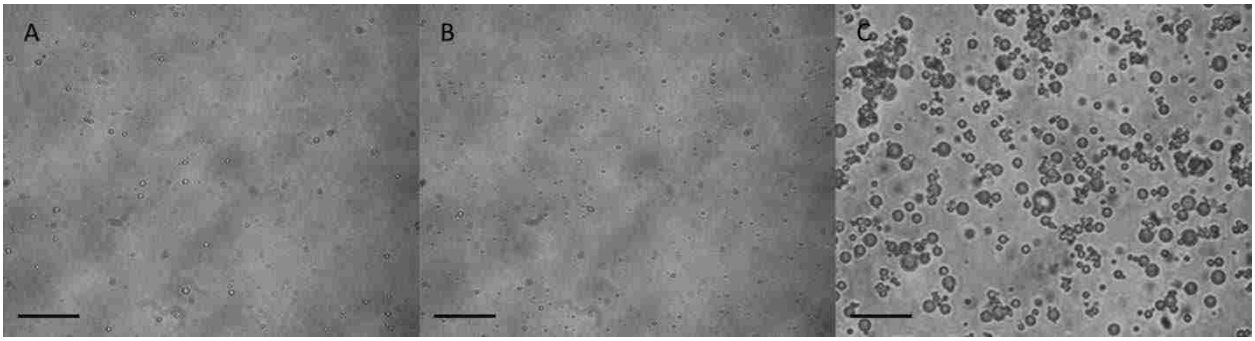

Figure 13. Large PFC5 emulsion before heating (A) and before (B) and after (C) ultrasound exposure at 37°C. Emulsion droplets were placed on a microscope slide under a coverslip and imaged initially (A). The slide was then heated to 37°C and imaged again prior to ultrasound exposure (B). 20-kHz ultrasound was then applied for 5 seconds at 1 W/cm^2 and the slide was imaged again (C). Heating above the normal boiling point had no significant effect on the appearance of the emulsion (A and B). After ultrasound exposure, droplets had vaporized and coalesced into much larger bubbles (B). Scale bars represent 50 µm.

The experiment was again repeated with small PFC5 emulsion droplets. Likewise, small emulsion droplets did not show any significant change after being heated to 37°C (Figure 14). Large bubbles formed after sonication. These bubbles were more numerous and more prominent than those formed from small PFC5 emulsions at room temperature, although still not as much as bubbles formed from large PFC5 droplets. It seems that the increase in temperature increased the ability of the droplets to vaporize and/or to combine with one another.

Figure 14. Small PFC5 emulsion before heating (A) and before (B) and after (C) ultrasound exposure at 37°C. The microscope slide was heated to 37°C and 20-kHz ultrasound was applied for 5 seconds at 1 W/cm^2. Heating had no significant effect on the appearance of the emulsion (A and B). After ultrasound exposure, droplets had vaporized and coalesced into much larger bubbles (B). However, these bubbles were less prominent than those formed from large PFC5 droplets. Scale bars represent 50 µm.

5.5.2 Acoustic evidence of vaporization

Vaporization of emulsion droplets was further verified by observing acoustic signals generated by emulsions and control water samples. Samples were exposed to 525 kHz with 1000 cycle pulses at a 20-Hz pulse repetition frequency. The acoustic signal was detected with a hydrophone. This signal was Fourier-transformed, creating a spectrum with peaks at frequencies according to the oscillations of entrained bubbles. The fundamental frequency of the ultrasound can be detected at practically any intensity. As the ultrasound intensity is increased harmonic peaks, subharmonic peaks, and a baseline jump can be observed, typically in that order. Figure 15 demonstrates examples of these phenomena with a fundamental frequency of 525 kHz.

The fundamental peak does not provide meaningful information about the behavior of the emulsion droplets. The presence of higher harmonic peaks (Figure 15B) is linked to the oscillation of these gas bubbles [30, 126]. Control samples are important because bubbles can also form from water vapor and/or from dissolved gases that nucleate at sufficiently high ultrasound intensities [30]. Lower thresholds in emulsion samples than in controls is likely indicative of vaporizing perfluorocarbons that begin to oscillate and behave as gas bubbles.

There is some debate in literature as to whether the subharmonic peak correlates to stable or collapse cavitation [114, 115, 118, 127-129]. For our purposes, the appearance of this peak can be considered evidence that cavitation is, at the very least, becoming more complex and chaotic in nature. A jump in the baseline is widely accepted as being correlated to widespread collapse cavitation; as shock waves are formed from collapsing bubbles they generate sound at all frequencies, and result in this jump in the baseline [21, 118, 119].

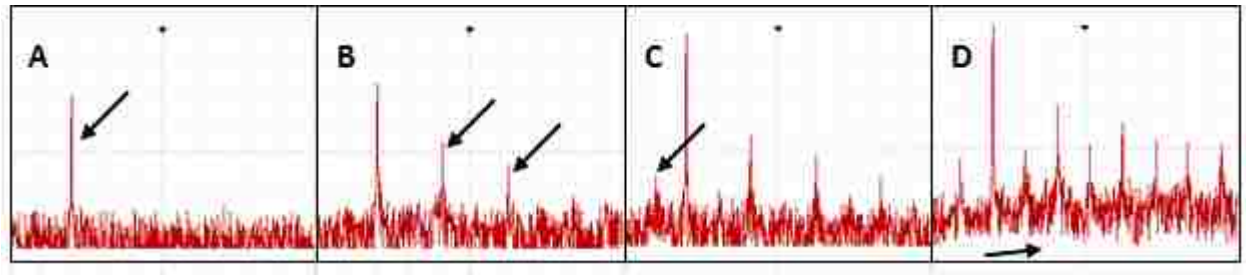

Figure 15. Fourier transforms of the acoustic signal collected from emulsion samples, providing examples of the fundamental peak (A), higher harmonic peaks (B), a subharmonic peak (C) and a baseline shift (D).

The left panel of Figure 16 compares the onset of these 3 phenomena for control samples (water) and for large (450 nm) and small (100 nm) PFC5 and PFC6 emulsion samples when exposed to 525 kHz ultrasound at room temperature. The initial onset of higher harmonic peaks was much lower in emulsion samples than in control samples of water, indicating that the emulsion droplets are indeed vaporizing when exposed to ultrasound. Interestingly, at room temperature, there is little difference among the various emulsion samples, regardless of whether they are formed from PFC5 or PFC6 and regardless of droplet size.

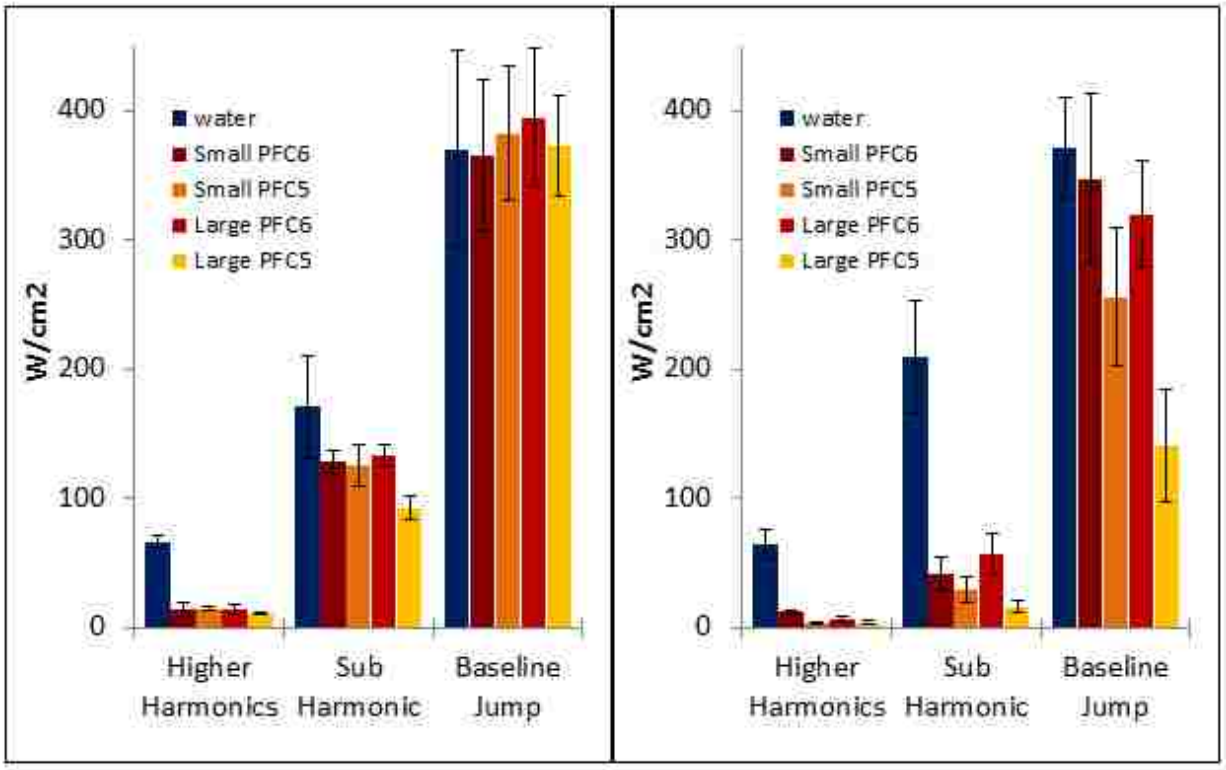

Figure 16. Threshold values for control samples and emulsions at 525 kHz. Emulsion samples were prepared from both PFC5 and PFC6 at 450 nm (large) and at 100 nm (small). Threshold values were observed at 24°C (left panel) and at 37°C (right panel). Higher harmonic peaks were observed at lower intensities in emulsion samples than in controls. At room temperature there was little to no difference in thresholds resulting in subharmonic peaks and for the baseline jump in emulsions or control samples. There was, however, a significant difference for intensities required to observe a subharmonic peak at 37°C. PFC5 samples also demonstrated a baseline jump at intensities lower than other samples. Data is reported as the mean average ± 1 standard deviation (n=5).

The onset of the subharmonic peak also occurred at lower intensities for the emulsion samples compared to controls. However, at room temperature the difference between control and emulsion samples was much less pronounced for this phenomenon. Because this peak is connected with more complex bubble dynamics, it may indicate the presence of more persistent bubbles. It appears that intensities required to observe this in room temperature emulsion samples are close to intensities required to nucleate persistent bubbles from water. This is not surprising as the water used for control samples was exposed to similar treatment as emulsion

samples and would therefore likely be saturated with dissolved gases. Compared to each of the other emulsion samples, large PFC5 droplets demonstrated a statistically significant lower intensity threshold for the emergence of the subharmonic peak. This lower intensity threshold suggests that large PFC5 droplets form persistent bubbles that can cavitate chaotically at lower intensities than the other emulsions. This is likely the result of PFC5 having a higher vapor pressure than PFC6. Also, larger droplets are expected to have less Laplace pressure than small droplets. Interestingly, at 24°C there was no difference in the onset of the baseline jump between controls or the various emulsion droplets. It seems that this intensity is sufficient to create bubbles and cause collapse cavitation regardless of the presence of emulsion droplets.

As the temperature was increased to 37°C, there was no difference ultrasound thresholds observed in control samples compared to the results at 24°C (See the right panel of Figure 16). For emulsion samples, the higher temperature is expected to result in a higher vapor pressure, making it easier to overcome the vapor pressure with the negative phase of an ultrasound wave. The thresholds for observing higher harmonic peaks were significantly lower at 37°C for all of the emulsion samples except for the small PFC6 emulsion. Again, this is likely because of the lower vapor pressure of PFC6 and the higher Laplace pressure imposed on small droplets. Compared to room temperature samples, the subharmonic peak was observed at much lower ultrasound intensities in emulsion samples at elevated temperature; these differences were statistically significant for each emulsion liquid and size (Student t-test, $p < 0.05$). This suggests that the increased temperature makes it easier to form bubbles, and that these bubbles can persist more readily in order to approach a state of transient cavitation. For control samples and for PFC6 samples, the emergence of the baseline shift was not significantly different at 37°C compared to room temperature. However, a baseline shift was observed in PFC5 emulsion

samples at much lower ultrasound intensities when the sample was heated to 37°C, suggesting that in higher vapor pressure liquids the temperature can play a role in their ability to form bubbles and to subsequently undergo collapse cavitation. It should also be noted that large PFC5 emulsions underwent this phenomenon at a lower intensity than small PFC5 emulsions, once again supporting the hypothesis that Laplace pressure has an effect on the ability of emulsion droplets to form bubbles and to undergo collapse cavitation.

Experiments with acoustic phenomena were repeated at 1.58 MHz (Figure 17). The trends observed at 525 kHz were all essentially the same, but the intensities required for the onset of each phenomenon were much higher at 1.58 MHz. For example, the higher harmonic peaks were first observed at 67 W/cm^2 for controls and at approximately 14 W/cm^2 for emulsion samples at 525 kHz. These peaks were not observed until 216 W/cm^2 in water and approximately 90 W/cm^2 in emulsion samples at 1.58 MHz. Likewise, the baseline shift was observed in all samples at about 380 W/cm^2 at 525 kHz. The baseline shift was not observed until 3500 W/cm^2 at 1.58 MHz. Increasing temperature from room temperature to 37°C also had similar results at 1.58 MHz compared to results at 525 kHz. Most notably, the threshold for the baseline jump remained approximately the same in control samples and in PFC6 samples but was significantly reduced in PFC5 samples.

It should be noted that the phenomena that were observed are linked with bubble dynamics, not necessarily droplet vaporization. While the presence of these phenomena does indicate the presence of a gas phase and provide hints about the behavior of the emulsion droplets, it does not necessarily provide precise threshold values of emulsion droplet vaporization behavior. The discrepancy between controls and emulsion samples, however, does support the hypothesis that ultrasound has the ability to vaporize emulsion droplets by

demonstrating that ultrasound-induced droplet vaporization leads to the introduction of a gas phase at much lower intensities when emulsion droplets are present.

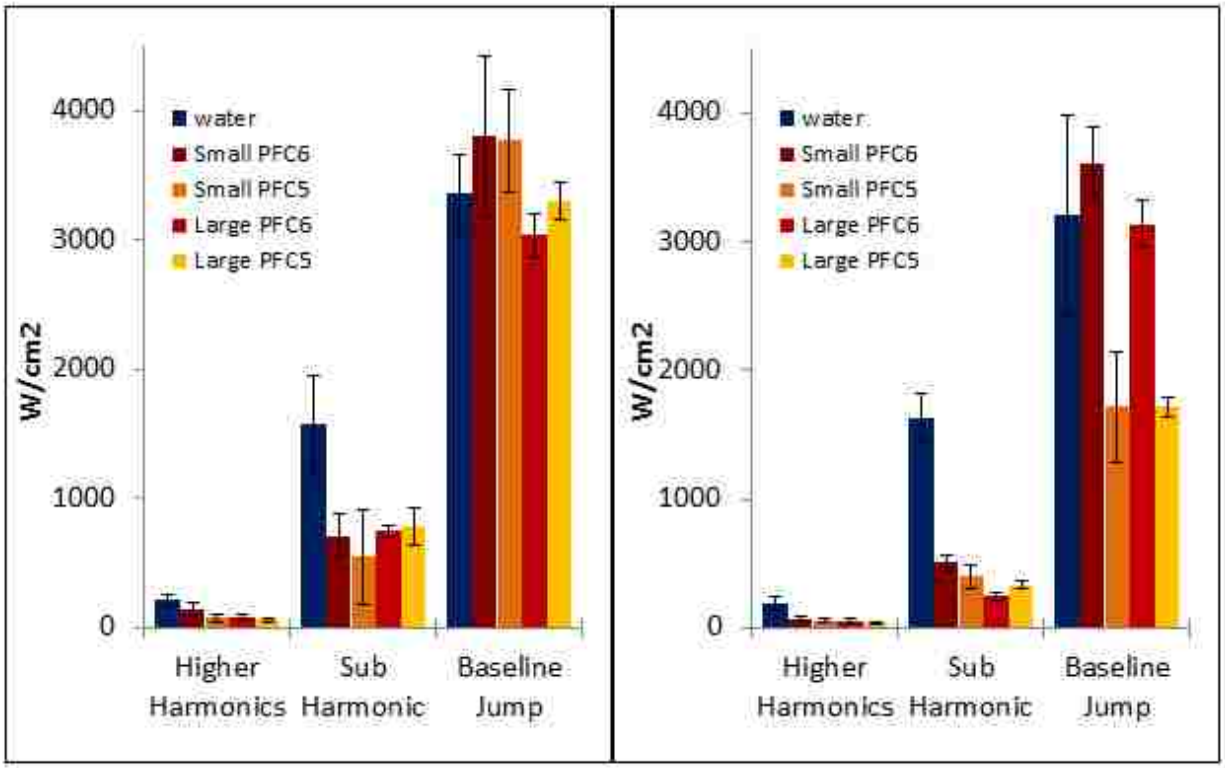

Figure 17. Threshold values for control samples and emulsions at 1.58 MHz. Emulsion samples were prepared from both PFC5 and PFC6 at 450 nm (large) and at 100 nm (small). Threshold values were observed at 24°C (left panel) and at 37°C (right panel). Data is reported as the mean average ±1 standard deviation (n=5).

Experiments were repeated at 500 cycles/pulse with no significant difference in results, suggesting that 500 ultrasound cycles are capable of creating the same vaporization and cavitation events observed at 1000 cycles. Experiments were also repeated with a continuous wave. Counter intuitively, the thresholds for the various peaks were higher with a continuous wave. These results suggest that acoustic decoupling may be occurring when a continuous wave is applied. Acoustic decoupling is a phenomenon in which incoming high intensity ultrasound

induces the formation of cavitating bubbles at the entry of the sample. The bubbles then scatter ultrasound and prevent it from penetrating deeper into the sample. Thus it appears to the observer that there is less cavitation occurring in the sample as the acoustic intensity increases. There was no evidence of acoustic decoupling when short pulses were applied.

5.6 Emulsion-aided release from conventional liposomes

While emulsions have shown some promise as drug and gene carriers, they also have several disadvantages compared to other types of drug carriers. For example, many drugs are not very soluble in the very hydrophobic oil phase. This limits the amount of drug that can be carried by emulsions to the amount that can be attached to the surface or carried in the surfactant layer. Because the drug load is most likely carried on the surface of the droplets, emulsions also have only a limited ability to sequester the drug and prevent interactions with non-target tissues. In contrast, liposomes and micelles have a larger interior volume that can carry and sequester their payload. Liposomes, as mentioned previously, are a particularly versatile drug carrier. However, liposomes are not inherently responsive to ultrasound and ultrasound-mediated release from them is largely dependent on neighboring bubbles. The size of these neighboring bubbles limits the ability to take advantage of the EPR effect in combination with ultrasound-induced drug targeting.

It is possible that using liposomes together with emulsion droplets may provide a method to utilize the advantages of both particles. The liposome may add versatility, increased drug loading and effective sequestering. Co-administered emulsion droplets could vaporize into bubbles and provide cavitation nuclei while retaining the ability to extravasate with the liposomes due to their small size. DPPC liposomes containing calcein at a self-quenching

concentration were prepared by film hydration in a 15 mM calcein solution and extruded through a 200 nm filter. Some of the external calcein was removed on a GE PD-10 spin column. A PFC5 emulsion was prepared with an average diameter of 200 nm. In order to investigate the possibility of increasing ultrasound-induced drug release from liposomes with emulsion droplets, 20 μL of the liposome solution and 20 μL of the emulsion were diluted into 2 mL of PBS. The encapsulated calcein did not add to overall fluorescence and the surrounding solution was within the linear range of the fluorescence versus concentration curve for calcein. As calcein was released from the liposomes and diluted into the surrounding solution, the fluorescence of the solution increased.

Figure 18 shows the amount of calcein released from liposomes with and without the presence of PFC5 emulsion droplets. Exposure time was varied from 2 second to 50 seconds and experiments were performed at 0.5 W/cm^2, 1 W/cm^2 and 2 W/cm^2. At short times there was not a significant difference in calcein release from liposomes with or without external emulsion droplets. As time increased, there was increased release of calcein from samples with emulsion droplets compared to those without; this difference was significant at times longer than 30 seconds. It was unexpected that this amount of time was required to observe an increase in calcein release from liposomes with external emulsion droplets. This could indicate that the emulsion droplets require time to vaporize and/or to coalesce into large oscillating bubbles with the ability to contribute to calcein release. At short times, droplet vaporization may have not generated enough mechanical shear to affect the liposomes. At longer times, the droplets may have coalesced into larger bubbles and/or aided in the nucleation of dissolved gasses to add to cavitation.

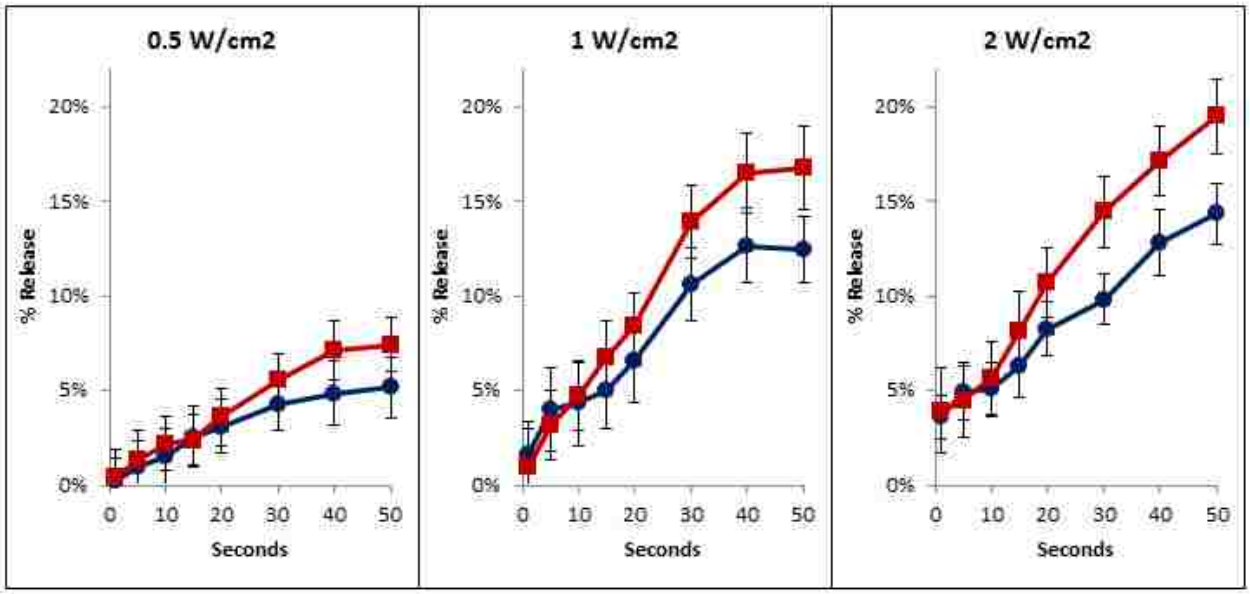

Figure 18. Calcein release from 200 nm DPPC liposomes with (■) and without (●) the presence of 200 nm PFC5 emulsion droplets. Exposure time was varied from 2 to 50 seconds and samples were exposed to 0.5, 1 or 2 W/cm^2 ultrasound at 20 kHz. Each point represents the average of 3 experiments ± 1 standard deviation.

It should be noted that while there was a significant increase in calcein release at longer exposure times, the increase was not substantial. For example, liposomes with external emulsion droplets released 19% of their calcein after 50 seconds of ultrasound at 2 W/cm^2 and control liposomes released 14% after this same exposure. This increase of 5%, although statistically significant, offers little practical improvement.

6 eLIPOSOMES

6.1 eLiposome definition and motivation

In order to better take advantage of the versatility of liposomes together with the ultrasound sensitive nature of emulsion droplets, a novel drug carrier was developed. The proposed drug carrier is called an eLiposome, defined as a liposome containing vaporizable emulsion droplets. The eLiposomes would have the advantages of conventional liposomes while adding an ultrasound responsive component. The emulsion droplets may vaporize when exposed to ultrasound and form an oscillating gas bubble that could increase drug release from the eLiposome. Furthermore, the expanding vapor phase may be able to disrupt the bilayer membrane without ongoing cavitation and/or gas nucleation. In contrast to bubbles and other ultrasound sensitive particles, the nano-sized emulsion droplets allow the carrier to take on an ultrasound sensitive component without sacrificing key characteristics of liposomes. Specifically, eLiposomes must have the ability to be formed at nano-scales sizes. Also, the versatility of liposomes that comes from the ability to tune the lipid composition should be retained in eLiposomes. Lastly, eLiposomes must retain the ability to sequester and protect a therapeutic payload.

During the low pressure phase of an ultrasound wave, the local pressure drops below the high vapor pressure of the liquid emulsions, creating a thermodynamic potential to vaporize. The expanding vapor phase stretches and disrupts the surrounding membrane and releases the

encapsulated material because lipid bilayers can sustain only about a 3% expansion [130, 131]. Two possible representations of this are illustrated in Figure 19. As the vapor phase expands it may stretch the membrane, creating small rips and expelling the encapsulated material (Figure 19A). This scenario is perhaps most likely with small droplets relative to eLiposome size and with lower vapor pressure liquids; as discussed in Chapter 5, perfluorocarbons with lower vapor pressures may be more difficult to vaporize and will collapse back to liquid droplets when no longer exposed to the low pressure phase of an ultrasound wave. In this scenario, the gaps formed in the stretching membrane could potentially close during each cycle of ultrasound and following ultrasound exposure. Alternatively, if the expansion is more violent and/or if the volume of perfluorocarbon is more substantial, the membrane could be fragmented by the expanding vapor phase and associated cavitation events (Figure 19B).

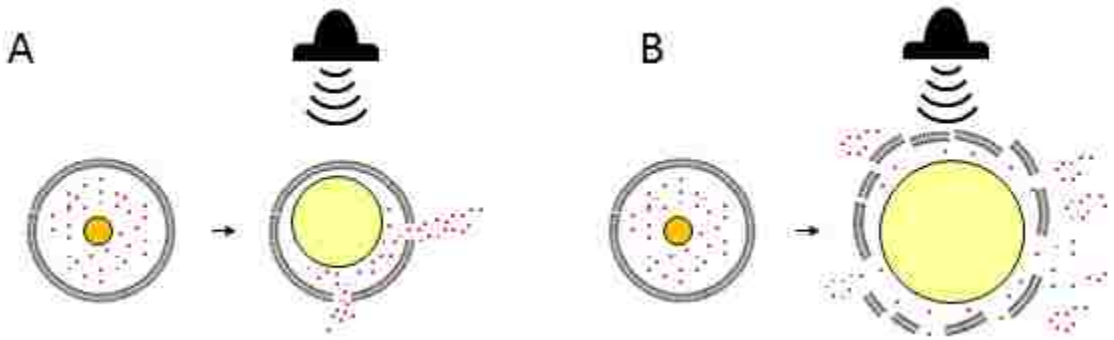

Figure 19. Proposed mechanisms of ultrasound-induced release from eLiposomes. Small red circles represent calcein or encapsulated drugs. In each panel the medium-sized circle inside the liposome represents a liquid perfluorocarbon emulsion droplet. When exposed to the low pressure phase of an ultrasound wave, the droplet vaporizes and expands, disrupting the bilayer membrane and releasing the contents from the eLiposome. A small expansion may stretch and rip the membrane and force out some of the payload (A), or it may more completely destroy the liposome by fragmenting the bilayer membrane (B).

6.2 eLiposome formation via the 2-step sheet refolding method

Lipid sheets were formed by adding alcohol to a solution of DPPC SUV's (small unilamellar vesicles). A DPPC lipid solution was prepared at 30 mg/mL. Initially after hydration, this concentrated DPPC solution was opaque and white. After SUV's were formed by sonication or by extrusion, the solution had a translucent bluish color (see Figure 20A and 20B). Ethanol was added dropwise while stirring to the SUV's to slightly above a sheet-formation threshold value (approximately 2-3 M) [98]. As the ethanol was added, the color of the solution transitioned from a translucent bluish hue to opaque white (Figure 20C). The viscosity of the solution increased substantially as the SUV's unfolded into sheets and the liquid solution transitioned to a gel (see Figure 20D). This change in appearance and viscosity is indicative of the formation of lipid sheets. As alcohol interacts with the bilayer membrane, the lipid heads tend to swell. The membrane becomes thinner and stiffer as the lipids transition from a bilayer gel phase (L_{β}) to an interdigitated gel phase ($L_{\beta I}$) [132, 133]. This stiffening reduces the ability of the membrane to bend into small spheres, and small liposomes unfold into sheets. The layering of continuous sheets compared to the suspension of independent spheres is responsible for the physical changes described above. These sheets remain stable when maintained below the lipid transition temperature even after the removal of the alcohol due to the inability of the lipids to flow and assume a new formation. When heated above the transition temperature, however, the lipid bilayer transitions to a liquid crystalline phase (L_{α}) [134]. As the membrane becomes more fluid, the sheets will refold into spherical vesicles.

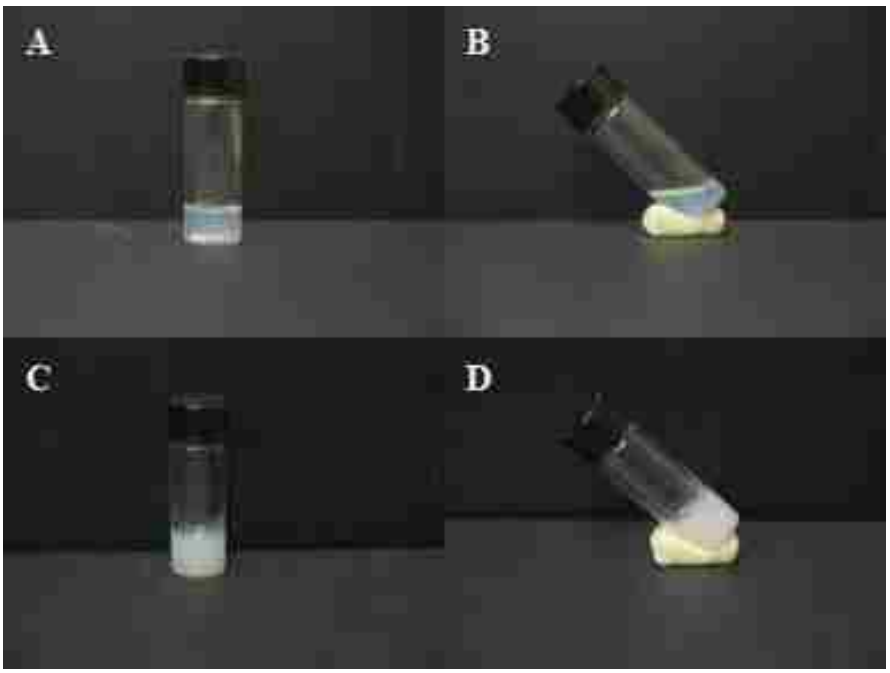

Figure 20. SUV's before (A and B) and after (C and D) the addition of alcohol. Upon alcohol addition, the solution becomes opaque and white, accompanied with a large increase in viscosity. The vial was tipped on its side in images B and D to demonstrate this increase in viscosity.

eLiposomes were formed by heating sheets in the presence of emulsion droplets (see Figure 1). During heating and stirring, the gel-like sheet solution decreased in viscosity as the lipid sheets were heated above their transition temperature, became more fluid and refolded into vesicles. Resulting vesicles typically had average diameters greater than 1 μm and very broad size distribution as observed by DLS and by light microscopy. Although some vesicles reformed at sizes as small as 250 nm, others formed at much larger sizes, sometimes as large as 5 to 20 μm. The eLiposomes were resized by extrusion through an 800-nm polycarbonate filter. Figure 21 shows the DLS data from a typical sample of extruded eLiposomes. There are two peaks present, one of which is assigned to the emulsion droplets (130 nm) and the other to the lipid bilayer vesicles (795 nm). The emulsion size before mixing with the lipid sheets was 120 nm. The eLiposome peak in this example ranges from 400 to 1200 nm, with a median diameter of

795 nm. This experiment was repeated 10 times with the lipid peak having an average median size of 869.84±102 (standard deviation) and the emulsion peak having an average median size of 123±38. This demonstrates the ability to resize the eLiposomes after they have encapsulated emulsion droplets. This is crucial because of the large average diameter and wide size distribution observed after sheet heating and vesicle formation. The ability to reduce the average diameter and narrow the size distribution is crucial in order to take advantage of the EPR effect. While the average diameter of the outer eLiposome membrane was slightly larger than the filter, the average size of the vesicles was significantly reduced compared to before extrusion and controlled to a size near the filter size. The slight descrepency in filter size and vesicle diameter could be due to the relatively large filter size being used, allowing for some motion and flexibility as the vesicles are forced through the filter.

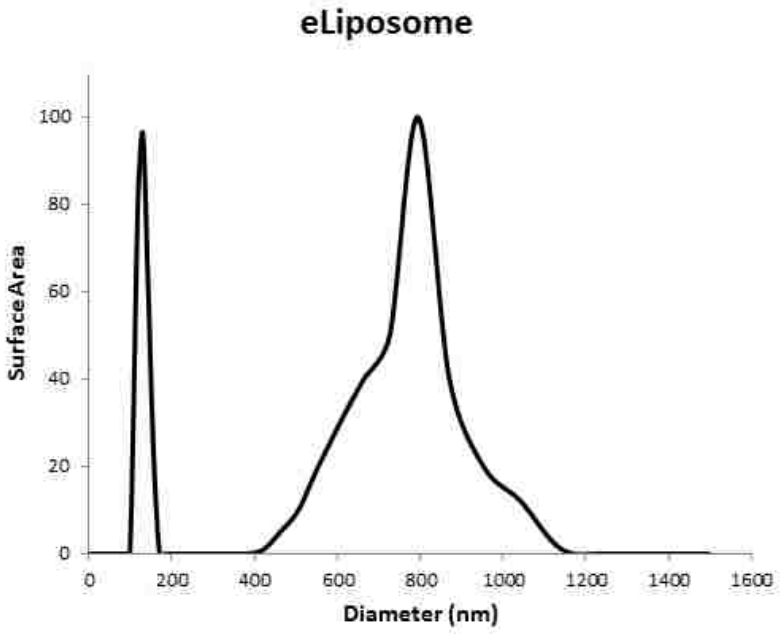

Figure 21. Typical DLS data from an eLiposome sample after extrusion through an 800 nm filter. The peak at 130 nm is assigned to emulsion droplets. The peak at 795 is assigned to the outer lipid membrane.

6.3 TEM imaging of eLiposomes

6.3.1 Negative staining

eLiposomes were imaged by TEM using negative staining to verify the formation of closed vesicles. Negative staining images are presented in Figure 22 and Figure 23. The sample preparation process may have altered the appearance of these lipid structures; folds and creases in the surface of the membrane may have formed as the sample dried. Alternately, some of these creases and folds could be the result of lipid sheets that did not completely refold and recombine. Regardless, the images confirm the closed 3-dimensional structure of the lipid membranes. This is an important point as it provides evidence that our refolding technique via heating was able to form new vesicles from lipid sheets. The TEM images also show that at least some of the refolded lipid vesicles are multilamellar (See Figure 22). The negative staining images also showed emulsion droplets (distinguished by smooth edges and smaller size).

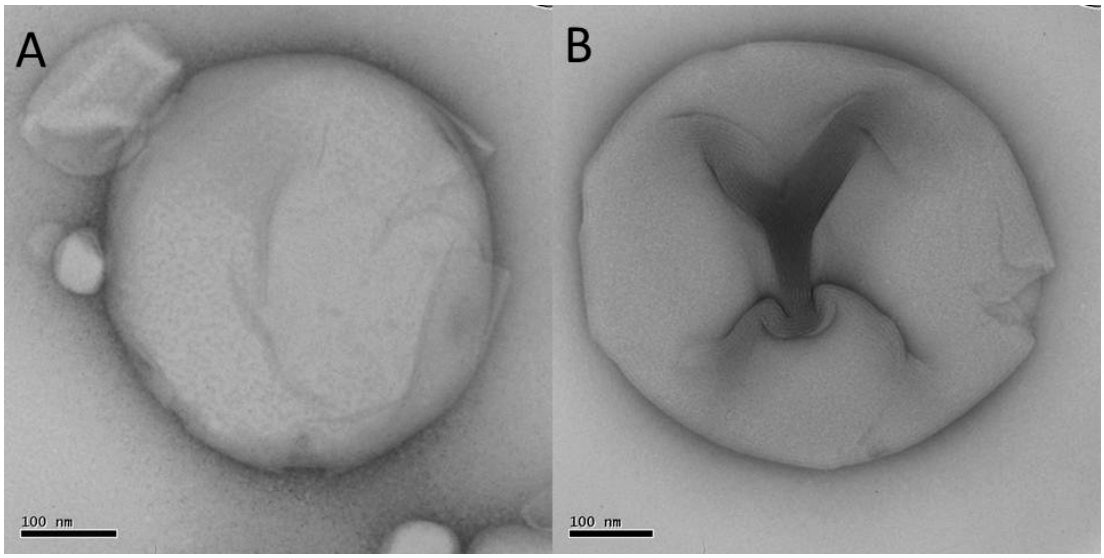

Figure 22. Examples of eLiposomes as imaged with negative staining. These images show the closed vesicles formed from lipid sheets during the reheating step. It can also be observed that at least some of these vesicles are multilamellar.

Figure 23 shows examples where emulsion droplets - the smaller structures from 50-150 nm - were observed as well. Some of these emulsion droplets are indicated with black arrows. These TEM images also confirm sizes measured by DLS; the negative staining images confirm the presence of 400-800 nm vesicles. While negative staining was useful for showing the structure of eLiposome vesicles, it could not conclusively show droplet encapsulation. While there are some droplets that appear to be inside of the membrane, their location is inconclusive do to the nature and limitations of the staining and drying process.

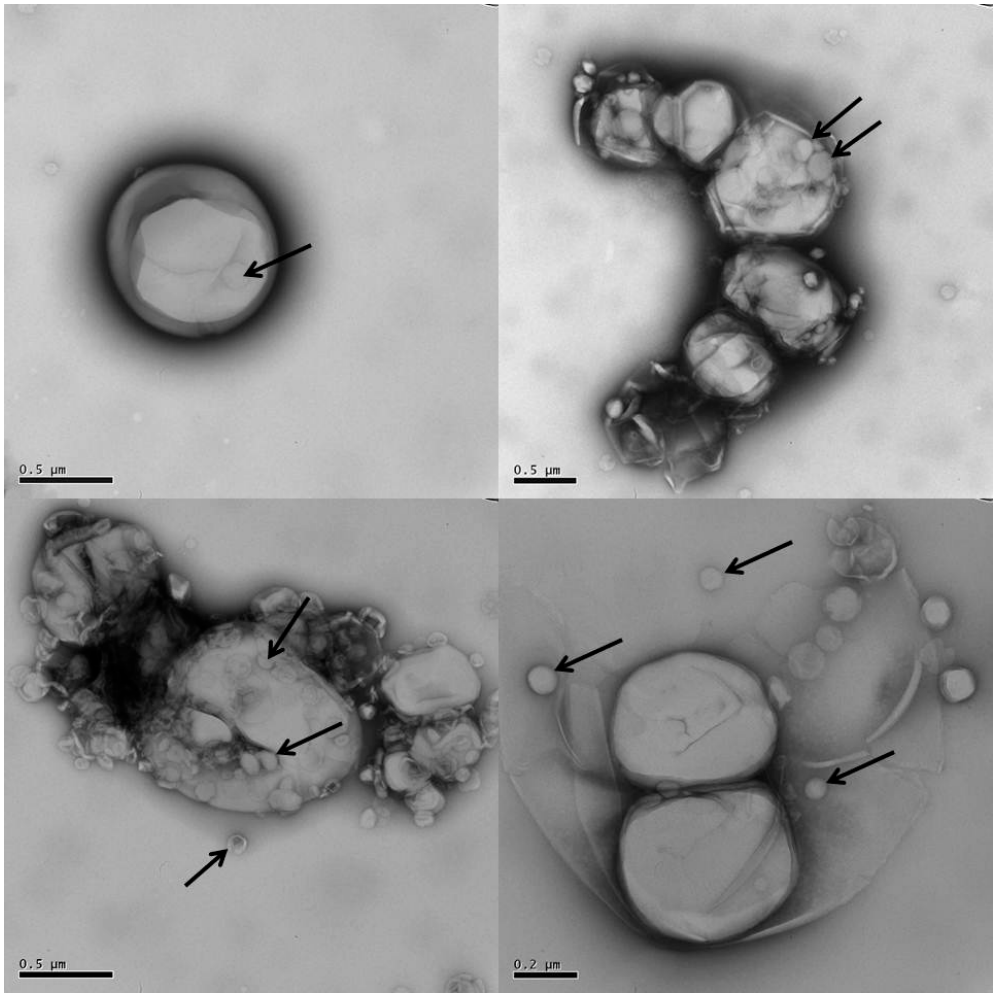

Figure 23. Several examples of eLiposomes imaged with negative staining. The images show the variety of vesicle diameters and appearances as observed by TEM. Emulsion droplets - the small round structures from 50 to 150 nm - were observed as well. Some of these emulsion droplets are indicated with black arrows.

6.3.2 CryoTEM imaging of eLiposomes

Figure 24 shows images of eLiposomes obtained by cryoTEM. The eLiposomes in Figure 24A-F were prepared using an emulsion with an average diameter of about 100 nm. The eLiposome in Figure 24G-I was prepared with an emulsion with an average diameter of about 475 nm. Emulsion droplets that were observed with cryoTEM retained the 3 possible appearances discussed previously (Chapter 5.4). Namely, they either appeared as dark electron dense spots, as very light spots or as a dark circle surrounding a lighter one.

Cryo-TEM allows the viewing of unstained specimens that are embedded in a layer of vitreous (non-crystalline) ice. Internal as well as external features can be seen because the method relies on the inherent contrast within the specimen, not on contrast provided by an applied stain. The fibrous structures in Figure 24 are the carbon-formvar support that lies on the copper grid and supports the vitreous ice layer. The micrographs show an outer lipid membrane, and emulsion droplets encapsulated inside of the membrane. In order to verify that the emulsion droplets were truly encapsulated, the microscope stage was rotated to -45°, 0°, and +45° to verify that the images of the emulsion droplets remained enclosed within the image of the lipid membrane.

Figure 24A-C shows an example of a 600-nm eLiposome containing 3 emulsion droplets ranging from 100 to 150 nm in size. As the stage is rotated through 90°, the images of these droplets remain inside of the liposomal boundary. Likewise, Figure 24D-F shows an example of a 500-nm eLiposome with two large emulsion droplets as well as a number of smaller emulsion droplets. This eLiposome also has additional polygonal structures encapsulated. These structures are most likely additional DPPC vesicles of various sizes that may have collapsed. Rotation of the microscope stage again demonstrates encapsulation of these structures inside of

the liposomal membrane. The sheet refolding technique showed the ability to encapsulate both large and small emulsion droplets as shown in Figure 24. Figure 24G-I shows an example of an 800-nm eLiposome with one 475-nm emulsion droplet as well as two smaller droplets.

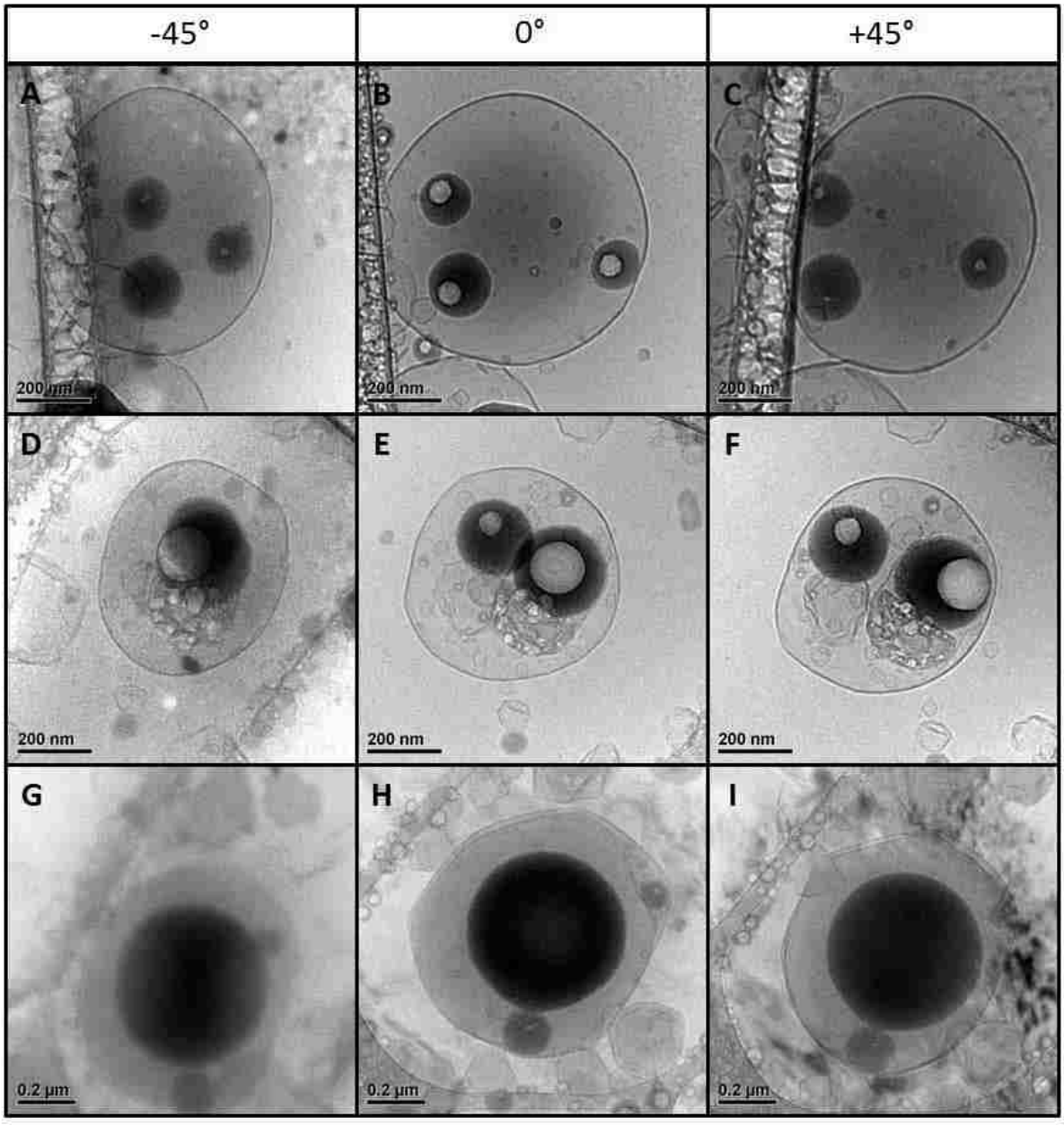

Figure 24. eLiposomes with encapsulated emulsion droplets imaged via cryoTEM. The microscope stage was rotated to -45° (A, D, and G), 0° (B, E, and H), and +45° (C, F, and I) to demonstrate encapsulation of droplets.

Freezing samples for cryoTEM and rotating the stage allowed a unique and novel method to verify encapsulation of the emulsion droplets. Being able to view the droplets inside of the eLiposome membrane at various angles provides solid proof of their encapsulation. In contrast, Figure 25 shows examples of non-encapsulated structures that appear to be inside of the liposome boundary until the stage is rotated. The arrows in Figure 25 identify droplets that might appear to be encapsulated. When rotated by 45°, however, these droplets can be observed to be outside of the membrane, and thus are not encapsulated.

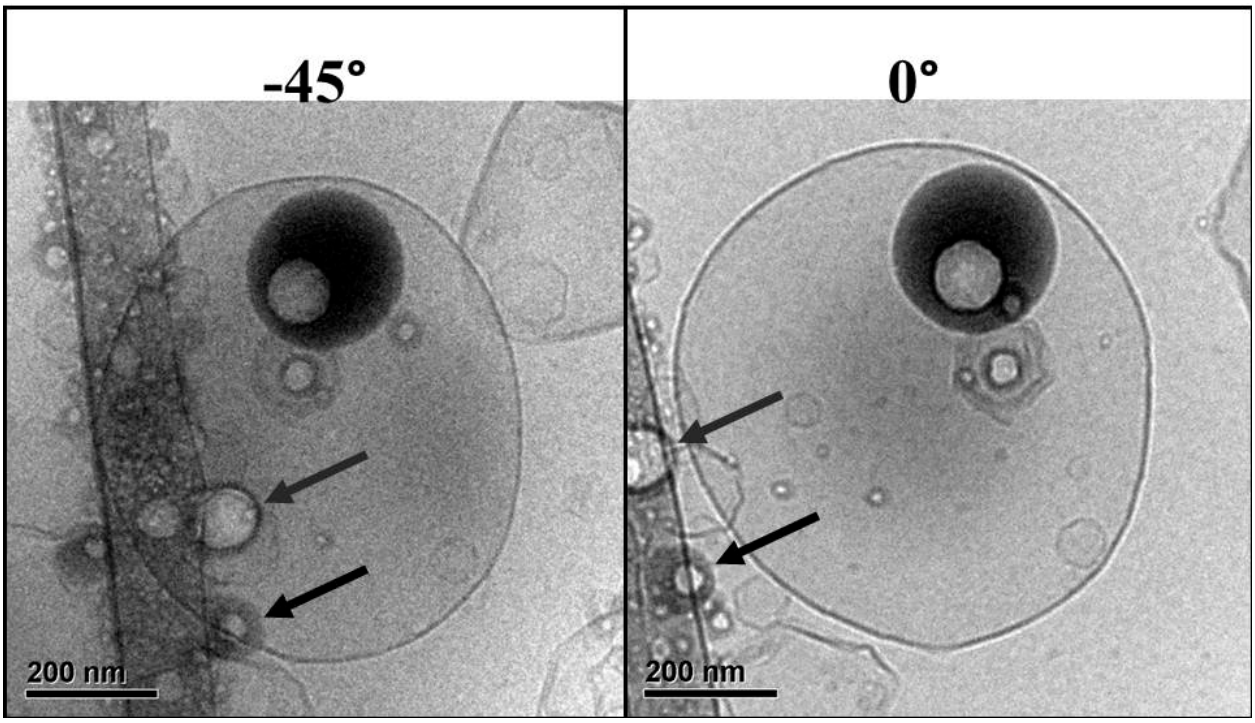

Figure 25. Cryo-TEM image of an eLiposome with internal and external emulsion droplets, as shown by rotating the microscope stage by 45°. The arrows in the left panel point to specific droplets that appear to be encapsulated (top arrow) or unencapsulated (bottom arrow). However, when rotated by 45° (right panel), both droplets are clearly outside of the membrane.

Figure 26 shows examples of control lipid vesicles, made by refolding lipid sheets without emulsion present. The appearance of the lipid membranes can be observed, as well as the absence of emulsion droplets that were present in the eLiposomes of Figure 24 and Figure

25. Similar to the structures observed in Figure 24D-F, there are again additional polygonal structures. Their presence in the absence of emulsion supports the possibility that these structures are DPPC vesicles that have partially collapsed and become polygonal.

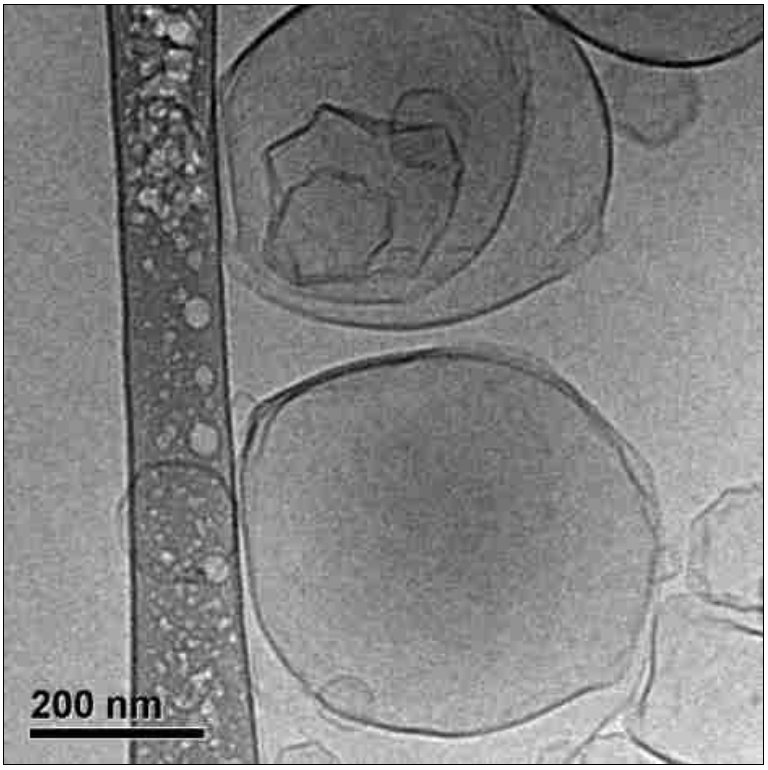

Figure 26. CryoTEM images of empty liposomes formed by refolding DPPC sheets without any emulsion present.

6.4 Ultrasound induced release of calcein from eLiposomes at 20 kHz

In order to test their efficacy as ultrasound-sensitive drug carriers, eLiposomes were exposed to 20 kHz ultrasound and compared to controls of conventional liposomes with and without external emulsion droplets. Concentrated (self-quenched) calcein was encapsulated inside of eLiposomes and some of the excess was removed from the outside so that the interior calcein would not add to the fluorescent signal generated by the solution. The eLiposome

sample was then diluted in a cuvette to create a system in which calcein released from the eLiposome would be detectable by a fluorometer and in which the released calcein would fall within the linear range of the fluorescence versus concentration plot for calcein. 20-kHz ultrasound was chosen in order to employ an acoustic system using a small-diameter tipped probe sonicator. This allowed the application of ultrasound within an optical cuvette. While ultrasound from a probe sonicator would not be used in a clinical setting due to focus and potential safety limitations, the work performed at 20 kHz has provided meaningful insights into the behavior of eLiposomes compared to conventional liposomes when exposed to ultrasound. Short exposure times and relatively low intensities were chosen in order to provide ultrasound exposures that would be comparable to higher frequency ultrasound administered in short pulses over a longer period of time. Most ultrasound parameters that were used correspond to mechanical indices below the FDA approved limit of 1.9. Acoustic droplet vaporization of perfluorocarbons has been reported by others at higher frequencies and similar mechanical indices [44, 45, 56]. In some cases higher intensities were employed in order to explore the behavior of eLiposomes and conventional liposomes at higher intensity.

6.4.1 Release at 20 kHz and short exposure times

When exposed to 20-kHz ultrasound for short exposure times, eLiposome samples demonstrated an increase in calcein release compared to controls. Figure 27 shows the percent released after 100 milliseconds (ms) of exposure to 20-kHz ultrasound (n=3, and error bars represent one standard deviation). Ultrasound intensity was varied between 0.5 W/cm^2 and 5 W/cm^2. eLiposomes were prepared with large (450 nm) and small (100 nm) emulsion droplets. The amount of release increased as ultrasound intensity increased. After 100 ms of ultrasound

exposure, PFC5 eLiposomes released approximately 3 to 4 times more calcein than controls at each intensity (Figure 27A). For example, at 5 W/cm^2 eLiposomes with large PFC5 emulsion droplets released 39% and eLiposomes containing small PFC5 emulsion droplets released 31%, while control samples released only 10% of the encapsulated calcein.

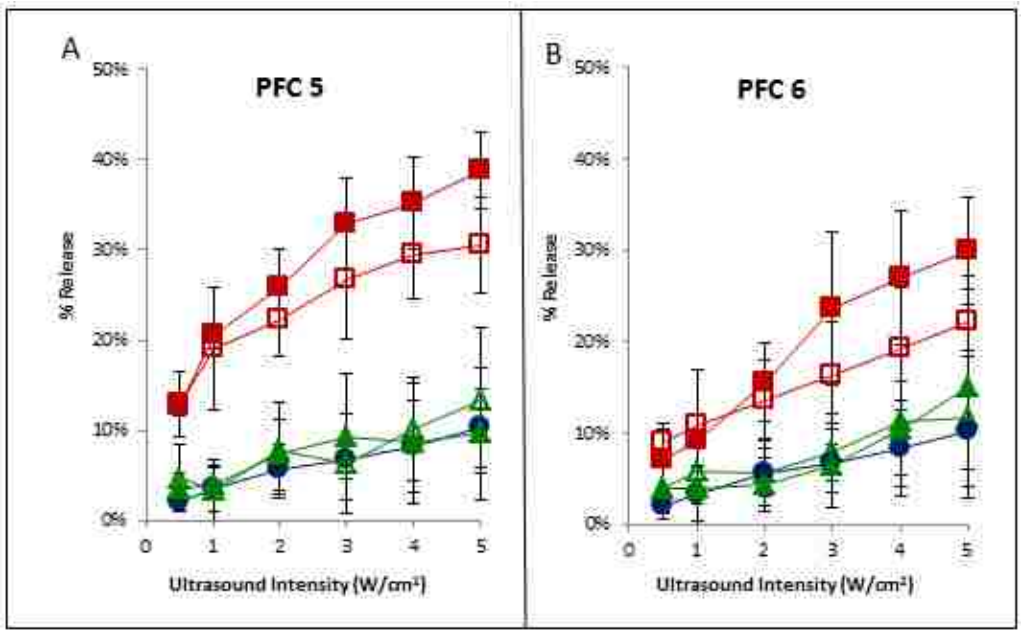

Figure 27. Calcein release from PFC5 eLiposomes (A) and PFC6 eLiposomes (B) when exposed to 100 milliseconds of 20-kHz ultrasound at varying intensities. Data is presented for eLiposomes with large (■) and small (□) emulsion droplets, control vesicles without emulsion (●), and control vesicles with large (▲) or small (△) emulsion droplets added to the exterior solution. Error bars represent ± 1 standard deviation.

PFC6 eLiposomes also released more of the encapsulated calcein than control samples. Figure 27B shows calcein release from PFC6 eLiposomes after 100 ms of insonation. While this release was slightly less than observed from PFC5 eLiposomes, PFC6 eLiposomes also released up to 3 times more calcein than control samples. After 100 ms at 5 W/cm^2, eLiposomes with 100-nm PFC6 emulsions released 22% of the available calcein. The difference in calcein release between controls and eLiposomes was statistically significant (Student t-test, $p < 0.05$) for both

PFC5 eLiposomes with both large and small emulsion droplets and PFC6 eLiposomes with large droplets.

Negative controls included both empty vesicles and empty vesicles with emulsion droplets added to the exterior. All of these negative controls released less of their encapsulated calcein than eLiposome samples. At 100 ms of ultrasound exposure there was no significant difference ($p > 0.05$) between empty control liposomes and empty liposomes with emulsion droplets added to the outside solution, regardless of emulsion size or material (see Figure 27). There was, however, more variability in samples with emulsion droplets added to the outside of the vesicles; empty vesicles had an average standard deviation of 3% compared to a standard deviation of 5% when emulsion droplets were added to the exterior solution (n=3). There was no significant difference ($p > 0.05$) between release from empty vesicles with small exterior droplets and release from empty vesicles with large exterior droplets.

After 100 ms of ultrasound exposure, the difference in calcein release from eLiposomes with large PFC5 emulsion droplets was statistically significant ($p < 0.05$) compared to eLiposomes with small droplets at intensities of 2 W/cm^2 or greater. In PFC6 samples exposed to 100 ms of ultrasound, the difference in calcein release from eLiposomes with large emulsion droplets was statistically significant compared to eLiposomes with small droplets at intensities of 3 W/cm^2 or greater.

6.4.2 Release at 20 kHz with longer exposure times

Although there was an increase in calcein release from eLiposomes compared to conventional liposomes after 100 ms, there was still a significant portion of the encapsulated calcein that was not released. While in theory droplet vaporization and associated drug release

could occur within the first few ultrasound cycles, there may be factors that delay ultrasound-induced release from eLiposomes. For this reason, calcein release at longer exposure times was also investigated. Because the motivation behind eLiposomes is to release a large amount of the encapsulated load at mild ultrasound parameters, exposure times were maintained relatively short (10 seconds and less). The objective of these experiments was to investigate a) if the time of exposure has a significant effect on release and b) if a majority of encapsulated calcein can be released from eLiposomes while maintaining mild ultrasound intensities and energy exposures.

The effect of time was investigated by varying the length of ultrasound exposure from 100 ms to 10 seconds for eLiposomes and control samples. This was performed at 0.5, 1, and 2 W/cm^2 (MI = 0.87, 1.22, and 1.73). Each data point presented is the mean of three measurements. Longer exposure times at higher intensities were not explored because the mechanical index would be greater than 1.9. Not only is this the limit imposed by the FDA, but these higher intensities would be more likely to produce significant heating and tissue damage at long exposure times.

eLiposomes containing large PFC5 emulsion droplets released the majority of their drug load when exposed to ultrasound for 10 seconds (see Figure 28). Samples exposed to 0.5, 1, and 2 W/cm^2 for this length of time released 75%, 94% and 94% of their drug load, respectively. This was much more release than observed in control samples, which released approximately 15%, 20% and 30% at these intensities. Furthermore, this release was quite rapid, with the majority of release taking place within the first 5 seconds of ultrasound exposure at all 3 intensities. While exposure at 2 W/cm^2 did not produce additional release after 10 seconds of exposure when compared to 1 W/cm^2, it should be noted that the amount of release after 1 and 5 seconds was significantly greater at the higher intensity. It should also be noted that although

PFC5 eLiposome samples with large droplets approached 100% release with these relatively mild ultrasound parameters, other eLiposome configurations did not.

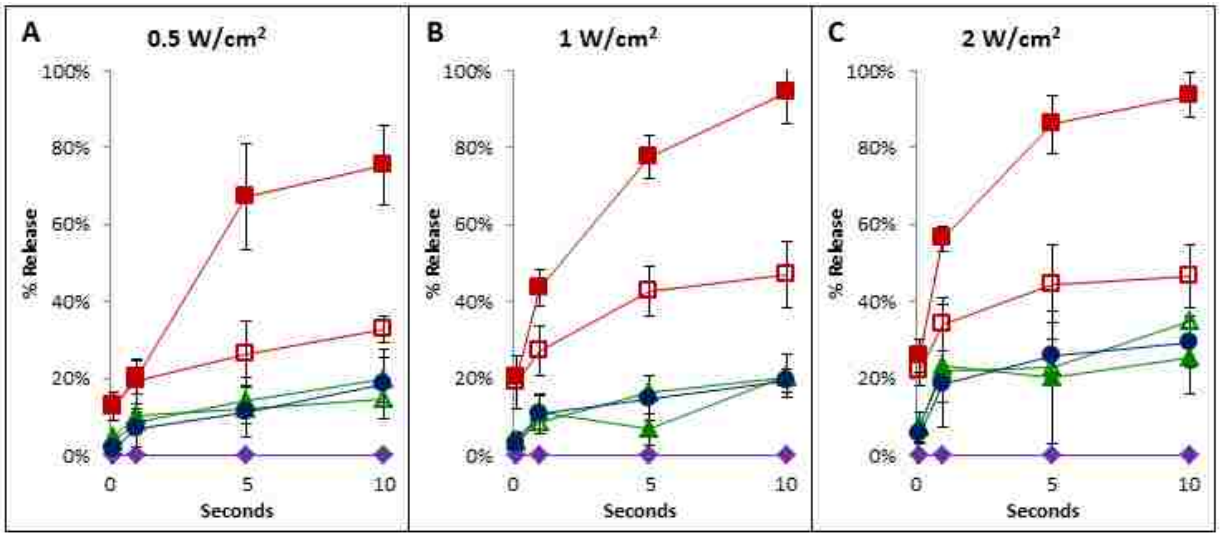

Figure 28. Calcein release from PFC5 eLiposomes when exposed to 20-kHz ultrasound at 0.5, 1 or 2 W/cm^2 for varying times. Data is presented for eLiposomes with large (■) and small (□) emulsion droplets, empty control vesicles (●), and empty vesicles with large (▲) or small (△) emulsion droplets added to the exterior solution. Sham experiments (no ultrasound) were also performed using eLiposomes with large droplets (◆). Error bars represent ± 1 standard deviation.

While the size of the emulsion droplets had only a small effect at 100 ms of ultrasound (Figure 28), this effect became more pronounced with PFC5 eLiposomes at longer ultrasound exposures; eLiposomes with large emulsion droplets released approximately twice as much calcein as those with small droplets after 10 seconds of ultrasound exposure at all three intensities tested. PFC5 eLiposomes with 450-nm emulsion droplets released approximately 75% of encapsulated calcein after 10 seconds of 0.5 W/cm^2 ultrasound while PFC5 eLiposomes with 100-nm droplets released only 33% after 10 seconds (Figure 28A). Similarly, PFC5 eLiposomes with 450-nm emulsion droplets released approximately 94% of encapsulated calcein after 10 seconds of 1 W/cm^2 or 2 W/cm^2 ultrasound while PFC5 eLiposomes with 100-nm

droplets released only 47% (Figure 28B and 28C). These differences between calcein release from eLiposomes with large PFC5 emulsion droplets and calcein release from eLiposomes with small PFC5 emulsion droplets were significant at all time points for samples exposed to 2 W/cm^2. The differences were significant for samples exposed to 1 W/cm^2 for 1 second or longer and for samples exposed to 0.5 W/cm^2 for 5 seconds or longer. Although not as much calcein release was observed from eLiposomes containing small droplets, this release was still significantly higher than control samples at every time point for each intensity.

The difference in release from eLiposomes with droplets of different sizes is most likely due to the additional Laplace pressure on the smaller droplets (see Chapter 5.1). At 0.5 W/cm^2, the ultrasound imposes a negative pressure of 122 kPa, sufficient to overcome the difference in the atmospheric pressure and the vapor pressure of PFC5 (see Table 1). This amplitude is also sufficient to overcome the Laplace pressure of approximately 36 kPa on a 450-nm droplet. However, this amplitude is not sufficient to overcome the Laplace pressure of approximately 160 kPa on a 100-nm droplet. At this smaller size 1 W/cm^2 is required to overcome the additional Laplace pressure, with ultrasound at this intensity imposing 173 kPa of negative pressure. The large difference observed in calcein release from eLiposomes with large and small droplets at 1 W/cm^2 and 2 W/cm^2 indicates that either additional pressure beyond the theoretical requirements is required to vaporize the droplets, or that a more consistent or violent vapor expansion may occur from the larger droplets.

Figure 29 shows the amount of calcein release from PFC6 eLiposomes at times varying from 100 ms to 10 seconds. PFC6 eLiposomes released more than controls with increasing time. At 0.5 and 1 W/cm^2, eLiposomes released approximately 2 times as much calcein as controls. Although the increase in release was much less than observed in PFC5 samples, these differences

were statistically significant ($p < 0.05$). At 2 W/cm^2, however, only eLiposomes with large PFC6 emulsion droplets showed a significant increase in calcein release compared to controls, with eLiposomes releasing about 1.5 times as much calcein. Calcein release from eLiposomes with small PFC6 droplets was not statistically different than control samples.

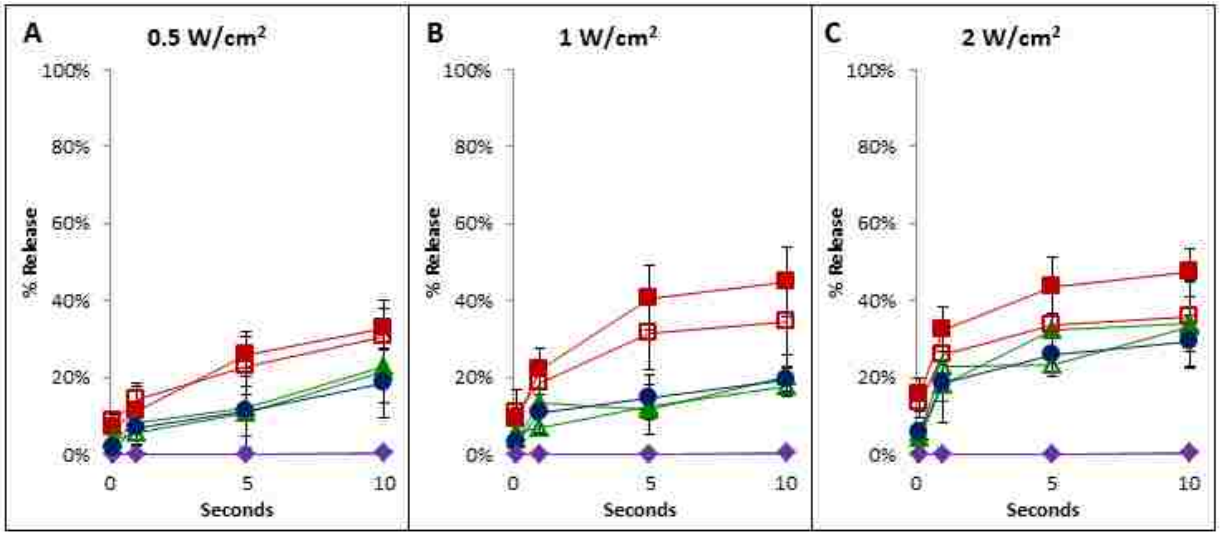

Figure 29. Calcein release from PFC6 eLiposomes when exposed to 20-kHz ultrasound at 0.5, 1 or 2 W/cm^2 for varying times. Data is presented for eLiposomes with large (■) and small (□) emulsion droplets, empty control vesicles (●), and empty vesicles with large (▲) or small (△) emulsion droplets added to the exterior solution. Sham experiments (no ultrasound) were also performed using eLiposomes with large droplets (◆). Error bars represent ± 1 standard deviation.

As intensity was increased from 1 W/cm^2 to 2 W/cm^2, there was no significant change in the amount of calcein released from any of the eLiposome samples. However, all control samples (both empty and with external emulsion) showed a statistically significant increase in calcein release at 10 seconds of ultrasound when the intensity was increased from 1 W/cm^2 to 2 W/cm^2. Similar to results shown in Figure 27, control samples with external emulsion droplets released the same average amount as empty negative controls, but showed more variability.

In contrast to PFC5-containing eLiposomes, there was no difference in calcein release from PFC6 eLiposomes with small droplets compared to those with large droplets when exposed to 0.5 W/cm^2 ultrasound (Figure 29A). There was, however, a statistical difference in PFC6 eLiposomes with small and large droplets when exposed to 1 W/cm^2 or 2 W/cm^2 for 5 seconds or longer (Figure 29B and 29C). While there was a statistical difference between these samples, the difference was much less pronounced than it had been with PFC5 eLiposomes. For example, after 10 seconds of exposure to 0.5, 1, and 2 W/cm^2, eLiposomes containing 450-nm PFC6 droplets released 31%, 45% and 47% of the encapsulated calcein, respectively. In comparison, eLiposomes with 100-nm PFC6 droplets released 31%, 34%, 36%.

Sham experiments were also performed to verify that the laboratory manipulations and procedures were not responsible for the observed calcein release. eLiposomes with large emulsion droplets were submitted to the entire release procedure, including insertion of the probe into the cuvette for the same amount of time as active experiments. These sham experiments showed no evidence of payload leakage or eLiposome damage from the experimental procedure (see Figures 28 and 29). The sham experiments suggest not only that the calcein release reported was not induced by the experimental procedure, but also seem to indicate that the eLiposomal membrane and structure are sufficiently robust to sequester a drug load despite various steps of manipulation and handling.

In order to verify that temperature was not playing a significant role in calcein release, the temperature of the solution was measured after sonication using a thermocouple. The temperatures of samples exposed to 2 W/cm^2 for 10 seconds increased by an average of approximately 4°C and those of samples exposed to 2 W/cm^2 for 5 seconds increased by approximately 2°C. Increased temperature was not measureable in other samples at lower

intensities and times. Because the resulting temperatures were still well below the transition temperature for DPPC and below the temperature at which the nano emulsions were extruded (50°C), it is unlikely that the increase in temperature was responsible for the increase in calcein release from eLiposomes or from control samples.

In summary, it was found that eLiposomes did release additional calcein with increasing ultrasonic exposure. This may partly be explained by the experimental setup; it is likely that there are regions of the cuvette, such as the sides and corners, where the effective ultrasound intensity is significantly lower than it is near the tip of the ultrasound probe. This would mean that eLiposomes in the low-exposure regions would require ultrasound-induced convection in the cuvette in order to be fully exposed to ultrasound; without full exposure to ultrasound at the expected intensity, eLiposomes may not release their contents. Therefore, the time necessary for mixing would increase to the amount of time required to observe full release. In order to test the rate of mixing, a small drop of calcein solution was carefully added to a corner of the cuvette and sonicated at intensities from 0.5 W/cm^2 to 5 W/cm^2. The amount of time required for the dye to mix throughout the cuvette and for the solution to become uniform in color was measured. At 0.5 W/cm^2, the dye was fully mixed through the cuvette after approximately 1.8 seconds. At 1 W/cm^2, the dye had mixed through the cuvette after approximately 0.5 seconds. Mixing at higher intensities was too rapid to measure. Therefore, the initially slower release at 0.5 W/cm^2 may have been, in part, due to inadequate mixing, but this is unlikely to have had a significant effect at longer times or at higher intensities. At times or intensities where there was inadequate mixing, it is possible that some vesicles were not exposed to full-intensity ultrasound because of the use of a continuous wave. In order to consider this possibility, large PFC5 and PFC6 eLiposomes were exposed to 100 ms bursts of 0.5 W/cm^2 and 1 W/cm^2 ultrasound at 1 Hz for 10

seconds, so that the overall exposure was equal to a single 1 second exposure. During the period where the ultrasound was "off" between the short bursts of ultrasound, the solution would have continued to mix, but overall ultrasound exposure was the same. Results from this comparison are presented in Table 3. Despite allowing more complete mixing in the pulsed sample, there was not a significant difference in calcein release between the pulsed sample and the continuous sample, suggesting that mixing did not have a large effect and the ultrasound may have efficiently induced release throughout the entire cuvette. Other effects, such as delayed vapor nucleation, likely play a role in the time-dependency of release.

Table 3. Large PFC5 and PFC6 eLiposomes were exposed to 1 second of 20-kHz ultrasound at 0.5 W/cm^2 and at 1 W/cm^2. The ultrasound was delivered continuously in some samples. Other samples were exposed to 10 bursts of 100 ms at a 1 Hz pulse repetition frequency. All values reported are the mean of 3 measurements ± 1 standard deviation.

	PFC5		PFC6	
	Continuous	Pulsed	Continuous	Pulsed
0.5 W/cm^2	20 ± 4%	23 ± 4%	11 ± 6%	14 ± 3%
1 W/Cm^2	44 ± 5%	43 ± 5%	22 ± 5%	21 ± 4%

It is also interesting that the amount of release often seemed to level off as time increased, especially at the higher intensities tested. For example, PFC5 eLiposomes with 100 nm emulsion droplets released 43% of encapsulated calcein in the first 5 seconds of ultrasound exposure, and only released an additional 4% with 5 seconds more of ultrasound. Similarly, negative controls released an average of 15% of encapsulated calcein in the first 5 seconds of ultrasound exposure, followed by only 4% additional release in the last 5 seconds of ultrasound. This suggests that an equilibrium point exists for both conventional liposomes and eLiposomes where increased time of exposure will not increase drug release. It is especially important that for most eLiposome samples, this leveling-off occurred well before 100% release. This could

be due to eLiposomes that did not initially contain emulsion droplets or due to a portion of the population from which emulsion droplets had escaped or dissolved away prior to complete membrane rupture and drug release. Either of these scenarios would lead to an intermediate level of release that is less than 100%, but more than that observed in control samples. As an additional explanation, there could be some eLiposomes that contain only very small emulsion droplets that, due to increased Laplace pressure, fail to vaporize at the ultrasound parameters applied.

6.4.3 Effect of eLiposome size

The eLiposomes described to this point have a diameter cutoff of approximately 800 nm. Eventually, in order to best take advantage of the EPR effect, eLiposomes will have to be formed with vesicle diameters between 150 and 300 nm. This lower range of sizes would help allow penetration of the eLiposomes into leaky tissues (such as cancerous tumors). Literature also suggests that the smaller vesicles may be internalized more readily into cells themselves. eLiposomes containing small-diameter emulsion droplets (75-100 nm) were extruded through 200 nm filters in order to explore the possibility of forming smaller eLiposomes. DLS confirmed that the resulting eLiposomes typically had average diameters of approximately 150-250 nm. Figure 30 shows an example of the data collected by DLS. In this example there are two distinct peaks, with the peak at 200 nm attributed to the outer membrane of the eLiposomes and the peak at 80 nm attributed to emulsion droplets. However, in contrast to the larger eLiposome samples, there were not always two obvious peaks when eLiposomes were extruded through 200 nm filters. Some samples had a bimodal distribution, while others did not. Those that did not often

had a very wide distribution. This is perhaps due to the DLS algorithm being unable to differentiate two distributions that are close to each other.

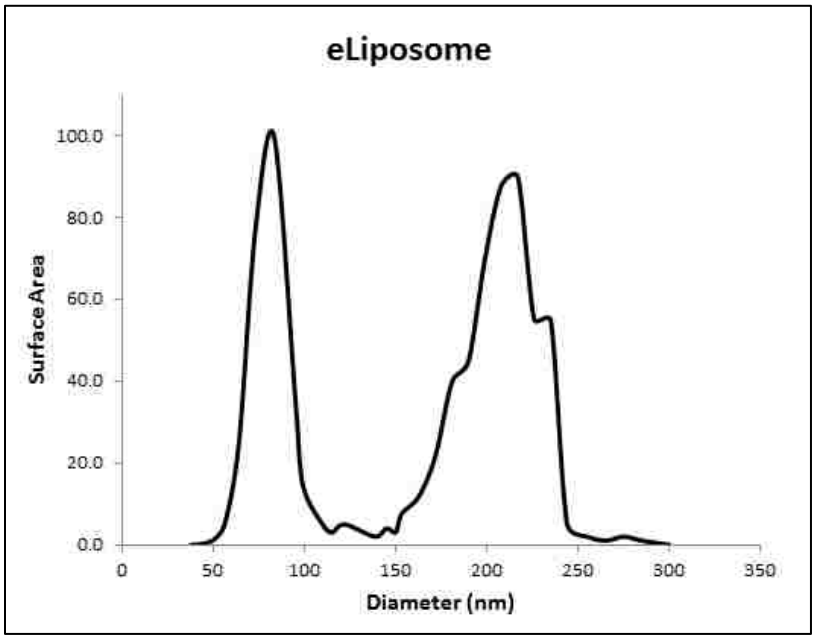

Figure 30. Typical DLS data from an eLiposome sample after extrusion through a 200 nm filter. The peak at 80 nm is assigned to emulsion droplets. The peak at 200 nm is assigned to the outer lipid membrane.

Figure 31A shows the amount of calcein released from 200 nm eLiposomes after 100 milliseconds (ms) of exposure to 20-kHz ultrasound. Each data point represents the average of 3 repeated experiments. Ultrasound intensity was once again varied between 0.5 W/cm^2 and 5 W/cm^2. In contrast to results with large eLiposomes samples (Chapter 6.4.1), there was not a significant difference in release from small PFC6 eLiposomes and small PFC5 eLiposomes after 100 ms of ultrasound exposure. After 100 ms at 5 W/cm^2, small eLiposomes released approximately 13% of the available calcein regardless of perfluorocarbon liquid, while control liposomes released approximately 4% of their calcein. The difference in calcein release between

controls and eLiposomes was statistically significant (Student t-test, $p < 0.05$) for both PFC5 and PFC6.

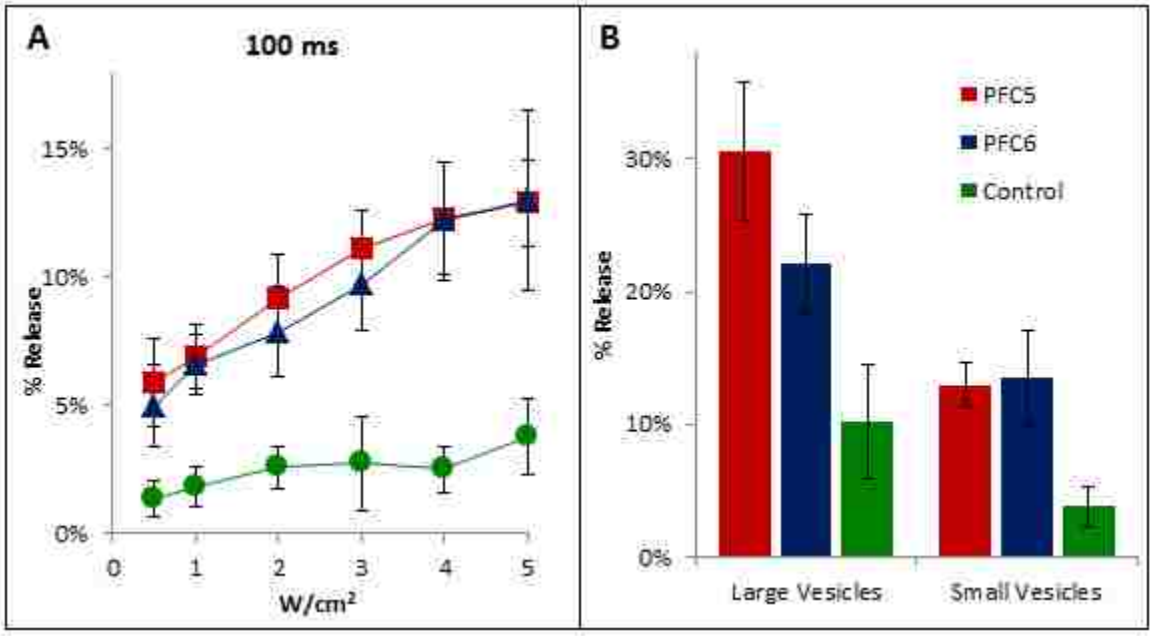

Figure 31. A) Calcein release from conventional DPPC liposomes (●) and from 200 nm eLiposomes formed with PFC5 (■) and PFC6 (▲) when exposed to 20 kHz ultrasound for 100 ms. B) Comparison of calcein release from large (800 nm) vesicles and from small (200 nm) vesicles after 100 ms of exposure to 20 kHz ultrasound at 5 W/cm^2.

Figure 31B provides a comparison between calcein release from large (800 nm) vesicles and small (200 nm) vesicles at 100 ms exposure time and 5 W/cm^2. All eLiposomes samples used for this comparison were prepared with 100 nm emulsion droplets. Small eLiposomes released less of the encapsulated calcein than their large counterparts. Large PFC5 eLiposomes with small droplets released 31% of the encapsulated calcein, while small PFC5 eLiposomes released 13%. Similarly, large PFC6 eLiposomes released 22% of the encapsulated calcein, while small PFC6 eLiposomes released 13%. The decrease in release was also consistent for

conventional liposome controls; large control liposomes also released more than small liposomes (10% and 4%, respectively).

This decreased ability of small eLiposomes to release their encapsulated load is also apparent with increased exposure times. Large PFC5 eLiposomes with small emulsion droplets exposed to 0.5, 1, and 2 W/cm^2 for 10 seconds released 33%, 47%, and 47% of their drug load, respectively (see Figure 28). In contrast, the amount of release from small PFC5 eLiposomes exposed to 0.5, 1, and 2 W/cm^2 for 10 seconds was approximately 18%, 25% and 27% (See Figure 32).

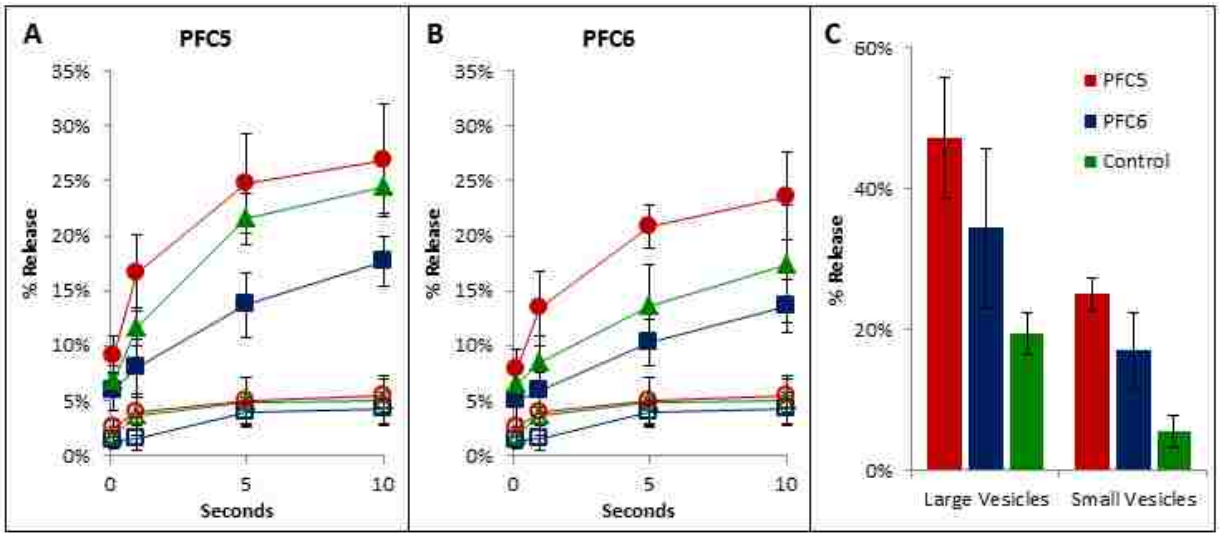

Figure 32. A) Calcein release from 200 nm PFC5 eLiposomes (solid symbols) and from conventional DPPC liposomes (empty symbols). 20-kHz ultrasound was applied at 0.5 W/cm^2 (blue squares), 1 W/cm^2 (green triangles) and 2 W/cm^2 (red circles). B) Calcein release from 200 nm PFC6 eLiposomes and from conventional DPPC liposomes. C) Comparison of calcein release from large (800 nm) vesicles with small emulsion droplets and from small (200 nm) vesicles after 10 seconds of exposure to 20-kHz ultrasound at 1 W/cm^2.

Figure 32A shows the amount of calcein release from small PFC5 eLiposomes at 0.1, 1, 5, and 10 seconds. Once again, the amount of release from eLiposomes increased with time. Ultrasound was applied at intensities of 0.5, 1, and 2 W/cm^2. As would be expected, release also

increased with intensity. At 1 and 2 W/cm^2, calcein release was quite rapid, with the majority of the released calcein escaping within the first 5 seconds. At 0.5 W/cm^2, release was more gradual and continued to increase significantly through 10 seconds. Control vesicles released much less of their encapsulated calcein compared to eLiposomes samples. Interestingly, there was no significant difference in small control samples exposed to 0.5, 1 or 2 W/cm^2 after 10 seconds, with all of these controls releasing approximately 5% of the encapsulated calcein. Furthermore, calcein release from small control liposomes seemed to have leveled off between 1 and 5 seconds.

While there was no difference between small PFC5 and PFC6 eLiposomes at short times (Figure 31), this difference was again apparent at longer times (see Figure 32). For example, while small eLiposomes containing PFC5 droplets released 18%, 25% and 27% of encapsulated calcein after 10 seconds of ultrasound at 0.5, 1 and 2 W/cm^2, small eLiposomes with PFC6 droplets released 13%, 17%, and 24% at these same intensities (see Figure 32B).

Similar to results at short times, small vesicles released less of the encapsulated calcein than large vesicles containing small emulsion droplets (see Figure 32C). At 10 seconds of exposure to 1W/cm^2 ultrasound, large PFC5 eLiposomes with small droplets released 47% of the encapsulated calcein, while small PFC5 eLiposomes released 25%. Similarly, large PFC6 eLiposomes released 34% of the encapsulated calcein, while small PFC6 eLiposomes released 17%. Large control liposomes also released more than small liposomes at an exposure time of 10 seconds (19% and 6%, respectively).

Because small conventional liposomes also released less than their large counterparts, there was still a significant increase in release from small control liposomes to small eLiposomes. In some cases, this increase was more substantial than this comparison at large

vesicle sizes. After 100 ms of ultrasound exposure small eLiposomes with PFC5 or PFC6 released approximately 3 to 5 times more calcein than control samples at the intensities tested (Figure 31A). Interestingly, this ratio is the same as was observed with large eLiposomes with short exposure times. After 10 seconds at 1 W/cm^2, small PFC5 eLiposomes released 3 to 6 times as much calcein as controls and small PFC6 eLiposomes released 2 to 4 times as much calcein compared to controls. Because the motivation for producing smaller vesicles would be to take advantage of the EPR effect, comparisons among samples of similar size are perhaps the most relevant comparisons.

It is interesting that size has a significant effect on release from both the eLiposome and control liposome samples. This tendency of small liposomes to be less-susceptible to ultrasound than larger liposomes has been previously documented [80, 135]. While the role that size plays on the interactions between ultrasound and liposomes is not fully understood, it has been hypothesized that smaller liposomes lack the ability to elongate and break up when exposed to the shear forces provided by cavitating bubbles [86]. This previously observed phenomenon may play a role in the decreased release from eLiposomes at smaller sizes. However, while this is likely a contributing factor, it is possible that other factors play a role as well. For example, smaller vesicles will have fewer encapsulated emulsion droplets and therefore the inability of encapsulated droplets to combine into larger droplets or bubbles

6.4.4 Effect of temperature

In order for emulsions and eLiposomes to be useful as drug delivery vehicles, their stability and behavior at 37°C (biological temperature) must also be explored. As mentioned previously, emulsion droplets persisted despite being heated during processing. While

occasional foaming did occur when heating to 50°C for extrusion, this foaming was limited and controlled by allowing the extruder to cool before removing the syringes. The persistence of emulsion droplets was verified by centrifuging the solution on a sucrose cushion and observing the collection of a pellet below the dense sucrose phase. Because eLiposome stability at 37°C is of particular interest, the stability and ability to sequester calcein at 37°C was examined with fluorometry. It was determined that approximately 3 minutes were required to warm the solution to 37°C in a water bath. eLiposome samples were diluted in 2 mL of buffer solution as described in Chapter 4.2.8. The fluorescence was measured initially after dilution and the sample was placed in a heated water bath for 3 minutes. After 3 minutes, no evidence of calcein release could be observed. The sample was heated and fluorescence was again measured after 10, 20, and 30 minutes of heating. This process was repeated for large eLiposomes containing large PFC5 or large PFC6 droplets and for small eLiposomes containing small PFC5 or small PFC6 droplets. No significant amount of calcein release could be detected in any of these measurements. The eLiposomes were lysed with Triton X-100 after the 30 minute fluorescence measurement to verify the encapsulation of calcein. In all samples the fluorescence increased with the addition of Triton X-100, indicating that the vesicles had remained intact and continued to sequester calcein throughout the heating process.

Release experiments were repeated with heated samples. The optical cuvette was heated in a 37°C water bath for 3 minutes and transferred to the fluorometer quickly to avoid cooling before the measurement. After a 10 second baseline was collected, the sample was moved back to the heated water bath and sonicated while being heated. Fluorescence was again measured and the sample was lysed with Triton X-100 to measure 100% release. Figure 33A shows the percent released from 800 nm eLiposomes with large emulsion droplets after 100 milliseconds

(ms) of exposure to 20-kHz ultrasound when heated to 37°C. Ultrasound intensity was once again varied between 0.5 W/cm^2 and 5 W/cm^2. After 100 ms of ultrasound exposure at 5 W/cm^2, large PFC5 eLiposomes released approximately 49% of the available calcein and large PFC6 eLiposomes released 31%. Large control liposomes released approximately 12% of their calcein.

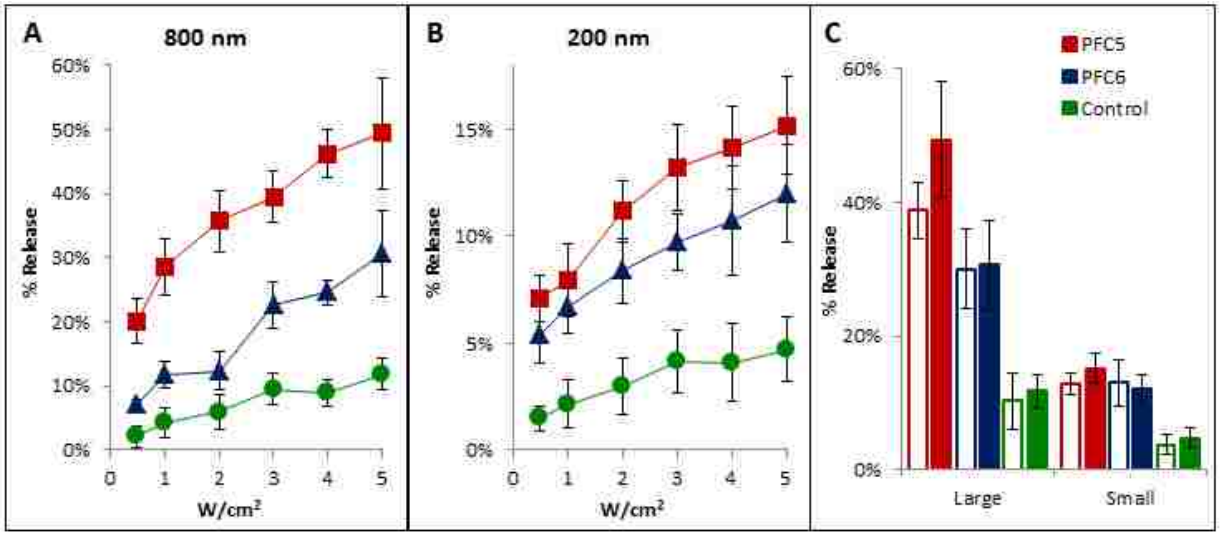

Figure 33. Calcein release at 37°C from 800 nm vesicles (A) and from 200 nm vesicles (B) exposed to 100 ms of ultrasound at intensities from 1 to 5 W/cm^2. Experiments were performed on PFC5 eLiposomes (■), PFC6 eLiposomes (▲) and conventional liposomes (●). (C) Comparison of calcein release from eLiposomes and control liposomes at room temperature (empty bars) and at 37°C (filled bars).

Figure 33B shows the percent released from 200 nm eLiposomes after 100 milliseconds (ms) of exposure to 20-kHz ultrasound. While small eLiposomes at room temperature had not shown a difference in release from PFC5 and PFC6 samples, this difference was again evident at elevated temperature after 100 ms of ultrasound exposure. Small PFC5 eLiposomes released approximately 15% of the available calcein and small PFC6 eLiposomes released 12%. Small control liposomes released approximately 5% of their calcein. The difference in release between

PFC5 and PFC6 eLiposome samples at 37°C was statistically significant for both large and small vesicles (Student t-test, $p < 0.05$), as well as each eLiposome sample compared to control samples.

Figure 33C compares the release of calcein from large or small vesicles at 37°C to release at room temperature after 100 ms of exposure at 5 W/cm^2. Empty bars represent room temperature release measurements and solid bars represent calcein release at 37°C. All reported values are the average of three measurements and error bars represent ± 1 standard deviation. There was not typically a significant increase in calcein release from the eLiposomes or from conventional liposomes as temperature was increased from room temperature to 37°C. However, the difference in release from large PFC5 eLiposomes was significant as temperature was increased from room temperature to 37°C.

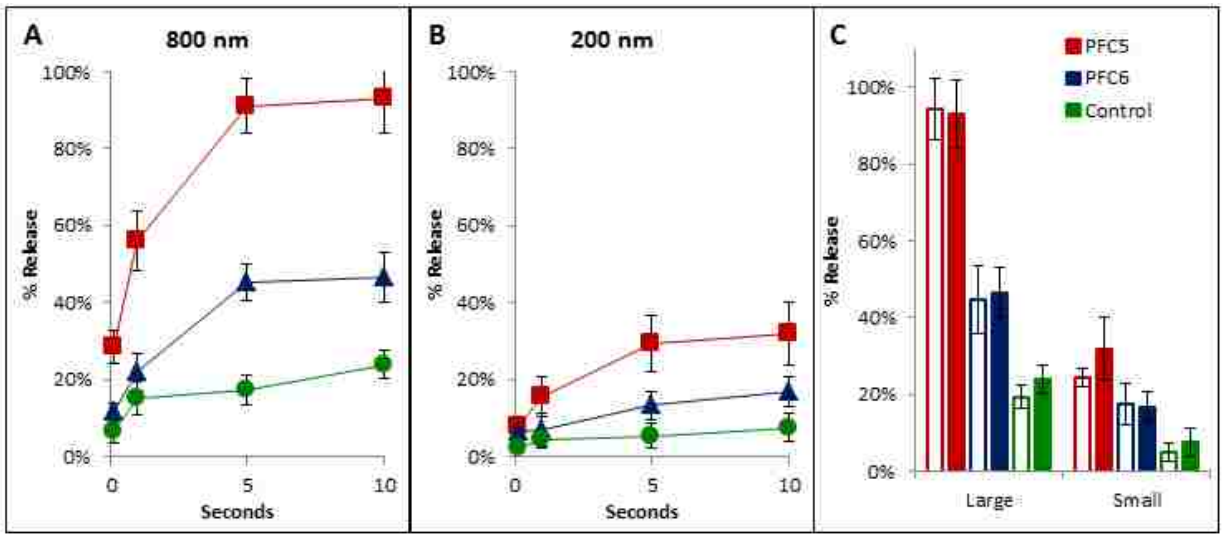

Figure 34. Calcein release from 800 nm vesicles (A) and from 200 nm vesicles (B) exposed to 1 W/cm^2 ultrasound at 37°C. Exposure time was varied from 100 ms to 10 seconds. Experiments were performed on PFC5 eLiposomes (■), PFC6 eLiposomes (▲), and conventional liposomes (●). (C) Comparison of calcein release from eLiposomes and control liposomes at room temperature (empty bars) and at 37°C (filled bars).

Figure 34A shows the percent of calcein released from 800 nm eLiposomes with large emulsion droplets exposed to 1 W/cm^2 ultrasound at 37°C. Exposure time was varied from 100 ms to 10 seconds. At 10 seconds, large PFC5 eLiposomes released approximately 93% of the available calcein and large PFC6 eLiposomes released 47%. Large control liposomes released approximately 24% of their calcein. Figure 34B shows the percent released from 200-nm eLiposomes exposed to 20-kHz ultrasound at 1 W/cm^2 at 37°C. Despite the increased temperature, small eLiposomes still released much less of their encapsulated calcein compared to large eLiposomes (Figure 34A and 34B). Small PFC5 eLiposomes released approximately 32% of the available calcein and small PFC6 eLiposomes released 17%. Small control liposomes released approximately 8% of their calcein.

Figure 34C compares the release of calcein from large or small vesicles at 37°C to release at room temperature after 10 seconds of exposure to ultrasound at 1 W/cm^2; empty bars represent room temperature release measurements and solid bars represent calcein release at 37°C. Interestingly, after 10 seconds of ultrasound exposure at 1 W/cm^2 there was little or no increase in release at 37°C compared to room temperature in any of the samples. Only control liposomes and small PFC5 eLiposomes released statistically more calcein at 37°C, and increases were relatively small. While Figures 33C and 34C provide only a comparison at 5 W/cm^2 after 100 ms and at 1 W/cm^2 after 10 seconds, these results were typical for all data points collected; generally, PFC5 eLiposomes released more calcein at the higher temperature while PFC6 eLiposomes did not. However, while these differences in release from PFC5 eLiposomes were statistically significant, they were only noteworthy in large PFC5 eLiposome samples at short exposure times.

It is interesting that release did not increase more despite increasing temperatures. Because increasing the temperature raises the vapor pressure of the perfluorocarbon liquids, the ultrasound pressure requirements should decrease. The vapor pressure of PFC5 increases from about 84 kPa to about 135 kPa, a 60% increase. The vapor pressure of PFC6 increases from about 28 kPa to 48 kPa, a 79% increase. At the increased temperature, lower ultrasound intensities should be required to overcome the droplet vapor pressure and induce vaporization. For example, at 24°C, ultrasound intensities of 0.5 and 1 W/cm^2 are below the theoretical threshold for vaporization of 100-nm droplets. However, at 37°C, 1 W/cm^2 is above the theoretical threshold for vaporization. Also, the higher temperature was expected to increase release even at other intensities tested due to a more substantial sub-pressurization that is expected to aid in gas nucleation by increasing the thermodynamic potential for vaporization. While the trends observed in the experimental results did somewhat mirror this hypothesis, the increase in release was not as significant as expected. Furthermore, there was no obvious jump in release from small droplets at 1 W/cm^2 as the temperature increased. It is possible that the lack of sharp thresholds and jumps in release is due to the size distribution of droplets. Threshold calculations assume a homogeneous size, but there are larger and smaller droplets. These droplets would therefore have different thresholds for vaporization and could result in the observed lack of expected thresholds in the data. Once again, gas nucleation is a potential limiting factor, and a comparison of short and long ultrasound exposures may suggest that the time required to nucleate a gas is more important than providing additional driving force.

6.5 Ultrasound induced release of calcein from eLiposomes at 525 kHz

As mentioned previously, 20-kHz ultrasound would not typically be used in a medical setting because low frequency ultrasound is more difficult to focus within the body and is often cited as having health concerns [136-138]. The experiments at 20 kHz that are detailed in this dissertation provide insight into eLiposome and emulsion behavior compared to conventional liposomes when exposed to ultrasound. Furthermore, the results are relevant for research and laboratory applications. Ultrasound parameters such as intensity, mechanical index, and energy exposure were chosen to be comparable to medically relevant parameters. However, experiments at a higher frequency are also needed to verify the potential of eLiposomes to release drugs at higher frequencies and to compare this release to comparable ultrasound parameters at low frequency. It is expected that drug release will be similar at similar energy exposures or at similar ultrasound intensities.

Ultrasound used in medical setting is typically 500 kHz and above; frequencies of 700 kHz to 3 MHz are used for therapeutic and drug delivery applications while frequencies above 1 MHz are used in imaging [139]. The HIFU transducer used in this study operates at 525 kHz. At this frequency, ultrasound can be focused to a focal point of approximately 1.5 mm, making it practical for clinical drug targeting applications. Short exposure times and/or pulsed ultrasound were used in order to mimic medically relevant ultrasound parameters that would avoid heating and tissue damage. Pulses of 1,000 cycles/pulse were applied at a pulse repetition frequency of 20 Hz. For some samples, single pulses of 50,000 cycles were used for short single burst exposures.

6.5.1 Exposure to 525 kHz at varying times and intensities

Release experiments were performed similar to those at 20 kHz. However, after collecting the initial fluorescence baseline, the sample was transferred to the bulb of a 3 mL transfer pipet. The bulb containing the sample was placed at the focal point of ultrasound within a water bath. Short exposure times and/or pulsed ultrasound were used to maintain similarity to parameters typically used in medical applications to avoid heating and tissue damage. Furthermore, it is likely that our experimental setup was prone to acoustic decoupling when continuous wave ultrasound at high intensities was applied.

Figure 35 shows the amount of calcein release from small (200 nm) eLiposomes containing PFC5 emulsions and control vesicles when exposed to 525 kHz ultrasound at 5 W/cm^2 and 35 W/cm^2. These intensities were chosen because the mechanical indices are low enough to make these parameters medical relevant (MI = 0.53, and 1.41, respectively) and relatively low intensity; the FDA allows ultrasound to be applied at mechanical indices up to 1.9. Pulses of 1000 cycles were applied at a pulse frequency of 20 Hz. As mentioned in Chapter 5.5.2, acoustic decoupling was not detected at these parameters. The time of exposure was varied from 2 seconds to 30 seconds, making the overall energy exposure relatively low.

The amount of release increased with exposure time, with PFC5 eLiposomes releasing 29% and 50% of the encapsulated calcein after 30 seconds of exposure to 5 W/cm^2 and 35 W/cm^2, respectively. In comparison, control liposomes released 14% and 16% of the calcein at these same intensities. In general eLiposome samples released 2 to 3 times as much of their encapsulated load compared to control vesicles when exposed to 5 W/cm^2 and 3 to 3.5 times as much of the calcein when exposed to 35 W/cm^2.

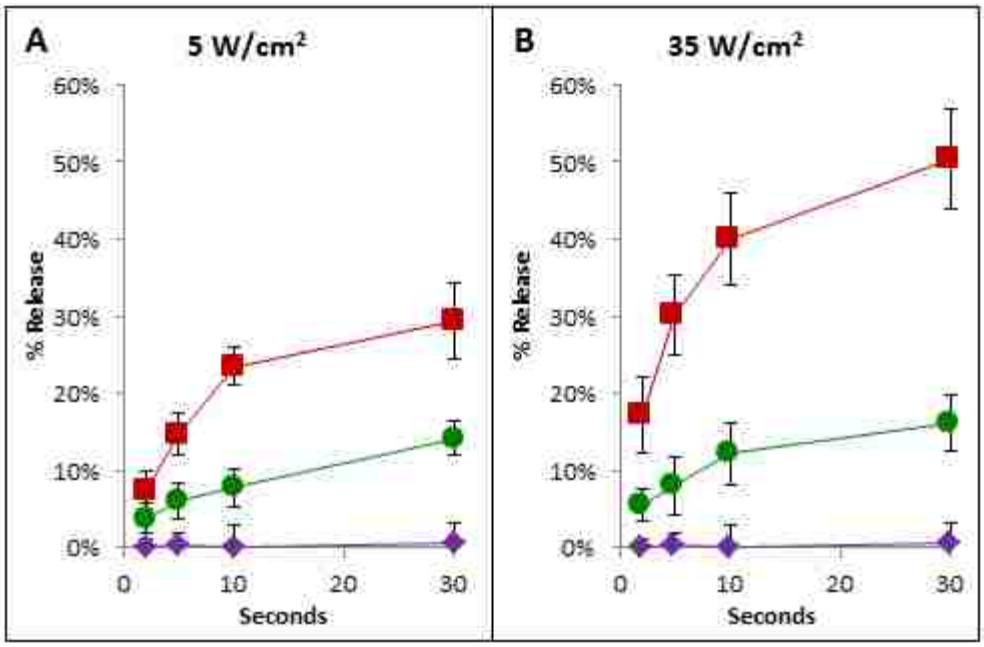

Figure 35. Calcein release from small (200 nm) PFC5 eLiposomes (■) and from control liposomes (●) at 525 kHz. Ultrasound was applied at 5 W/cm^2 and at 35 W/cm^2 in 1000 cycle bursts at a pulse frequency of 20 Hz. Exposure time was varied from 2 to 30 seconds. Sham experiments were performed by exposing samples to the complete procedure but without ultrasound exposure (◆). Each point represents the average of triplicate measurements and error bars represent ± 1 standard deviation.

The differences between calcein released from eLiposomes compared to control samples were significant at each point tested. The increase in calcein released from eLiposomes as the intensity was increased from 5 to 35 W/cm^2 was also significant at each point examined. Interestingly, there was not a significant increase in calcein release from control vesicles as ultrasound intensity was increased.

Sham experiments were also performed in which samples were handled the same as active experiments, including the length of time that they were left in water bath, but without ultrasound exposure (see Figure 35). Release from sham experiments was negligible.

6.5.2 Effect of intensity at 525 kHz and comparisons to acoustic phenomena

In order to further explore the effect that intensity of 525 kHz ultrasound has on eLiposomes, ultrasound intensity was varied from 5 W/cm^2 to 425 W/cm^2. The intensities tested were chosen to examine the effect of intensity as well as to allow a comparison to the acoustic phenomena described in Chapter 5.5.2. Figure 36 shows calcein release from PFC5 and PFC6 eLiposomes as well as control liposomes when exposed to 10 seconds of 525 kHz ultrasound at 5, 35, 150, and 425 W/cm^2. At 5 W/cm^2 and at 35 W/cm^2, there was a significant contrast between eLiposome samples and control samples, with eLiposomes releasing approximately 3 times as much of the encapsulated calcein. At 150 W/cm^2, eLiposomes released only slightly more calcein than controls (approximately 1.3 times as much); at 150 W/cm^2, this difference was only significant between PFC5 eLiposomes and conventional liposomes. At 425 W/cm^2 there was no significant difference in the release from eLiposomes and from control samples. It is worth noting that the mechanical indices at 5 and 35 W/cm^2 are within limits set by the FDA, while 150 and 425 W/cm^2 are beyond these limits.

Referring back to Figure 16, 5 W/cm^2 is below the threshold for the detection of higher harmonics. As these peaks are typically associated with stable cavitation of bubbles, the fact that there is a significant increase in calcein release from eLiposomes compared to control liposomes at this intensity suggests that droplet vaporization and expansion may begin to occur before stable cavitation is detectable. At 5 W/cm^2, both PFC5 and PFC6 are expected to be well beyond the thresholds for vaporization based on their vapor pressures and the calculation of Laplace pressure compared to ultrasound pressure amplitude (see Chapter 6.4.2). It appears from release data at this intensity that vaporization is indeed occurring. This vaporization and expansion could be partially or completely reversible and may not lead to a consistent cavitating bubble.

Alternatively, bubble oscillations at this intensity could simply be below the thresholds for detection of the higher harmonic peaks.

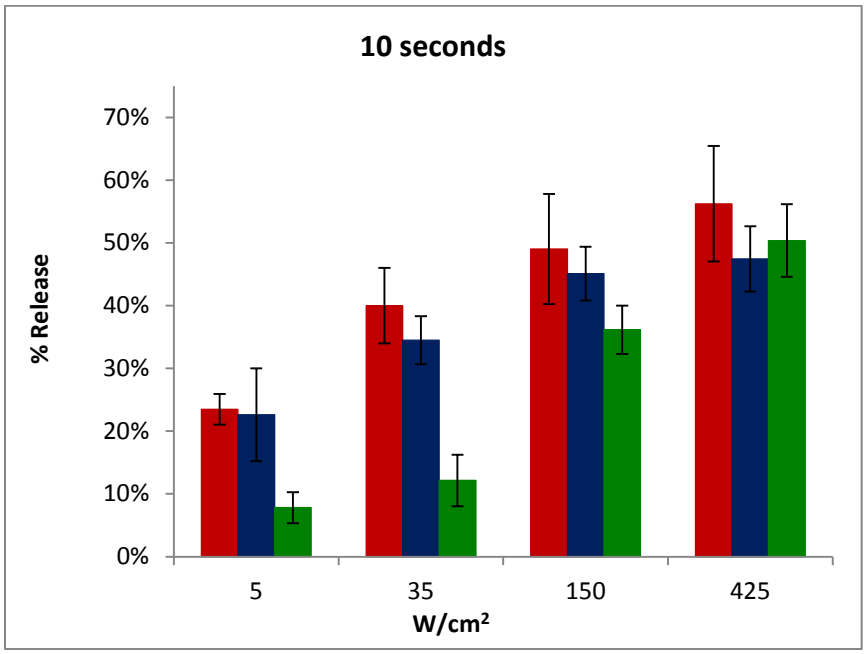

Figure 36. Calcein release from small PFC5 eLiposomes (Red bars), PFC6 eLiposomes (blue bars), and conventional liposomes (Green bars) as ultrasound intensity is increased from 5 to 425 W/cm^2. Error bars represent ± 1 standard deviation (n=3).

35 W/cm^2 is above the threshold for higher harmonic peaks for both emulsion samples, but below the threshold for water. The observation of these peaks in emulsion samples provides evidence of persistent stable cavitation, suggesting that droplets have vaporized to form persistent bubbles. The absence of higher harmonic peaks in the control samples at this intensity (Figure 16) suggests that gas nucleation and cavitation does not occur in water at these intensities. The fact that there is still a large difference in calcein release from eLiposomes and control vesicles provides further evidence that the expanding and cavitating perfluorocarbon phase is responsible for calcein release from eLiposomes. Furthermore, the difference in calcein

release from eLiposome samples exposed to 5 W/cm^2 and 35 W/cm^2 is significant. This suggests that the presence of a persistent gas phase and cavitation (as evidenced by the observation of higher harmonic peaks in samples with emulsions) likely results in increased calcein release.

150 W/cm^2 is above the threshold for higher harmonics in all samples and above the threshold for the sub-harmonic peak in the emulsion samples. The presence of the higher harmonic peaks in the control samples at this intensity seems to correlate well with a large increase in release from the control samples (see Figure 36), suggesting that consistent cavitating bubbles are formed at this intensity and contribute to calcein release from conventional liposomes. This result is in agreement with results at lower intensities in the eLiposome samples; calcein release seems to be most strongly correlated with the expansion and cavitation of a gas phase. As intensity was increased from 35 W/cm^2 to 150 W/cm^2 there was a slight increase in release from eLiposome samples, suggesting that the onset of collapse cavitation contributes only slightly to calcein release (sub-harmonic peaks were observed in emulsion samples at 150 W/cm^2, suggesting more chaotic cavitation and the onset of collapse cavitation). The majority of the release seems to be correlated with the presence of a vapor phase, and is not as strongly dependent on collapse cavitation.

Lastly, when ultrasound is applied at 425 W/cm^2, which is above the thresholds for collapse cavitation, there was no observable difference in release between samples. At this intensity, all samples are expected to be well above the threshold for collapse cavitation. The difference in release at 150 W/cm^2 and 425 W/cm^2 was only significant for PFC5 eLiposomes and for control samples. Although significant, this increase in release was not as substantial as increases between other intensities, especially for control samples. This evidence further

supports the hypothesis that while collapse cavitation may slightly enhance release from liposomes, release is most strongly correlated with stable cavitation.

6.5.3 Effect of size at 525 kHz

It was previously reported that vesicle and emulsion size had a significant effect on release from eLiposomes and conventional liposomes at 20 kHz. In order to determine if vesicle size had a similar effect at 525 kHz, large (800 nm) eLiposome samples were prepared with small (100 nm) emulsion droplets of both PFC5 and PFC6. Large control samples were also prepared, and samples were exposed to 525 kHz ultrasound at 5 W/cm^2 and 35 W/cm^2 for 10 seconds. Figure 37 compares the release of calcein from these large vesicles to release from small (200 nm) vesicles.

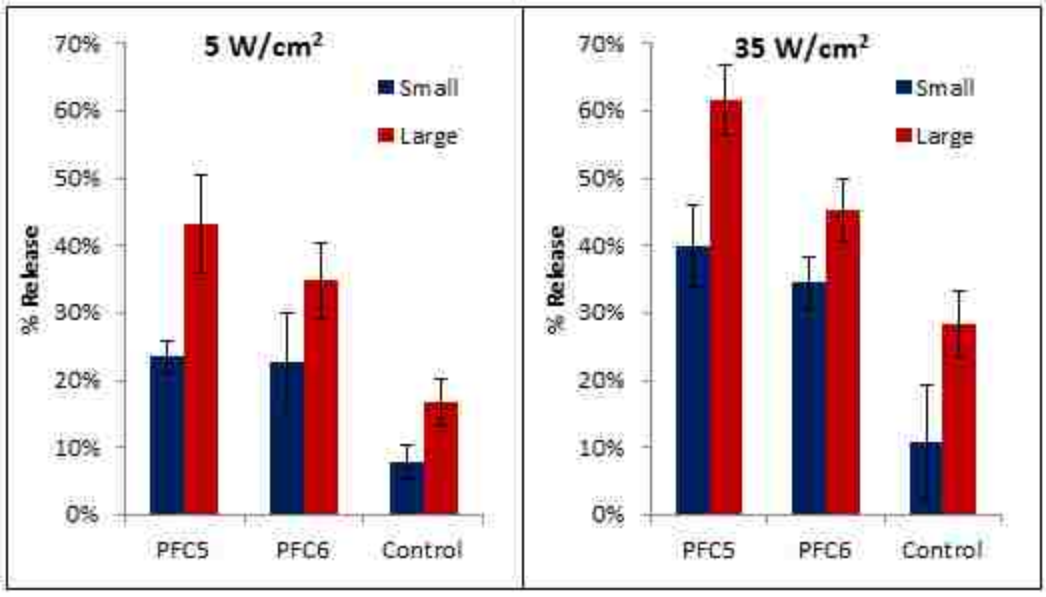

Figure 37. Comparison of calcein release from large (800 nm) and small (200 nm) eLiposomes and from large and small control vesicles when exposed to ultrasound at 525 kHz.

Similar to results at 20 kHz, the large eLiposomes released significantly more calcein than their smaller counterparts. This pattern was consistent at 5 and 35 W/cm^2. This increase in release with vesicle size was slightly smaller at 525 kHz; large eLiposomes released 1.3 to 1.8 times as much calcein as small eLiposomes when exposed to 525 kHz compared to approximately 1.6 to 2.4 times as much when exposed to 20 kHz. Large control vesicles also released significantly more calcein than small control vesicles; large conventional liposomes released 2 to 2.5 times as much calcein at 525 kHz compared to approximately 2.5 to 3.5 times as much at 20 kHz.

6.5.4 Short exposure times and comparisons to lower frequency

Ultrasound at 525 kHz was also applied in a single burst of 50,000 cycles and at low intensities in order to investigate the ability of short exposures (approximately 100 ms) at low intensity to induce calcein release from the eLiposomes. These parameters also allow direct comparison to calcein release at 20 kHz ultrasound with similar parameters. Acoustic decoupling was not detected from these single burst exposures; the short burst of ultrasound was probably not enough time to form a field of bubbles.

Figure 38 shows calcein release from small PFC5 and PFC6 eLiposomes as well as control liposomes when exposed to a single 100 ms pulse of 525-kHz ultrasound. There was a significant increase in release from the control vesicles to eLiposome samples; PFC5 eLiposomes released approximately 5 times as much calcein compared to control liposomes and PFC6 eLiposomes released approximately 4 times as much. The difference between calcein release from eLiposome samples and control samples was significant at each intensity tested.

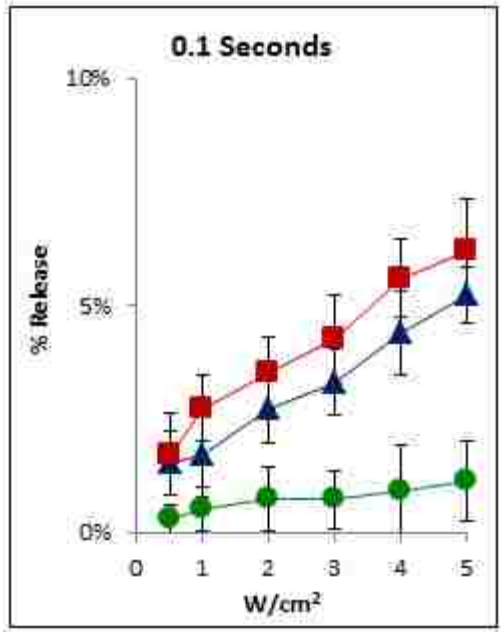

Figure 38. Calcein release from small (200 nm) PFC5 eLiposomes (■), PFC6 eLiposomes (▲) and from control liposomes (●). 525 kHz Ultrasound was applied in a single 50,000 cycle burst and intensity was varied from 0.5 W/cm^2 to 5 W/cm^2. Each point represents the average of triplicate measurements and error bars represent ± 1 standard deviation.

While the difference in release from control vesicles to eLiposomes at short exposure times was significant, the amount of release was relatively low. A single pulse of 100 ms at 525 kHz does not seem to be able to create a substantial amount of calcein release. For example, PFC5 eLiposomes released only 6% of the loaded calcein when exposed to a single 100 ms burst of ultrasound at 5 W/cm^2. However, it does appear that calcein will continue to be released as ultrasound is delivered in pulses; there was not a significant difference between calcein release from eLiposomes exposed to 525 kHz ultrasound at 5 W/cm^2 in a single 100 ms burst compared to relatively similar ultrasound exposure times divided into 1000 cycle pulses. This is particularly relevant as short bursts are typically preferred in medical applications to limit heating and tissue damage.

Single short bursts (100 ms) of ultrasound were applied at 525 kHz at intensities at mechanical indices of 0.87, 1.73, and 2.45. These mechanical indices correspond to those employed at 20 kHz. Figure 39 provides a comparison of calcein release from eLiposomes when exposed to 20 kHz and 525 kHz. When the ultrasound intensity and burst length was identical, exposure to 20 kHz ultrasound produced significantly more release; on average, 2.5 times as much calcein was released when exposed to 20 kHz compared to 525 kHz at the intensities investigated. However, when the mechanical index was identical, there was no significant difference in calcein release observed at the two frequencies. This occurred at all 3 values of mechanical index.

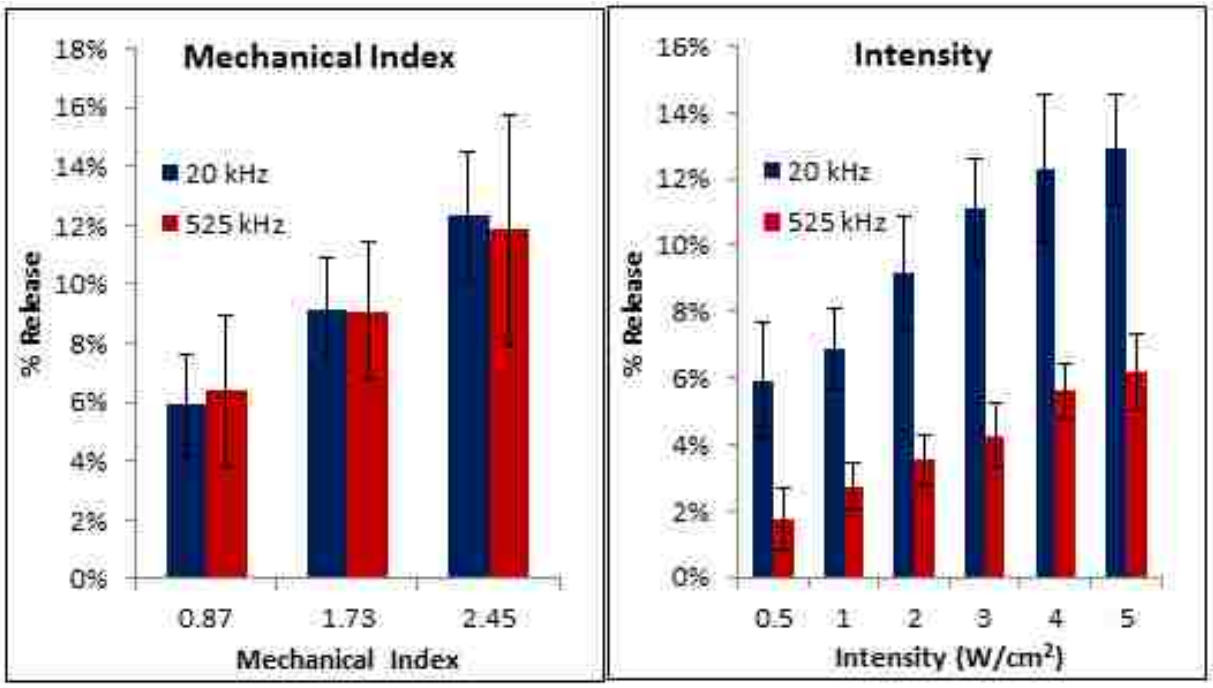

Figure 39. Calcein release from small PFC5 eLiposomes when exposed to short (100 ms) exposure times of 20 kHz and 525 kHz at identical intensities and mechanical indices. Error bars represent ± 1 standard deviation (n=3).

Although the negative pressure corresponding to lower ultrasound intensities should, in theory, be sufficient to overcome the vapor pressure of PFC5, the intensity of the 525 kHz ultrasound had to be increased in order to produce similar release to that observed when samples were exposed to 20 kHz ultrasound. This result provides further evidence that overcoming vapor pressure is not the only relevant factor affecting drug release from eLiposomes. The ability to nucleate a gas phase is likely a controlling factor in the droplet vaporization process. Low frequencies of ultrasound have longer wavelengths, resulting in a longer period of low pressure with each cycle. This longer period of low pressure may allow more time for nucleation and expansion of a gas phase. Pitt, et al. developed a mathematical model of acoustic droplet vaporization that describes a similar phenomenon; when the negative pressure applied by ultrasound is held constant, the volume expansion of a vaporizing emulsion droplet is much larger at lower frequencies due to the longer duration of the negative phase of the ultrasound cycle [140]. Calcein release from eLiposomes suggests that the mechanical index, which was developed to predict the likelihood of cavitation, may be a more effective way to account for the effects of ultrasound applied at different frequencies.

6.6 Summary

eLiposomes released a higher percentage of encapsulated calcein than conventional liposomes at all of the ultrasound parameters and exposure times tested. This release could be observed at very short (100 ms) exposure times and increased with intensity. Release also increased significantly as exposure time was increased. This increased release with time suggests that providing sufficient ultrasound pressure for vaporization is not the only parameter that effects droplet vaporization. Other factors, such as the time required to nucleate a gas phase,

likely play a significant role. In many cases, this increased release with increasing time had leveled off or slowed down after about 5 seconds of ultrasound exposure for samples exposed to 20-kHz ultrasound. A similar leveling-off was observed at 525 kHz as well. There was generally a significant increase in calcein release from eLiposomes containing PFC5 droplets compared to those containing PFC6 droplets, probably due to the higher vapor pressure of PFC5.

Vesicle and emulsion droplet size also had a significant effect on calcein release. eLiposomes containing large emulsion droplets released significantly more calcein than those with small droplets. This difference can be attributed to the increased Laplace pressure on smaller diameter droplets. The overall size of the vesicle also had a significant effect on calcein release, with larger vesicles releasing significantly more calcein than small vesicles. This pattern was observed in conventional liposomes as well as in eLiposomes.

Release experiments were also performed at 525 kHz, with eLiposomes once again demonstrating increased calcein release compared to controls. While the patterns observed at 20 kHz remained consistent, eLiposomes and control vesicles released less calcein at the higher frequency when intensity was maintained constant. Interestingly, there was a stronger correlation between mechanical index and release than between ultrasound intensity and calcein release. This result supports the hypothesis that the rate of gas nucleation may be a limiting factor in emulsion vaporization and subsequent calcein release even after a thermodynamic potential for vaporization has been attained. Higher frequencies have shorter cycles of negative pressure compared to lower frequencies, and therefore provide less time for a vapor phase to nucleate with each cycle. When operating at high frequency, medium to long ultrasound pulses administered at a relatively low pulse repetition frequency will probably be most efficient for drug release; such parameters could provide sufficient time per pulse to encourage nucleation

and still have a low time-averaged energy exposure. The amount of release would be expected to continue to increase with each additional pulse until the 'leveling-off" point mentioned above had been reached. It is even possible that the increased opportunity for vapor nucleation with each burst may increase this limit.

It was anticipated that increased temperatures would lead to increased calcein release due to the resulting higher vapor pressures of the perfluorocarbon liquids. Unexpectedly, increasing temperature resulted in only a small increase of drug release from most samples. While this increase was usually statistically significant, it was not substantial.

Lastly, comparison of drug release to acoustic spectra (Chapter 5.5.2) suggests that vaporization may induce release before sustained cavitation occurs; there was a significant increase in release from eLiposomes compared to conventional liposomes at frequencies below the threshold for higher harmonic peaks in the acoustic spectra. There was a significant additional increase in release from eLiposomes at intensities where stable cavitation had been detected in emulsion samples, suggesting that the presence of a persistent and oscillating gas phase adds to release from eLiposomes. The evidence of significant release from eLiposomes at thresholds where persistent and violent bubble oscillations were not detected may indicate that the mechanism of release could be largely correlated with increasing vapor volume that causes holes or rips in the membrane (see Figure 19A). Although further increasing ultrasound intensity did lead to an increase in calcein release from eLiposomes, this increase was relatively small. Conventional liposomes followed this same trend; the most significant increase in calcein release was observed at intensities that were correlated with stable cavitation. It should be noted that although there was little or no difference between release from eLiposomes and conventional

liposomes at high intensities, these intensities are well above acceptable ultrasound parameters for clinical use.

7 IN VITRO CELL STUDIES

eLiposomes and emulsions have advantages over other potential drug carriers due to the ability to extravasate into tissues followed by ultrasound-mediated drug release. This strategy may enhance drug targeting to tumors due to the combination of the EPR effect together with ultrasound-mediated targeting. Many treatments, however, require therapeutic internalization into cells in order to have their effect. Ideally, the drug carriers and ultrasonic targeting could be used to not only penetrate tissues, but also to deliver drugs to the cell cytosol. Targeting ligands can be attached to drug carriers in order to enhance their uptake into certain cells. For example, in this study folate was attached to drug carriers because cancer cells typically overexpress the receptors for folic acid. The binding of folate to these receptors induces endocytosis, thus increasing uptake of the carriers into cancer cells relative to other cells. Drugs and drug carriers are typically internalized into the cells via endocytosis. Because many molecules (for example, nucleic acids) are digested in the resulting endosome, endosomal escape is an area of intense research interest; in order to be effective, many therapeutics must be internalized into cells via endocytosis, and then must escape the endosome before being digested. An intriguing application of emulsions and eLiposomes as drug carriers is the potential ability to break open endosomal membranes. As the emulsion is vaporized and expands, this expanding vapor phase may not only break open the eLiposomal membrane, but could also disrupt the endosomal membrane and aid the escape of drugs or genes from the endosome.

7.1 Emulsions for endosomal release

Vaporizing emulsion droplets could be used to aid in endosomal escape by disturbing the endosome as they expand. The emulsion could act as the drug/gene carrier itself, or be part of another carrier such as an eLiposome. They could also be administered in combination with other drug delivery vectors and techniques.

HeLa cells were grown in order to investigate the ability of nanoemulsions to disturb the endosomal membrane when exposed to ultrasound. In order to encourage endocytosis of the emulsions, cells were grown in folate free media. Emulsions with average diameters of approximately 200 nm were prepared with PFC5 and with PFC6. The emulsions were stabilized with DPPC along with a small amount of DPPE-PEG2000-Folate. The emulsion was mixed 1:1 with concentrated calcein (30 mM). 200 μL of the resulting solution were added to HeLa cells that had been grown in 1.3 mL of folate-free media, resulting in an approximate calcein concentration of 4 mM around the cells. This concentration of calcein is sufficiently high to be in the self-quenching range. The cells were allowed to incubate for 2 hours in this solution to allow the emulsion and surrounding calcein-containing media to be endocytosed. As the folate-laced emulsion droplets were endocytosed, it was anticipated that the newly formed endosomes would contain calcein at a self-quenching concentration. The calcein would not create a strong fluorescent signal unless it was released from the endosomes and diluted into the cytosol. After 2 hours, the cells were thoroughly washed and some samples were exposed to 20-kHz ultrasound for 2 seconds at 1 W/cm^2. The cells were then scraped from the well surface and viewed by confocal microscopy. Control experiments were performed by repeating the procedure in the absence of emulsion droplets; a solution of calcein and DSPE-PEG2000-folate at similar

concentrations to the active experiments was added to the cells and ultrasound was applied to some wells.

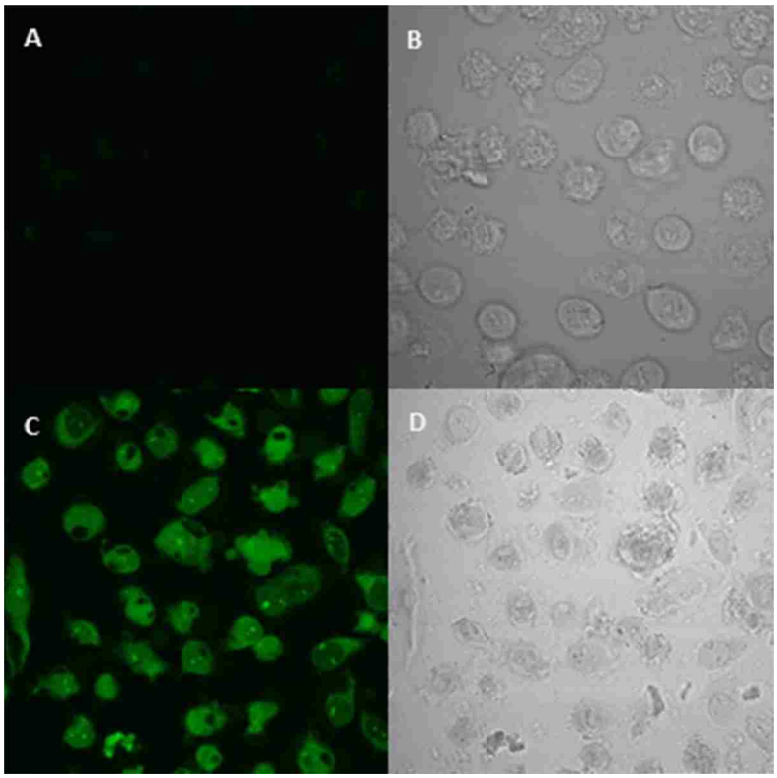

Figure 40. Folated PFC5 emulsions and concentrated calcein were endocytosed into HeLa cells. 20 kHz ultrasound was applied to some of the cells for 2 seconds at 1 W/cm^2. When cells were not exposed to ultrasound (A and B) the quenched calcein was not released into the cytosol. Calcein could be observed throughout the cells when exposed to ultrasound (C and D). Panels A and C are fluorescent confocal images and panels B and D are light images.

Figure 40 shows cells that had been incubated with PFC5 emulsion droplets. When the cells were not exposed to ultrasound (Figure 40A and 40B), almost no green could be detected within the cells. When the cells were exposed to ultrasound (Figure 40C and 40D), the cells were bright green, and green was observed throughout almost all of the cells (with the exception of the nucleus). This suggests that calcein had been incorporated into endosomes within the cells at a quenched concentration. With the application of ultrasound, the emulsion-containing

endosomes were disrupted and the encapsulated calcein was released into the cytosol and allowed to diffuse through most of the cell.

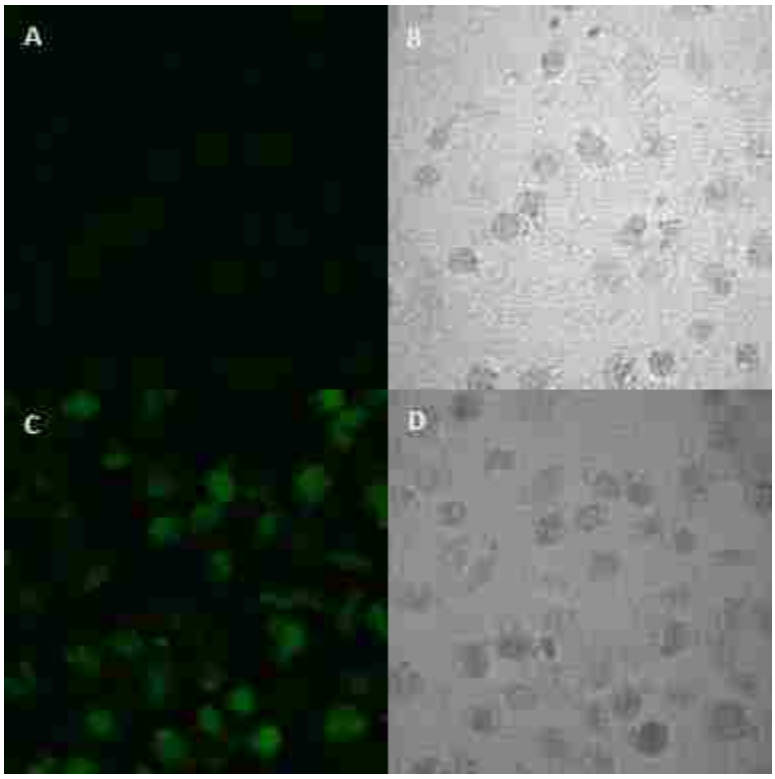

Figure 41. Folated PFC6 emulsions and concentrated calcein were endocytosed into HeLa cells. 20 kHz ultrasound was applied to some of the cells for 2 seconds at 1 W/cm^2. When cells were not exposed to ultrasound (A and B) the quenched calcein was not released into the cytosol. Calcein could be observed through the cells when exposed to ultrasound (C and D). Panels A and C are fluorescent confocal images and panels B and D are light images.

Figure 41 shows the results when cells were exposed to PFC6 emulsions. Similarly, there was a large increase in green fluorescence after exposure to ultrasound. However, the average fluorescence intensity per cell was significantly less than in cells that had been exposed to PFC5 as determined with ImageJ software. This suggests that the vaporization of PFC6 emulsions was less efficient for endosomal escape. This is most likely because of the lower vapor pressure of PFC6; fewer droplets may have vaporized, or the expansion and resulting cavitation events may

have been less violent. The difference in calcein release and subsequent fluorescence intensity seems analogous to release from eLiposomes; both PFC5 and PFC6 were able to generated release, but PFC5 was more complete or efficient.

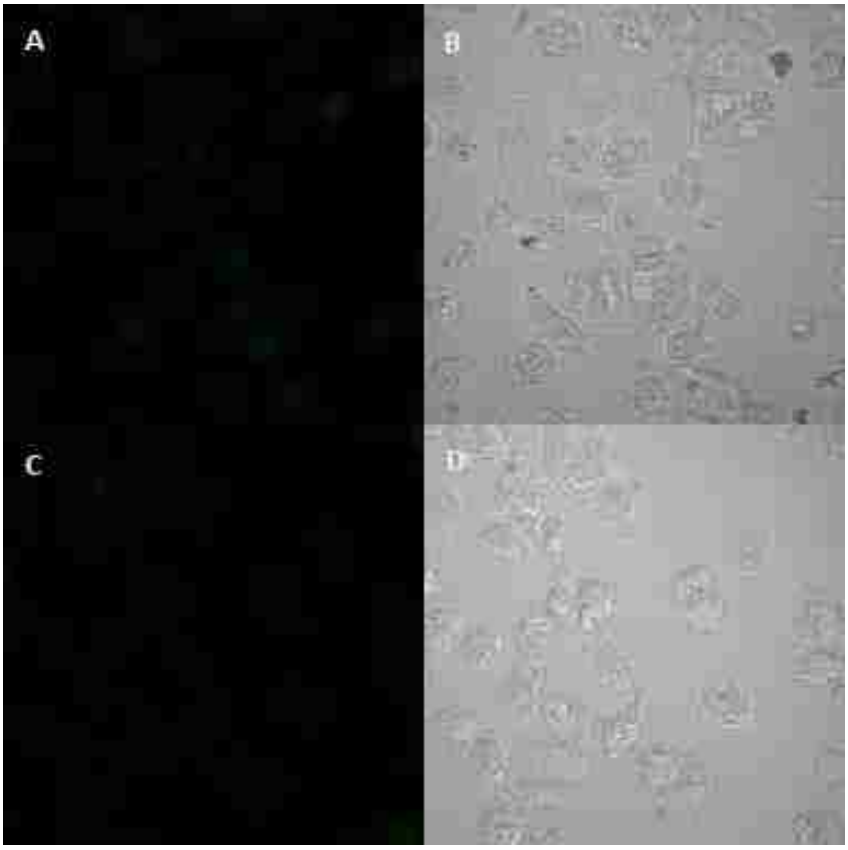

Figure 42. HeLa cells were incubated with calcein and DSPE-PEG2000-folate but without emulsion droplets. Cells in panels A and B were not exposed to ultrasound. Cells in panels C and D were exposed to 20 kHz ultrasound for 2 seconds at 1 W/cm^2. Without emulsion droplets present, there was not a significant difference in endosomal escape of the calcein when ultrasound was applied. Panels A and C are fluorescent confocal images and panels B and D are light images.

Figure 42 shows the results of a control experiment. Cells were exposed to the same concentrations of calcein and DSPE-PEG2000-folate as in active experiments, but without the presence of emulsion droplets. The cells in Figure 42C and 42D were exposed to 20-kHz ultrasound for 2 seconds at 1 W/cm^2. A slight green color can be seen in some cells. The

amount of green fluorescence is comparable to samples that had included emulsion droplets but not been exposed to ultrasound and is less than the amount of calcein observed throughout the cells when emulsion droplets are present and the cells are exposed to ultrasound. Control samples were viewed that had not been exposed to ultrasound and no green was detected at the microscope parameters that were used, indicating that this green is indeed from calcein and not from cell auto fluorescence. This baseline fluorescence could be due to some calcein passing through the cell membrane or escaping from the endosome without bursting the membrane when the cells are exposed to concentrated calcein. Confocal slices of some cells were viewed in order to verify that the green fluorescence could not be attributed to calcein on the surface of the cells. The resulting images verified that the observed calcein was on the interior of the cells.

Compared to controls, both PFC5 and PFC6 emulsions were able to induce endosomal escape, evidenced by the dilution of self-quenched calcein throughout the cell. It is likely that PFC5 emulsions form more persistent bubbles. The expansion of these persistent bubbles may be more complete, more chaotic or more violent than PFC6, resulting in more release from the endosomes. While PFC5 may have the advantage of more completely releasing contents from the endosome, PFC6 may also be useful due to increased stability of the droplets and the potential reversibility of the phase change. It is encouraging that both PFC5 and PFC6 emulsions have the potential to aid in endosomal escape when exposed to ultrasound.

7.2 Intracellular calcein delivery with eLiposomes

7.2.1 Vesicle uptake at different diameters

In order to test the ability of cells to endocytose vesicles the sizes of our eLiposomes, vesicles of DPPC and DSPE-PEG200-folate were prepared with 0.05 mM calcein at 800-nm and

at 200-nm by film hydration and extrusion through membranes with 800 nm and 200 nm filter pores. At this concentration, the calcein is not self-quenched, and the liposomes create a fluorescent signal when viewed via confocal microscopy. Cells were grown for the final 48 hours in folate free media. The calcein containing liposomes were added to the cells and allowed to incubate for 2 hours prior to being viewed on the confocal microscope.

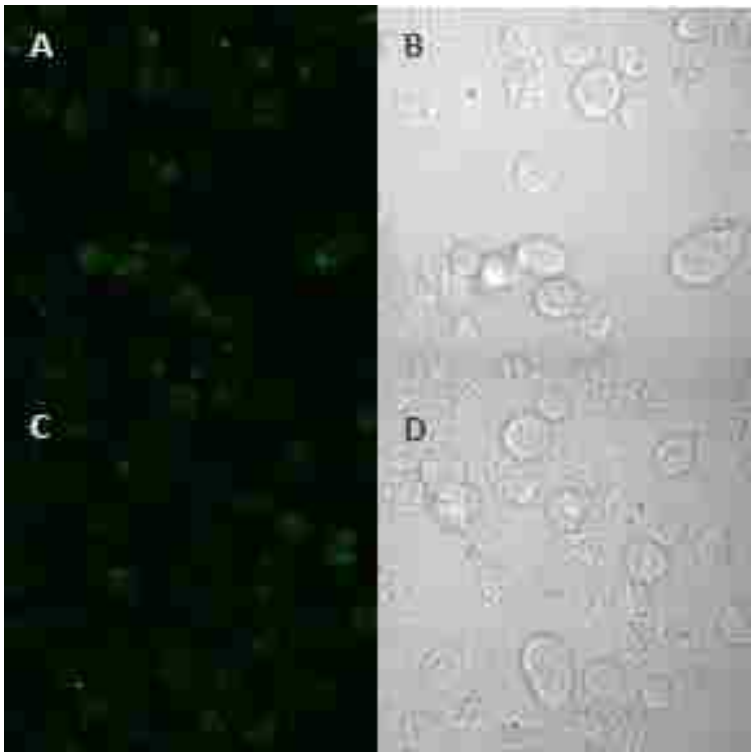

Figure 43. Cells were incubated with 200 nm (Panels A and B) or 800 nm (panels C and D) vesicles containing 0.05 mM calcein for 2 hours. Vesicles of both sizes were internalized into the cells. Panels A and C are fluorescent confocal images and panels B and D are light images.

Figure 43 demonstrates the uptake of vesicles of both sizes. Control samples (without folate) run at this calcein concentration did not show any green at the microscope settings that were used. The ability to detect green fluorescence with both 800-nm and 200-nm vesicles shows the ability of the cells to internalize both samples. It should also be mentioned that the

800-nm samples typically do contain some liposomes with smaller diameters, which may be internalized more readily than the vesicles with a true 800-nm diameter. While both sizes show the ability to endocytose in vitro, it is worth remembering that each size has advantages and disadvantages: the 200-nm vesicles release less of their drug load when exposed to ultrasound, but could penetrate deep into tissues via the EPR effect. In contrast, the 800-nm vesicles may be induced to release more of their drug load, but may not have the ability to extravasate into tissues.

7.2.2 In vitro ultrasound-induced delivery of calcein from eLiposomes to HeLa cells

In order to test the ability of eLiposomes to deliver a drug load to the cytosol of cells, 200 nm eLiposome samples were prepared with concentrated (15mM) calcein inside. This concentrated calcein does not fluoresce significantly while encapsulated inside of the vesicles. Fluorescence increases as the calcein is diluted into the larger volume of the cell. Conventional liposomes with encapsulated calcein at 15 mM were also prepared as a negative control. Some of the external calcein was removed by settling. Additional calcein and the external emulsion droplets were removed by the "sucrose cushion" technique. 200 μL of the various solutions were added to each well of cells and allowed to incubate for 2 hours to allow the cells to endocytose the vesicles. After the 2 hours of incubation, some cells were exposed to 20-kHz ultrasound at 1 W/cm^2 (MI = 1.22) for 2 seconds.

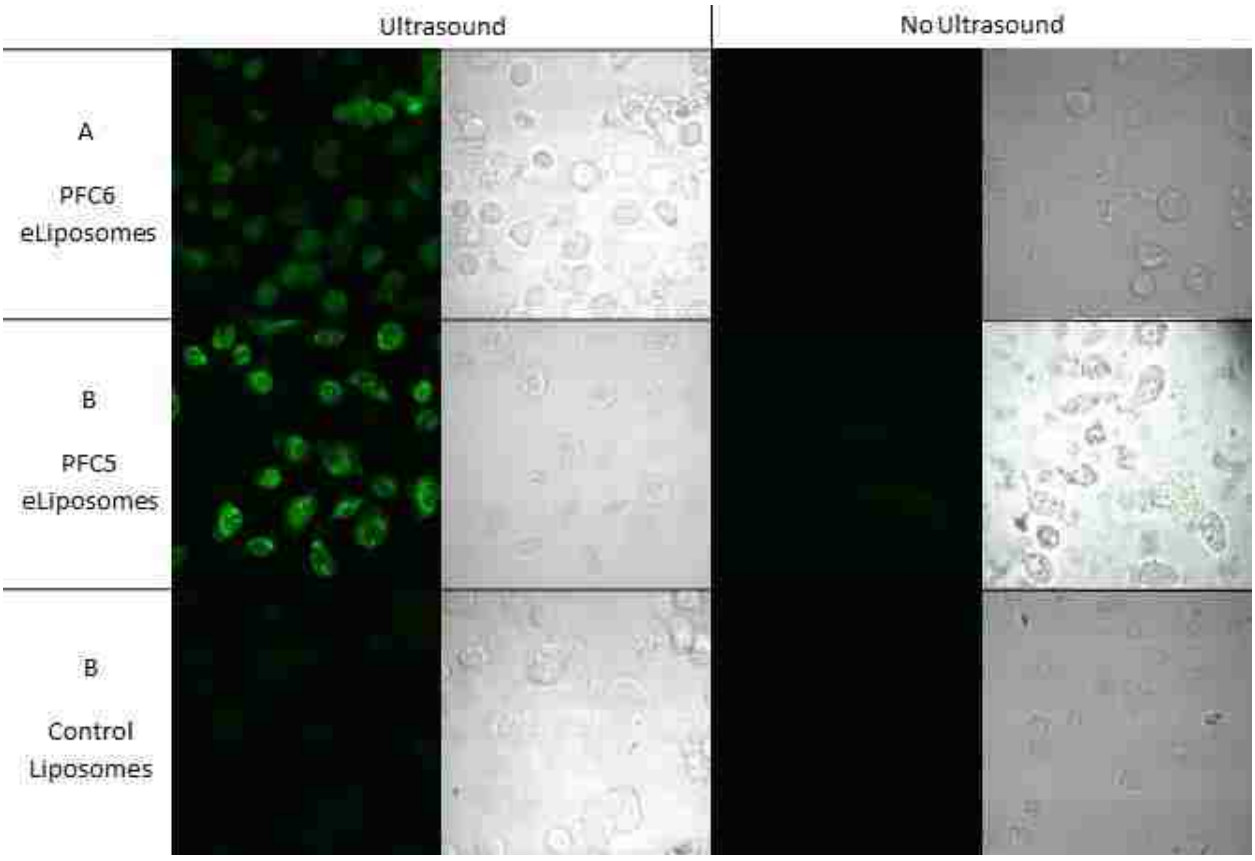

Figure 44. HeLa cells that have been incubated with 200-nm eLiposomes or control vesicles containing concentrated (self-quenched) calcein. After incubation to allow internalization of the vesicles, some samples were exposed to 2 seconds of 20-kHz ultrasound at 1 W/cm^2. eLiposome samples demonstrated much more calcein throughout the cells when exposed to ultrasound. Samples with control liposomes did not demonstrate significant amounts of calcein delivered to the cells with or without ultrasound exposure.

Figure 44 demonstrates the resulting calcein release to cells. PFC6 eLiposomes demonstrated the ability to sequester the majority of their calcein prior to insonation, followed by the release of calcein to the interior of the cells when exposed to ultrasound (Figure 44A). When ultrasound was not applied to the cells, the concentrated calcein was not released into the cytosol. The self-quenched calcein that remained inside of the eLiposomes did not add significantly to the fluorescence of the cells. Similarly, PFC5 eLiposomes demonstrated the ability to deliver calcein to the interior of the cells when exposed to ultrasound and the ability to sequester the calcein when not exposed to ultrasound (Figure 44 B). PFC5 eLiposomes were

able to deliver significantly more calcein to the cytosol than PFC6 as evidenced by increased green fluorescence intensity in the cells as measured by ImageJ. This could be due to an increased ability to vaporize and release from the eLiposomes (see Chapter 6) or from an increased ability to break out of the endosomes due to irreversible and/or more chaotic vaporization and gas cavitation. Control vesicles showed little to no ability to deliver the calcein to the interior of the cells with or without exposure to ultrasound (see Figure 44C).

7.2.3 Evidence of folate-induced endocytosis, and endosomal release

In order to verify the importance of folate on the surface of the eLiposomes to stimulate endocytosis, samples were prepared with encapsulated calcein at a self-quenching concentration. DSPE-PEG2000-folate was added to the surface of some of the samples. The eLiposome samples were incubated with HeLa cells for 2 hours, followed by exposing the cells to 20-kHz ultrasound at 1 W/cm^2 for 2 seconds. When the eLiposomes did not include folate, only a small amount of green fluorescence could be observed in the cells (see Figure 45A). In contrast, samples that contained folate on the surface of the eLiposomes demonstrated significant calcein release to the cells (Figure 45C). When cells were incubated with calcein without eLiposomes or emulsions and exposed to ultrasound there was not a significant amount of green fluorescence detected (see Figure 42). These results suggest that the eLiposomes are not internalized into cells without folate. When folate is included in the eLiposomes, they not only are internalized but can be induced to release their contents with ultrasound.

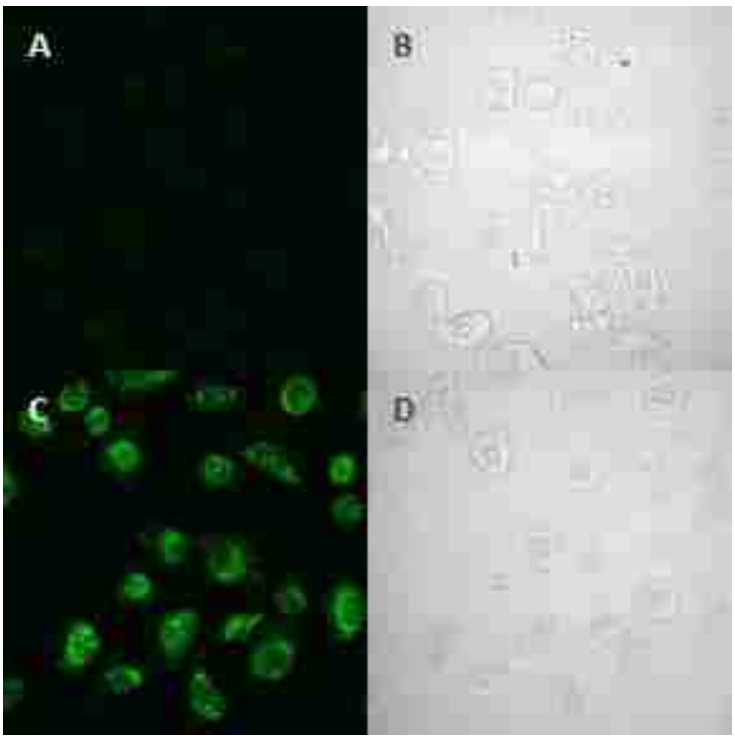

Figure 45. eLiposomes containing self-quenched calcein were prepared without folate (Panels A and B) or with folate (panels C and D). The eLiposomes were added to HeLa cells and allowed to incubate for 2 hours. The cells were then exposed to 2 seconds of 20-kHz ultrasound at 1 W/cm^2. Cells that had been incubated with folated eLiposomes had calcein throughout the cells. Panels A and C are fluorescent confocal images and panels B and D are light images.

In order to further investigate the location of eLiposomes in cells before and after sonication, eLiposome samples were prepared with a non-quenching calcein concentration (0.05 mM). LysoTracker was added to cells and allowed to incubate for at least 30 minutes in order to allow the dye to penetrate the cells. Various concentrations of LysoTracker red dye were tested to try to improve contrast and locate the endosomes. The best concentration was determined to be 50 nM; higher and lower concentrations did reveal the location of the endosomes, but at lower concentrations the contrast was poor, and at higher concentrations the red fluorescence tended to dominate the majority of the cell. The two fluorescent molecules were imaged in series; LysoTracker dye was imaged using the helium-neon laser and the calcein was imaged using the

argon laser. Figure 46 provides an example of cells with both dyes. When ultrasound was not applied, the calcein tended to be localized in bright bunches and spots that were co-localized with the LysoTracker Red, suggesting that the eLiposomes were located in endosomes and/or other acidic vesicles (see Figure 46A). After ultrasound exposure, the green calcein was spread throughout the cells. The location of the calcein and the LysoTracker Red dyes (green and red, respectively), was no longer co-localized. These results suggest that prior to ultrasound exposure, the eLiposomes were inside of the endosomes. After ultrasound, the calcein had not only been released from the eLiposomes, but had also escaped from the endosome (see Figure 46B).

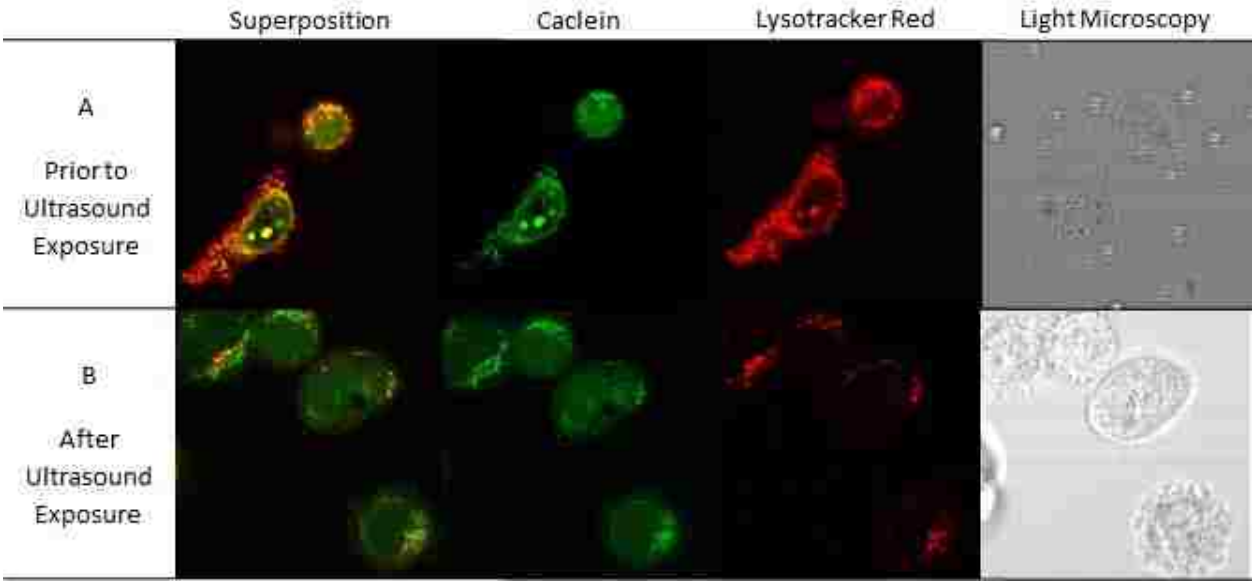

Figure 46. HeLa cells were incubated with PFC5 eLiposomes and with LysoTracker Red dye. Cells were imaged by confocal microscopy before (A) and after (B) ultrasound exposure. Calcein was co-localized with the LysoTracker in Cells that had not been exposed to ultrasound, indicating that eLiposomes were located in endosomes. After ultrasound exposure, the calcein had been released into the cytosol and spread throughout the cell.

8 CONCLUSIONS AND RECOMMENDATIONS

8.1 Summary and conclusions

The motivation behind this work was to explore the ability of ultrasound to vaporize emulsion droplets with high vapor pressures. This ultrasound-induced phase change may have applications in drug delivery; the emulsion droplets themselves may act as drug carriers or their vaporization may be able to trigger drug release from other drug carriers.

Emulsion droplets were successfully formed with PFC5 and PFC6. These perfluorocarbon liquids were chosen due to their biocompatibility, low solubility in water, and high vapor pressures. Due to its biocompatibility and its ability to stabilize the emulsion droplets at low concentrations, DPPC was chosen as a stabilizing surfactant. Sonication and mechanical shaking were explored as potential methods for emulsion formation, and sonication was chosen for the majority of this work due to its robust ability to form emulsions with relative ease of application. Because the liquids used for the emulsions have high vapor pressures, the emulsions were formed at low temperature on an ice bath. Attempts to form emulsions at room temperature resulted in premature vaporization and foam formation. After sonication, the droplets usually had a diameter between 200 and 400 nm and resulting emulsions were typically bimodal. The size of the emulsion droplets was effectively reduced and controlled by extrusion through polycarbonate filters with a 50 nm or 100 nm pore size. The resulting emulsions had average

diameters near the filter pore size. Extrusion also reduced multimodality. TEM was used to visualize the droplets and verified the average sizes.

Vaporization of the emulsion droplets when exposed to ultrasound was verified with microscopy and by examining the Fourier transform of the acoustic emissions produced by the emulsion samples. Both of these techniques verified that emulsion droplets are vaporized when exposed to ultrasound. The size of the emulsion droplets was determined to have an effect on droplet vaporization. Specifically, large emulsion droplets generated acoustic phenomena that are indicative of bubble cavitation at lower thresholds than small emulsion droplets. Large droplets also generated larger bubbles than small droplets when viewed under a microscope. This effect of droplet size is believed to be due to the Laplace pressure imposed on the droplet; the interior droplet pressure increases as the radius decreases, therefore increasing the ultrasound amplitude required for vaporization. In order to vaporize a liquid emulsion droplet with ultrasound, the applied negative pressure must overcome the liquid vapor pressure and the Laplace pressure imposed on the droplet. When these conditions are not met, the liquid droplet will remain in the liquid phase. At higher temperatures, the vapor pressure of the liquid is increased, and thresholds for vaporization are reduced.

Emulsion droplets were encapsulated inside of liposomes by forming interdigitated lipid sheets and subsequently refolding the sheets into closed vesicles in the presence of emulsion. The resulting eLiposomes initially had a very broad and random size distribution. The upper limit of this size distribution was controlled and reduced by extrusion. CryoTEM and negative staining TEM demonstrated the closed structure of the eLiposomes and the encapsulation of emulsion droplets.

When exposed to ultrasound, eLiposomes released more calcein than negative controls, including liposomes without any emulsions and liposomes with external emulsions. This is consistent with the hypothesis that internal emulsion droplets vaporize and expand when exposed to ultrasound. When the droplets are encapsulated inside of a liposome, the expanding gas phase seems to be able to disrupt the bilayer membrane. External emulsion droplets, however, did not have an effect on the vesicles at short ultrasound exposure times. As exposure time increased, external droplets had a slight effect, but only result in a slight increase in calcein release compared to control experiments without emulsion droplets. As expected, the size of the emulsion droplets had a significant effect on their ability to induce calcein release from eLiposomes; eLiposomes containing small emulsion droplets required higher ultrasound intensities in order to release a comparable amount of calcein than eLiposomes with large droplets. The size of the vesicles had an effect on the ability of eLiposomes and conventional liposomes to release their calcein, with larger vesicles releasing more of the encapsulated load.

Herein, many different combinations of eLiposome size, emulsion droplet size, and ultrasound parameters were explored. There are a number of aspects to be considered in order to design the "ideal" eLiposome. Namely, larger droplets and vesicles tend to release more of their encapsulated load, but smaller structures would be more useful for passive drug targeting. Also, the eLiposome should retain the ability to sequester a large drug load along with emulsion droplets. In general, it is likely that that an eLiposome with a 200 to 300-nm outer membrane containing 100-nm PFC5 droplets would best balance these competing parameters. For treatments where passive drug targeting is not desired, 800-nm vesicles with large droplets would be most efficient. Obviously there are a large number of experiments that need to be conducted in order to quantitate and optimize these design parameters.

After decreasing the pressure sufficiently, a vapor phase should nucleate and expand during phases of low pressure and rupture the eLiposome membrane. The required ultrasound intensity for vaporization and time for nucleation should result in some kind of intensity threshold for calcein release from eLiposomes. However, obvious thresholds were not observed with respect to time or intensity despite operating at ultrasound parameters above and below those calculated to overcome both the Laplace pressure on the droplets and the difference between the local pressure and the droplet vapor pressure. This lack of obvious thresholds is most likely due to the distribution of sizes in both emulsion droplets and eLiposomes. The distribution of emulsion sizes imposed different Laplace pressures from droplet to droplet. Some emulsion droplets will therefore require higher or lower negative pressure in order to vaporize and this distribution may be responsible for the lack of a sharp intensity threshold for calcein release. Furthermore, nucleation probably does not occur instantly, but may be a random process that is related to the degree of sub-pressurization of the emulsion. The experimental data indicate that nucleation occurs, but there may be a distribution in nucleation times that may smear out a theoretically sharp threshold in experimental data.

The effect of delayed gas nucleation is further evidenced by the effects of time. If droplet vaporization were instantaneous, a single ultrasound cycle with sufficient amplitude would rupture the eLiposomal membrane and release the encapsulated contents. However, calcein release from eLiposomes continued to increase with increasing exposure times up to at least 30 seconds. Furthermore, ultrasound frequency also had an effect on calcein release from eLiposomes. Theory would suggest that the amount of negative pressure imposed by the ultrasound wave should predict its ability to vaporize the emulsion droplet. However, as ultrasound frequency increased, much higher intensities were required to produce calcein release.

This increase in release at lower frequency is most likely tied to the longer duration of the rarefactional phase of ultrasound, thus providing more time for gas nucleation and expansion.

Temperature was expected to have a significant effect on calcein release from eLiposomes due to the increased vapor pressure of the perfluorocarbon liquids at increased temperature. While there was an increase in calcein release at higher temperatures, this increase was less substantial than expected based on the change in vapor pressure with temperature.

Folated emulsion droplets demonstrated the ability to be internalized into HeLa cells via endocytosis. Calcein was released from the resulting the endosome when ultrasound was applied. Likewise, both 200-nm and 800-nm eLiposomes were endocytosed into cells when the vesicles were folated. Upon ultrasound exposure, the calcein that had been encapsulated within the eLiposomes was not only released from the eLiposomes, but was also released into the cytosol.

8.2 Recommendations for future work

The work described in this dissertation explores the potential of acoustic droplet vaporization to be used in drug delivery applications. The details included herein add to the existing understanding of this process. Specifically, the ability of perfluorocarbon emulsions to vaporize and form persistent or non-persistent cavitating bubbles has been described. A hypothesis presented herein but not fully explored is that gas nucleation is a stochastic process and a limiting factor in this phase change. While the ultrasound parameters employed in this study were relatively mild, rapid drug release was not observed at predicted thresholds. An attempt to further understand gas phase nucleation in emulsion droplets would represent a significant advance in the understanding of acoustic droplet vaporization. It is possible that

additional nucleating agents could further lower time and intensity thresholds for emulsion vaporization.

For the purpose of drug delivery, it would be advantageous to speed up and enhance gas-phase nucleation so that emulsions may be used for drug delivery at ultrasound parameters with low energy exposures. If the nucleation process can be sped up, droplets could be induced to vaporize rapidly at high frequency in order to create a safe targeted system that behaves in an on/off fashion. Alternatively, it is possible that other targeting modalities such as heat or IR light could induce droplet vaporization in more of an on/off fashion compared to ultrasound.

Another area of potential exploration is a better understanding of the effect of frequency on droplet vaporization. This dissertation reports that higher frequencies required higher intensities in order to induce vaporization. However, only 2 frequencies were tested at only a handful of intensities. A study that explores several frequencies and a variety of ultrasound parameters, including intensity, pulse length, and pulse frequency, would not only add a more complete understanding of ultrasound-induced vaporization, but could also identify more useful ultrasound parameters.

While eLiposomes demonstrated an enhanced ability to release encapsulated contents when exposed to ultrasound, other techniques have also made similar advances. Namely, ultrasound sensitive liposomes have been developed using non-traditional lipids to form the bilayer, and "echogenic liposomes" have been developed with the claim that small amounts of gas or air are encapsulated in the liposome. While each of these systems will have its own set of advantages and disadvantages, an objective comparison may prove useful. Particularly, the following questions should be answered: how does the ultrasound-induced delivery of encapsulated contents compare at similar ultrasound intensities? Can the various types of

liposomes be formed with diameters between 100-300 nm in order to take advantage of the EPR effect? Do the lipids and other materials of construction allow the liposomes to efficiently sequester a drug load prior to ultrasound activation? How does this sequestering efficiency compare to conventional liposomes?

Purification of eLiposomes, including removal of external emulsion droplets and the removal of unencapsulated calcein (or drug), remains a challenge. The separation methods used herein include the sucrose cushion technique and vesicle settling. These techniques and/or other separation methods should be further developed and perfected.

The 2-step sheet refolding method for droplet encapsulation that is presented in this dissertation provided an interesting way to form eLiposomes, but also presents significant challenges. Using this 2-step process to form eLiposomes is complicated and cumbersome and is probably not practical on an industrial scale. Furthermore, there are formulation constraints that affect the ability to form and refold sheets. Most notably, cholesterol cannot be added to the sheets at concentrations that are typically used in liposomal formulations. As mentioned in Chapter 2, cholesterol is typically used in commercial liposomes and is cited as preventing the liposomes from being quickly broken down in the blood stream. Efforts have already begun to explore other techniques for forming eLiposomes that will allow more versatility with lipid formulations and also will allow the addition of cholesterol. These methods should be further explored and perfected. The finalized eLiposomes should include cholesterol and PEGylated lipids. The ultrasound sensitivity of the new eLiposome formulation should be characterized similar to the work performed in this dissertation.

After eLiposomes have been further developed, in vivo targeting will be an area of particular interest. This dissertation describes the intracellular delivery of calcein, enhanced by

folated drug carriers. The ability to selectively target cancerous tissues in vivo via active targeting ligands and by the EPR effect will be an important process to verify and to characterize. The effectiveness of eLiposomes to reduce tumor size should also be characterized. Prior to these studies, eLiposomes will need to be loaded with active anti-cancer drugs.

This dissertation has detailed initial in vitro studies that suggest that the vaporizing emulsion droplets can aid in drug delivery without killing the target cells. As is the case with all ultrasound-mediated drug delivery, there may be thresholds where the expanding vapor may damage and/or kill cells. A more quantitative study of cell viability when exposed to emulsion droplets and ultrasound may prove useful, especially when the emulsion droplets are taken into the cells and may have the potential to disrupt the cell membrane. Internal emulsion droplets have shown the potential to disrupt endosomal membranes, and there may be a fine balance in order to take advantage of that potential without damaging cells. Gene delivery is another potential use for vaporizing emulsion droplets, particularly because of the potential endosomal escape of the delivered nucleic acids. Emulsion droplets may be useful in this type of treatment individually or as part of eLiposomes. In order to explore this potential, an effective method for loading nucleic acids into eLiposomes should be developed. The potential to deliver a variety of nucleic acids could then be explored both in vitro and in vivo.

9 REFERENCES

1. Hobbs, S.K., et al., *Regulation of transport pathways in tumor vessels: Role of tumor type and microenvironment.* Proceedings of the National Academy of Sciences of the United States of America, 1998. **95**(8): p. 4607-4612.

2. Chari, R.V.J., *Targeted cancer therapy: Conferring specificity to cytotoxic drugs.* Accounts of Chemical Research, 2008. **41**(1): p. 98-107.

3. Kim, D.K. and J. Dobson, *Nanomedicine for targeted drug delivery.* Journal of Materials Chemistry, 2009. **19**(35): p. 6294-6307.

4. Gullotti, E. and Y. Yeo, *Extracellularly Activated Nanocarriers: A New Paradigm of Tumor Targeted Drug Delivery.* Molecular Pharmaceutics, 2009. **6**(4): p. 1041-1051.

5. Guo, D.P., et al., *Ultrasound-targeted microbubble destruction improves the low density lipoprotein receptor gene expression in HepG(2) cells.* Biochemical and Biophysical Research Communications, 2006. **343**(2): p. 470-474.

6. Tomanin, R. and M. Scarpa, *Why do we need new gene therapy viral vectors? Characteristics, limitations and future perspectives of viral vector transduction.* Current Gene Therapy, 2004. **4**(4): p. 357-372.

7. Zarnitsyn, V.G. and M.R. Prausnitz, *Physical parameters influencing optimization of ultrasound-mediated DNA transfection.* Ultrasound in Medicine and Biology, 2004. **30**(4): p. 527-538.

8. Rauch, C., *Toward a mechanical control of drug delivery. On the relationship between Lipinski's 2nd rule and cytosolic pH changes in doxorubicin resistance levels in cancer cells: a comparison to published data.* European Biophysics Journal with Biophysics Letters, 2009. **38**(7): p. 829-846.

9. Husseini, G.A. and W.G. Pitt, *The use of ultrasound and micelles in cancer treatment.* Journal of Nanoscience and Nanotechnology, 2008. **8**(5): p. 2205-2215.

10. Gabizon, A., et al., *Improved therapeutic activity of folate-targeted liposomal doxorubicin in folate receptor-expressing tumor models.* Cancer Chemotherapy and Pharmacology, 2010. **66**(1): p. 43-52.

11. Lee, R.J. and P.S. Low, *Folate-targeted liposomes for drug delivery.* Journal of Liposome Research, 1997. **7**(4): p. 455-466.

12. Bareford, L.A. and P.W. Swaan, *Endocytic mechanisms for targeted drug delivery.* Advanced Drug Delivery Reviews, 2007. **59**(8): p. 748-758.

13. Meers, P., *Enzyme-activated targeting of liposomes.* Advanced Drug Delivery Reviews, 2001. **53**(3): p. 265-272.

14. Simoes, S., et al., *On the formulation of pH-sensitive long circulation times.* Advanced Drug Delivery Reviews, 2004. **56**(7): p. 947-965.

15. Jagur-Grodzinski, J., *Polymers for targeted and/or sustained drug delivery.* Polymers for Advanced Technologies, 2009. **20**(7): p. 595-606.

16. Bae, Y.H. and K. Park, *Targeted drug delivery to tumors: Myths, reality and possibility.* Journal of Controlled Release, 2011. **153**(3): p. 198-205.

17. Leighton, T.G., *What is ultrasound?* Progress in Biophysics & Molecular Biology, 2007. **93**(1-3): p. 3-83.

18. Saad, A.H. and G.M. Hahn, *Ultrasound Enhanced Drug Toxicity on Chinese-Hamster Ovary Cells-Invitro.* Cancer Research, 1989. **49**(21): p. 5931-5934.

19. Tachibana, K., et al., *Enhanced cytotoxic effect of Ara-C by low intensity ultrasound to HL-60 cells.* Cancer Letters, 2000. **149**(1-2): p. 189-194.

20. Huber, P.E. and P. Pfisterer, *In vitro and in vivo transfection of plasmid DNA in the Dunning prostate tumor R3327-AT1 is enhanced by focused ultrasound.* Gene Therapy, 2000. **7**(17): p. 1516-1525.

21. Brujan, E.A., T. Ikeda, and Y. Matsumoto, *Jet formation and shock wave emission during collapse of ultrasound-induced cavitation bubbles and their role in the therapeutic applications of high-intensity focused ultrasound.* Physics in Medicine and Biology, 2005. **50**(20): p. 4797-4809.

22. Lawrie, A., et al., *Microbubble-enhanced ultrasound for vascular gene delivery.* Gene Therapy, 2000. **7**(23): p. 2023-2027.

23. Miura, S., et al., *In vitro transfer of antisense oligodeoxynucleotides into coronary endothelial cells by ultrasound.* Biochemical and Biophysical Research Communications, 2002. **298**(4): p. 587-590.

24. Prentice, P., et al., *Membrane disruption by optically controlled microbubble cavitation.* Nature Physics, 2005. **1**(2): p. 107-110.

25. Schlicher, R.K., et al., *Mechanism of intracellular delivery by acoustic cavitation.* Ultrasound in Medicine and Biology, 2006. **32**(6): p. 915-924.

26. Guzman, H.R., et al., *Ultrasound-mediated disruption of cell membranes. I. Quantification of molecular uptake and cell viability.* Journal of the Acoustical Society of America, 2001. **110**(1): p. 588-596.

27. Guzman, H.R., et al., *Equilibrium loading of cells with macromolecules by ultrasound: Effects of molecular size and acoustic energy.* Journal of Pharmaceutical Sciences, 2002. **91**(7): p. 1693-1701.

28. Rapoport, N.Y., et al., *Ultrasound-triggered drug targeting of tumors in vitro and in vivo.* Ultrasonics, 2004. **42**(1-9): p. 943-950.

29. Adamson, A., *Physical Chemistry of Surfaces*. 1982, New York: John Wiley and Sons.

30. Brennen, C.E., *Cavitation and Bubble Dynamics*. 1995, New York: Oxford University Press.

31. Liu, Y.Y., H. Miyoshi, and M. Nakamura, *Encapsulated ultrasound microbubbles: Therapeutic application in drug/gene delivery.* Journal of Controlled Release, 2006. **114**(1): p. 89-99.

32. Raisinghani, A. and A.N. DeMaria, *Physical principles of microbubble ultrasound contrast agents.* American Journal of Cardiology, 2002. **90**(10A): p. 3J-7J.

33. Tinkov, S., et al., *Microbubbles as Ultrasound Triggered Drug Carriers.* Journal of Pharmaceutical Sciences, 2009. **98**(6): p. 1935-1961.

34. Holland, C.K. and R.E. Apfel, *Thresholds for Transient Cavitation Produced by Pulsed Ultrasound in a Controlled Nuclei Environment.* Journal of the Acoustical Society of America, 1990. **88**(5): p. 2059-2069.

35. Treat, L.H., et al., *Targeted delivery of doxorubicin to the rat brain at therapeutic levels using MRI-guided focused ultrasound.* International Journal of Cancer, 2007. **121**(4): p. 901-907.

36. Unger, E.C., et al., *Acoustically active lipospheres containing paclitaxel - A new therapeutic ultrasound contrast agent.* Investigative Radiology, 1998. **33**(12): p. 886-892.

37. Anwer, K., et al., *Ultrasound enhancement of cationic lipid-mediated gene transfer to primary tumors following systemic administration.* Gene Therapy, 2000. **7**(21): p. 1833-1839.

38. Rocha, A., S. Ruiz, and J.M. Coll, *Improvement of DNA transfection with cationic liposomes.* J Physiol Biochem. 2002 Mar;58(1):45-56., 2002. **58**(1): p. 45-56.

39. Zobel, H.P., et al., *Effect of ultrasonication on the stability of oligonucleotides adsorbed on nanoparticles and liposomes.* J Microencapsul, 1999. **16**(4): p. 501-509.

40. Fang, J.Y., et al., *A study of the formulation design of acoustically active lipospheres as carriers for drug delivery.* European Journal of Pharmaceutics and Biopharmaceutics, 2007. **67**(1): p. 67-75.

41. Hwang, T.L., et al., *Development and Evaluation of Perfluorocarbon Nanobubbles for Apomorphine Delivery.* Journal of Pharmaceutical Sciences, 2009. **98**(10): p. 3735-3747.

42. Inayat, M.S., et al., *Oxygen carriers: A selected review.* Transfusion and Apheresis Science, 2006. **34**(1): p. 25-32.

43. Krafft, M.P., A. Chittofrati, and J.G. Riess, *Emulsions and microemulsions with a fluorocarbon phase.* Current Opinion in Colloid & Interface Science, 2003. **8**(3): p. 251-258.

44. Fabiilli, M.L., et al., *Delivery of Chlorambucil Using an Acoustically-Triggered Perfluoropentane Emulsion.* Ultrasound in Medicine and Biology, 2010. **36**(8): p. 1364-1375.

45. Rapoport, N., et al., *Ultrasound-mediated tumor imaging and nanotherapy using drug loaded, block copolymer stabilized perfluorocarbon nanoemulsions.* Journal of Controlled Release, 2011. **153**(1): p. 4-15.

46. Unger, E., et al., *Therapeutic applications of lipid-coated microbubbles.* Adv Drug Deliv Rev, 2004. **56**(9): p. 1291-1314.

47. Lemal, D.M., *Perspective on fluorocarbon chemistry.* Journal of Organic Chemistry, 2004. **69**(1): p. 1-11.

48. Krafft, M.P. and J.G. Riess, *Perfluorocarbons: Life sciences and biomedical uses - Dedicated to the memory of Professor Guy Ourisson, a true RENAISSANCE man.* Journal of Polymer Science Part a-Polymer Chemistry, 2007. **45**(7): p. 1185-1198.

49. Riess, J.G., *Fluorous micro- and nanophases with a biomedical perspective.* Tetrahedron, 2002. **58**(20): p. 4113-4131.

50. Correas, J.M., et al., *Human pharmacokinetics of a perfluorocarbon ultrasound contrast agent evaluated with gas chromatography.* Ultrasound in Medicine and Biology, 2001. **27**(4): p. 565-570.

51. Nieuwoudt, M., et al., *Non-toxicity of IV Injected Perfluorocarbon Oxygen Carrier in an Animal Model of Liver Regeneration Following Surgical Injury.* Artificial Cells Blood Substitutes and Biotechnology, 2009. **37**(3): p. 117-124.

52. Singh, R., G.A. Husseini, and W.G. Pitt, *Phase Transitions of nanoemulsions using ultrasound: Experimental observations.* Ultrasonics Sonochemistry, 2012. **19**(5): p. 1120-1125.

53. Giesecke, T. and K. Hynynen, *Ultrasound-mediated cavitation thresholds of liquid perfluorocarbon droplets in vitro.* Ultrasound in Medicine and Biology, 2003. **29**(9): p. 1359-1365.

54. Shiraishi, K., et al., *A facile preparation method of a PFC-containing nano-sized emulsion for theranostics of solid tumors.* International Journal of Pharmaceutics, 2011. **421**(2): p. 379-387.

55. Kawabata, K., et al., *Nanoparticles with multiple perfluorocarbons for controllable ultrasonically induced phase shifting.* Japanese Journal of Applied Physics Part 1-Regular Papers Brief Communications & Review Papers, 2005. **44**(6B): p. 4548-4552.

56. Sheeran, P.S., et al., *Formulation and Acoustic Studies of a New Phase-Shift Agent for Diagnostic and Therapeutic Ultrasound.* Langmuir, 2011. **27**(17): p. 10412-10420.

57. Sheeran, P.S., et al., *Design of ultrasonically-activatable nanoparticles using low boiling point perfluorocarbons.* Biomaterials, 2012. **33**(11): p. 3262-3269.

58. Gao, Z., et al., *Drug-loaded nano/microbubbles for combining ultrasonography and targeted chemotherapy.* Ultrasonics, 2008. **48**(4): p. 260-270.

59. Rapoport, N., Z.G. Gao, and A. Kennedy, *Multifunctional nanoparticles for combining ultrasonic tumor imaging and targeted chemotherapy.* Journal of the National Cancer Institute, 2007. **99**(14): p. 1095-1106.

60. Rapoport, N.Y., et al., *Controlled and targeted tumor chemotherapy by ultrasound-activated nanoemulsions/microbubbles.* Journal of Controlled Release, 2009. **138**(3): p. 268-276.

61. Lanza, G.M. and S.A. Wickline, *Targeted ultrasonic contrast agents for molecular imaging and therapy.* Progress in Cardiovascular Diseases, 2001. **44**(1): p. 13-31.

62. Hung, C.F., et al., *Development and evaluation of emulsion-liposome blends for resveratrol delivery.* Journal of Nanoscience and Nanotechnology, 2006. **6**(9-10): p. 2950-2958.

63. Jesorka, A. and O. Orwar, *Liposomes: Technologies and Analytical Applications.* Annual Review of Analytical Chemistry, 2008. **1**: p. 801-832.

64. Allen, T.M., et al., *Liposomes Containing Synthetic Lipid Derivatives of Poly(Ethylene Glycol) Show Prolonged Circulation Half-Lives Invivo.* Biochimica Et Biophysica Acta, 1991. **1066**(1): p. 29-36.

65. Ogris, M., et al., *PEGylated DNA/transferrin-PEI complexes: reduced interaction with blood components, extended circulation in blood and potential for systemic gene delivery.* Gene Therapy, 1999. **6**(4): p. 595-605.

66. Gabizon, A.A., Y. Barenholz, and M. Bialer, *Prolongation of the Circulation Time of Doxorubicin Encapsulated in Liposomes Containing a Polyethylene Glycol-Derivatized Phospholipid - Pharmacokinetic Studies in Rodents and Dogs.* Pharmaceutical Research, 1993. **10**(5): p. 703-708.

67. Medina, O.P., Y. Zhu, and K. Kairemo, *Targeted liposomal drug delivery in cancer.* Current Pharmaceutical Design, 2004. **10**(24): p. 2981-2989.

68. Gabizon, A., et al., *Prolonged Circulation Time and Enhanced Accumulation in Malignant Exudates of Doxorubicin Encapsulated in Polyethylene-Glycol Coated Liposomes.* Cancer Research, 1994. **54**(4): p. 987-992.

69. Koch, S., et al., *Ultrasound enhancement of liposome-mediated cell transfection is caused by cavitation effects.* Ultrasound in Medicine and Biology, 2000. **26**(5): p. 897-903.

70. Akita, H., et al., *Multi-layered nanoparticles for penetrating the endosome and nuclear membrane via a step-wise membrane fusion process.* Biomaterials, 2009. **30**(15): p. 2940-2949.

71. Cattel, L., M. Ceruti, and F. Dosio, *From conventional to stealth liposomes a new frontier in cancer chemotherapy.* Tumori, 2003. **89**(3): p. 237-249.

72. Andresen, T.L., S.S. Jensen, and K. Jorgensen, *Advanced strategies in liposomal cancer therapy: Problems and prospects of active and tumor specific drug release.* Progress in Lipid Research, 2005. **44**(1): p. 68-97.

73. Gregoriadis, G. and A.T. Florence, *Liposomes in Drug Delivery - Clinical, Diagnostic and Ophthalmic Potential.* Drugs, 1993. **45**(1): p. 15-28.

74. Seymour, L.W., *Passive Tumor Targeting of Soluble Macromolecules and Drug Conjugates.* Critical Reviews in Therapeutic Drug Carrier Systems, 1992. **9**(2): p. 135-187.

75. Ishida, T., et al., *Development of pH-sensitive liposomes that efficiently retain encapsulated doxorubicin (DXR) in blood.* International Journal of Pharmaceutics, 2006. **309**(1-2): p. 94-100.

76. Needham, D., et al., *A new temperature-sensitive liposome for use with mild hyperthermia: Characterization and testing in a human tumor xenograft model.* Cancer Research, 2000. **60**(5): p. 1197-1201.

77. Ning, S.C., et al., *Hyperthermia Induces Doxorubicin Release From Long-Circulating Liposomes and Enhances Their Antitumor Efficacy.* International Journal of Radiation Oncology Biology Physics, 1994. **29**(4): p. 827-834.

78. Andresen, T.L., D.H. Thompson, and T. Kaasgaard, *Enzyme-triggered nanomedicine: Drug release strategies in cancer therapy (Invited Review).* Molecular Membrane Biology, 2010. **27**(7): p. 353-363.

79. Zhang, Z.Y., et al., *Formation of fibrinogen-based hydrogels using phototriggerable diplasmalogen liposomes.* Bioconjugate Chemistry, 2002. **13**(3): p. 640-646.

80. Chen, D. and J.R. Wu, *An in vitro feasibility study of controlled drug release from encapsulated nanometer liposomes using high intensity focused ultrasound.* Ultrasonics, 2010. **50**(8): p. 744-749.

81. Klibanov, A.L., et al., *Ultrasound-triggered release of materials entrapped in microbubble-liposome constructs: A tool for targeted drug delivery.* Journal of Controlled Release, 2010. **148**(1): p. 13-17.

82. Evjen, T.J., et al., *Ultrasound-mediated destabilization and drug release from liposomes comprising dioleoylphosphatidylethanolamine.* European Journal of Pharmaceutical Sciences, 2011. **42**(4): p. 380-386.

83. Schroeder, A., et al., *Controlling liposomal drug release with low frequency ultrasound: Mechanism and feasibility.* Langmuir, 2007. **23**(7): p. 4019-4025.

84. Husseini, G.A. and W.G. Pitt, *Micelles and nanoparticles for ultrasonic drug and gene delivery.* Advanced Drug Delivery Reviews, 2008. **60**(10): p. 1137-1152.

85. Lasic, D.D., *The Mechanism of Vesicle Formation.* Biochemical Journal, 1988. **256**(1): p. 1-11.

86. Richardson, E.S., W.G. Pitt, and D.J. Woodbury, *The role of cavitation in liposome formation.* Biophysical Journal, 2007. **93**(12): p. 4100-4107.

87. Wu, J.R., *Shear stress in cells generated by ultrasound.* Progress in Biophysics & Molecular Biology, 2007. **93**(1-3): p. 363-373.

88. Pong, M., et al., *In vitro ultrasound-mediated leakage from phospholipid vesicles.* Ultrasonics, 2006. **45**(1-4): p. 133-145.

89. Lin, H.Y. and J.L. Thomas, *PEG-Lipids and oligo(ethylene glycol) surfactants enhance the ultrasonic permeabilizability of liposomes.* Langmuir, 2003. **19**(4): p. 1098-1105.

90. Lin, H.Y. and J.L. Thomas, *Factors affecting responsivity of unilamellar liposomes to 20 kHz ultrasound.* Langmuir, 2004. **20**(15): p. 6100-6106.

91. Evjen, T.J., et al., *Distearoylphosphatidylethanolamine-based liposomes for ultrasound-mediated drug delivery.* European Journal of Pharmaceutics and Biopharmaceutics, 2010. **75**(3): p. 327-333.

92. Schroeder, A., J. Kost, and Y. Barenholz, *Ultrasound, liposomes, and drug delivery: principles for using ultrasound to control the release of drugs from liposomes.* Chemistry and Physics of Lipids, 2009. **162**(1-2): p. 1-16.

93. Small, E.F., et al., *Ultrasound-induced transport across lipid bilayers: Influence of phase behavior.* Colloids and Surfaces a-Physicochemical and Engineering Aspects, 2011. **390**(1-3): p. 40-47.

94. Suzuki, R., et al., *Effective gene delivery with novel liposomal bubbles and ultrasonic destruction technology.* International Journal of Pharmaceutics, 2008. **354**(1-2): p. 49-55.

95. Buchanan, K.D., et al., *Encapsulation of NF-kappa B decoy oligonucleotides within echogenic liposomes and ultrasound-triggered release.* Journal of Controlled Release, 2010. **141**(2): p. 193-198.

96. Huang, S.L. and R.C. MacDonald, *Acoustically active liposomes for drug encapsulation and ultrasound-triggered release.* Biochimica Et Biophysica Acta-Biomembranes, 2004. **1665**(1-2): p. 134-141.

97. Xu, X.M., M.A. Khan, and D.J. Burgess, *Predicting hydrophilic drug encapsulation inside unilamellar liposomes.* International Journal of Pharmaceutics, 2012. **423**(2): p. 410-418.

98. Kisak, E.T., et al., *The vesosome - A multicompartment drug delivery vehicle.* Current Medicinal Chemistry, 2004. **11**(2): p. 199-219.

99. Polozova, A., et al., *Formation of homogeneous unilamellar liposomes from an interdigitated matrix.* Biochimica Et Biophysica Acta-Biomembranes, 2005. **1668**(1): p. 117-125.

100. Wong, B., et al., *Design and In Situ Characterization of Lipid Containers with Enhanced Drug Retention.* Advanced Materials, 2011. **23**(20): p. 2320-2325.

101. Mou, J.X., et al., *Alcohol Induces Interdigitated Domains in Unilamellar Phosphatidylcholine Bilayers.* Biochemistry, 1994. **33**(33): p. 9981-9985.

102. Boyer, C. and J.A. Zasadzinski, *Multiple lipid compartments slow vesicle contents release in lipases and serum.* Acs Nano, 2007. **1**(3): p. 176-182.

103. Chithrani, B.D. and W.C.W. Chan, *Elucidating the mechanism of cellular uptake and removal of protein-coated gold nanoparticles of different sizes and shapes.* Nano Letters, 2007. **7**(6): p. 1542-1550.

104. Rejman, J., et al., *Size-dependent internalization of particles via the pathways of clathrin- and caveolae-mediated endocytosis.* Biochemical Journal, 2004. **377**: p. 159-169.

105. Yanagisawa, K., et al., *Phagocytosis of ultrasound contrast agent microbubbles by Kupffer cells.* Ultrasound in Medicine and Biology, 2007. **33**(2): p. 318-325.

106. Caspi, A., R. Granek, and M. Elbaum, *Enhanced diffusion in active intracellular transport.* Physical Review Letters, 2000. **85**(26): p. 5655-5658.

107. Mellman, I., *Endocytosis and molecular sorting.* Annual Review of Cell and Developmental Biology, 1996. **12**: p. 575-625.

108. Pillay, C.S., E. Elliott, and C. Dennison, *Endolysosomal proteolysis and its regulation.* Biochemical Journal, 2002. **363**: p. 417-429.

109. Boussif, O., et al., *A Versatile Vector for Gene and Oligonucleotide Transfer into Cells in Culture and in-Vivo - Polyethylenimine.* Proceedings of the National Academy of Sciences of the United States of America, 1995. **92**(16): p. 7297-7301.

110. Sonawane, N.D., F.C. Szoka, and A.S. Verkman, *Chloride accumulation and swelling in endosomes enhances DNA transfer by polyamine-DNA polyplexes.* Journal of Biological Chemistry, 2003. **278**(45): p. 44826-44831.

111. Varkouhi, A.K., et al., *Endosomal escape pathways for delivery of biologicals.* Journal of Controlled Release, 2011. **151**(3): p. 220-228.

112. Sasaki, K., et al., *An artificial virus-like nano carrier system: enhanced endosomal escape of nanoparticles via synergistic action of pH-sensitive fusogenic peptide derivatives.* Analytical and Bioanalytical Chemistry, 2008. **391**(8): p. 2717-2727.

113. Fretz, M.M., et al., *Cytosolic delivery of liposomally targeted proteins induced by photochemical internalization.* Pharmaceutical Research, 2007. **24**(11): p. 2040-2047.

114. Gudra, T. and K.J. Opielinski, *Applying spectrum analysis and cepstrum analysis to examine the cavitation threshold in water and in salt solution.* Ultrasonics, 2004. **42**(1-9): p. 621-627.

115. Mestas, J.L., P. Lenz, and D. Cathignol, *Long-lasting stable cavitation.* Journal of the Acoustical Society of America, 2003. **113**(3): p. 1426-1430.

116. Miller, D.L., *Ultrasonic-Detection of Resonant Cavitation Bubbles In a Flow Tube by Their 2nd-Harmonic Emissions.* Ultrasonics, 1981. **19**(5): p. 217-224.

117. Dejong, N., R. Cornet, and C.T. Lancee, *Higher Harmonics of Vibrating Gas-Filled Microspheres 2. Measurements.* Ultrasonics, 1994. **32**(6): p. 455-459.

118. Husseini, G.A., et al., *The role of cavitation in acoustically activated drug delivery.* Journal of Controlled Release, 2005. **107**(2): p. 253-261.

119. Nyborg, W.L., *Biological effects of ultrasound: Development of safety guidelines. Part II: General review.* Ultrasound in Medicine and Biology, 2001. **27**(3): p. 301-333.

120. Mishra, V., et al., *Development of novel fusogenic vesosomes for transcutaneous immunization.* Vaccine, 2006. **24**(27-28): p. 5559-5570.

121. Saul, J.M., et al., *Controlled targeting of liposomal doxorubicin via the folate receptor in vitro.* Journal of Controlled Release, 2003. **92**(1-2): p. 49-67.

122. Hartley, J., *Surface Modification of Liposomes Containing Nanoemulsions*, in *Chemical Engineering*. 2011, M.S. Thesis, Department of Chemical Engineering, Brigham Young University: Provo. p. 127.

123. Gabizon, A., et al., *Targeting folate receptor with folate linked to extremities of poly(ethylene glycol)-grafted liposomes: In vitro studies.* Bioconjugate Chemistry, 1999. **10**(2): p. 289-298.

124. Kabalnov, A., et al., *Phospholipids as Emulsion Stabilizers. 1. Interfacial Tensions.* Langmuir, 1995. **11**(8): p. 2966-2974.

125. Brown, R.L. and S.E. Stein, *NIST Chemistry WebBook, NIST Standard Reference Database Number 69, Eds. P.J. Linstrom and W.G. Mallard*.

126. Leighton, T.G., *The Acoustic Bubble*. 1997, Waltham, Massachusetts: Academic Press.

127. Phelps, A.D. and T.G. Leighton, *The subharmonic oscillations and combination-frequency subharmonic emissions from a resonant bubble: Their properties and generation mechanisms.* Acustica, 1997. **83**(1): p. 59-66.

128. Tezel, A., A. Sens, and S. Mitragotri, *Investigations of the role of cavitation in low-frequency sonophoresis using acoustic spectroscopy.* Journal of Pharmaceutical Sciences, 2002. **91**(2): p. 444-453.

129. Birkin, P.R., et al., *Multiple observations of cavitation cluster dynamics close to an ultrasonic horn tip.* Journal of the Acoustical Society of America, 2011. **130**(5): p. 3379-3388.

130. Evans, E.A., R. Waugh, and L. Melnik, *Elastic Area Compressibility Modulus of Red-Cell Membrane.* Biophysical Journal, 1976. **16**(6): p. 585-595.

131. Netz, R.R. and M. Schick, *Pore formation and rupture in fluid bilayers.* Physical Review E, 1996. **53**(4): p. 3875-3885.

132. Cinelli, S., G. Onori, and A. Santucci, *Effect of ethanol on the main phase transition of distearoylphosphatidylcholine.* Colloids and Surfaces B-Biointerfaces, 2002. **25**(1): p. 91-96.

133. Pabst, G., et al., *On the propensity of phosphatidylglycerols to form interdigitated phases.* Biophysical Journal, 2007. **93**(2): p. 513-525.

134. Pabst, G., et al., *Stalk-free membrane fusion of cationic lipids via an interdigitated phase.* Soft Matter, 2012. **8**(27): p. 7243-7249.

135. Yamaguchi, T., et al., *Effects of frequency and power of ultrasound on the size reduction of liposome.* Chemistry and Physics of Lipids, 2009. **160**(1): p. 58-62.

136. O'Daly, B.J., et al., *High-power low-frequency ultrasound: A review of tissue dissection and ablation in medicine and surgery.* Journal of Materials Processing Technology, 2008. **200**(1-3): p. 38-58.

137. Schneider, F., et al., *Brain edema and intracerebral necrosis caused by transcranial low-frequency 20-kHz ultrasound - A safety study in rats.* Stroke, 2006. **37**(5): p. 1301-1306.

138. Daffertshofer, M., et al., *Transcranial low-frequency ultrasound-mediated thrombolysis in brain ischemia - Increased risk of hemorrhage with combined ultrasound and tissue plasminogen activator - Results of a phase II clinical trial.* Stroke, 2005. **36**(7): p. 1441-1446.

139. Ahmadi, F., et al., *Bio-effects and safety of low-intensity, low-frequency ultrasonic exposure.* Progress in Biophysics & Molecular Biology, 2012. **108**(3): p. 119-138.

140. Pitt, W.G., et al., *Phase Transitions of Perfluorocarbon Nanoemulsion Induced with Ultrasound: A Mathematical Model.* **Submitted**. Ultrasonics Sonochemistry, 2012.